Reports of the Department of Geodetic Science and Surveying

Report No. 383

GEOID UNDULATION COMPUTATIONS AT LASER TRACKING STATIONS

by

Vasilios K. Despotakis

Prepared for

National Aeronautics and Space Administration
Goddard Space Flight Center
Greenbelt, Maryland 20770

NASA Grant No. NGR 36-008-161
OSURF Project 783210

The Ohio State University
Department of Geodetic Science and Surveying
Columbus, Ohio 43210-1247

September 1987

ABSTRACT

Geoid undulation computations were carried out at 39 laser stations distributed around the world using a combination of terrestrial gravity data within a cap of radius 2° and a potential coefficient set (Rapp and Cruz, 1986b) up to degree 180. The traditional methods of Stokes' and Meissl's modification together with the new Molodenskii's method and the modified Sjöberg's method were applied. Performing numerical tests based on global error assumptions regarding the terrestrial data and the geopotential set we concluded that the modified Sjöberg's method is the most accurate and promising technique for geoid undulation computations. The numerical computations of the geoid undulations using all the four methods resulted in agreement with the "ellipsoidal minus orthometric" value of the undulations on the order of 60 cm or better for most of the laser stations in the eastern United States, Australia, Japan, Bermuda and Europe. A systematic discrepancy of about 2 meters for most of the western United States stations was detected and verified by using two relatively independent data sets. The cause of this discrepancy was not found. A correction due to the inconsistencies of the terrestrial data and the potential coefficients within the cap surrounding the laser station, called the "local average" correction improved the results by 30 cm and it seems necessary to apply this correction. For oceanic laser stations in the western Atlantic and Pacific oceans that no terrestrial data available, the adjusted GEOS-3 and SEASAT altimeter data were used for the computation of the geoid undulation in a collocation method.

FOREWORD

This report was prepared by Mr. Vasilios K. Despotakis, Graduate Research Associate, Department of Geodetic Science and Surveying, The Ohio State University. This research is supported by NASA Grant NGR36-008-161, The Ohio State University Research Foundation Project No. 783210. This project is under the direction of Richard H. Rapp, Professor, Department of Geodetic Science and Surveying. The grant covering this research is administered through the NASA Goddard Space Flight Center, Greenbelt, Maryland, 20771, Mr. Jean Welker, Technical Officer.

Some computer funds for the research described in this report were supplied through the Instruction and Research Computer Center.

This report is a slightly modified version of a thesis submitted in partial fulfillment of the requirements for the degree Master of Science in the Graduate School of The Ohio State University.

The reproduction and distribution of this report were carried out with funds supplied, in part, by the Department of Geodetic Science and Surveying.

ACKNOWLEDGMENTS

I am extremely grateful to my adviser, Dr. Richard H. Rapp who supervised and reviewed my work with a great deal of patience and fruitful cooperation. Dr. Urho A. Uotila reviewed my work and made some helpful suggestions. Dr. Clyde C. Goad helped me clarify some questions concerning the gravity data. Most of the software for the numerical application of Stokes' and Meissl's method was provided to me by Dr. Theodossios L. Engelis. Dr. Christopher Jekeli very kindly sent me some subroutines necessary for the numerical application of Molodenskii's method. Dr. Lars E. Sjöberg answered many questions I had when I started investigating his method in his reply to my letter. Mr. John W. Robbins clarified some problems about the laser station coordinates. Mr. Majid Kadar carried out sea surface height and anomaly computations using altimeter data in the vicinity of Bermuda.

Some computer funds were made available by the Instruction and Research Computer Center of the Ohio State University.

TABLE OF CONTENTS

LIST OF TABLES

LIST OF FIGURES

CHAPTER I

INTRODUCTION

The purpose of this investigation is the precise absolute geoid undulation computation for certain laser stations distributed around the world. The classical methods that combine terrestrial gravity data within a cap surrounding the computation point together with a high degree potential coefficient set through the use of integral formulas have been implemented to attack the problem. The only exception is the computation of the geoid undulation at four laser stations in the Pacific and two stations in West Atlantic that have been carried out using adjusted Geos-3 and SEASAT altimeter data in a collocation method. Chapter 2 will give the necessary truncation theory. The general formulation is given in section 2.1. The conventional method of Stokes' and Meissl's modification are presented in Section 2.1 as a review. The modification of Stokes' function with the ultimate goal to minimize certain errors in geoid undulation computations is a common concept for both Molodenskii's and modified Sjöberg's methods. This is why Molodenskii's and modified Sjöberg's methods are discussed together as "new" methods in Section 2.3.

After the theoretical background for the above four methods is established, numerical computations based on certain error models will

show us the behavior of the global root mean square (RMS) errors of the four methods as a function of the capsize. This is discussed in Chapter 3. We then will present information in Chapter 4 concerning the selected laser stations around the world. The available gravity data surrounding the laser stations were processed to be used in the integration formulas. This process is given in Chapter 5. The pre-processing of the data is first discussed in Section 5.1. Some prediction techniques which are necessary to transform the point data to mean values will be given in Section 5.2. The prediction procedure we used for the Bermuda area will be separately described in Section 5.3. The terrain corrections and the indirect effect for stations on high mountains is discussed in Section 5.4. To avoid the spherical approximation, ellipsoidal correction formulas will be given for the conventional methods, and will be derived for the new methods, in Chapter 6. A local average correction which is new in concept will be given in Chapter 7.

The numerical results for geoid unduation computations using all the four methods (Stokes', Meissl's, Molodenskii's and modified Sjöberg's methods) will be presented in Chapter 8: The details for the numerical application of the four methods will be given in Section 8.1; the results will be given in Section 8.2; a discussion of the results and comparisons will be given in Section 8.3. Emphasis will be given on the following comparisons:

a) Terrain corrected vs. uncorrected undulations.

b) Computed undulations using all the four method vs. the value of

the undulations computed as the difference ellipsoidal minus orthometric height.

c) Undulations computed using two different methods.

d) Undulations computed using the four methods and the values of the undulations taken from a high degree geopotential model.

e) Undulations computed excluding the local average correction vs. undulations computed including the local average correction.

The results will be presented by regions, for detection of any systematic differences that are correlated with a specific region. The collocation method was also used to compute undulations from altimeter data in the vicinity of Bermuda. These results together with the undulations obtained from the calibration of SEASAT will be compared to the gravimetric undulations and will be presented in Section 8.4. The undulations for five oceanic laser stations computed using altimeter data in a collocation method will be given in Section 8.5. Finally, summary and conslusions will be given in Chapter 9, and recommendations for future studies in Chapter 10.

An attempt has been made to maintain a uniform simple notation. The following will be adhered to:

N	geoidal undulation
R	mean earth radius
γ	mean value of the normal gravity
ψ_0	spherical cap of radius ψ_0 surrounding the computation

	point
$S(\cos\psi)$	Stokes' function
S_o	$S(\cos\psi_o)$
$W_i(\cos\psi)$	proper function subtracted from $S(\cos\psi)$
i=1	Stokes' method
i=2	Meissl's method
i=3	Molodenskii's method
i=4	Modified Sjöberg method
$S_i(\cos\psi)$	$S(\cos\psi) - W_i(\cos\psi)$
M	maximum degree of potential coefficients used
$\bar{n}$	maximum number of Fourier coefficinets of $W_i(\cos\psi)$
n_T	maximum degree of the terrestrial error degree variances
$\hat{\Delta}g_n^T$	n^{th} surface spherical harmonic of terrestrial Δ_g^T given on a sphere of radius R
$\hat{\Delta}g_n^s$	n^{th} surface spherical harmonic of Δ_g^s, based on a set of known potential coefficients given on a sphere of radius R
ε_n^T	degree error of $\hat{\Delta}_{gn}^T$ ($\Delta_{gn}^T = \hat{\Delta}_{gn}^T + \varepsilon_n^T$)
ε_n^s	degree error of $\hat{\Delta}_n^s$ ($\Delta g_n^s = \hat{\Delta}_{gn}^s + \varepsilon_n^s$)
$M(\cdot)$	global average operator
$C_n=M[(\Delta g_n)^2]$	degree variance of Δg_n for high degrees given on a sphere of radius R
$\delta C_n=M[(\varepsilon_n^s)^2]$	degree variance of ε_n^s
$\sigma_n=M[(\varepsilon_n^T)^2]$	degree variance of ε_n^T
Q_{in}	truncation coefficients

X_{in} Fourier coefficients of $S_i(\cos\psi)$

W_{in} Fourier coefficients of $W_i(\cos\psi)$

$P_n(\cos\psi)$ Legendre polynomial of degree n

CHAPTER II

TRUNCATION THEORY

2.1 General Formulation

The geoid undulation N with respect to a specified mean earth ellipsoid can be computed using gravity anomalies Δg on the geoid through the use of the Stokes' integral:

$$N = \frac{R}{4\pi\gamma} \iint_{\sigma} S(\cos\psi)\Delta g d\sigma \qquad (2.1)$$

A number of assumptions are associated with formula (2.1):

a) The boundary surface of the geoid is a sphere σ

b) Integration is done using global gravity data (on the sphere σ)

c) No masses external to the geoid exist

d) The mass of the reference ellipsoid equals the earth's mass

e) The normal potential on the ellipsoid equals the gravity potential on the geoid

f) The ellipsoid's center coincides wtih the earth's center of mass.

Assumption a) can be avoided by computing the ellipsoidal corrections (see Chapter 6); the error when doing assumption c) can be diminished by the use of the terrain-corrected gravity anomalies (see Section 5.4); assumptions d), e) and f) cannot be avoided and if they do not hold, a zero and first order term will have to be added to the

computed undulation. Finally, assumption b) can be more or less avoided if gravity anomalies within a cap σ_c surrounding the computation point and a given geopotential model are combined. All four methods that are described below will split the integral (2.1) into two parts (gravity anomalies within a cap and potential coefficient information) to avoid assumption b) which cannot be rigorously avoided due to the lack of global coverage of the existing gravity data.

The next step is to consider the basic modification of (2.1), so that certain errors are minimized. For all the four methods, denoting with $S_i(\cos\psi)$ the modified Stokes' function, the modification is done so that: (i = 1, 2, 3, 4 corresponds to the four methods: Stokes', Meissl's, Molodenskii's, modified Sjöberg's).

$$S_i(\cos\psi) = S(\cos\psi) - W_i(\cos\psi) \qquad (2.2)$$

where $W_i(\cos\psi)$ is a properly defined function of the spherical distance ψ. [For the original Stokes' method it is clear that no modification is done, but the notation in (2.2) will be kept even for i = 1, for convenience. It simply holds then $W_1(\cos\psi) = 0$; $S_1(\cos\psi) = S(\cos\psi)$].

Any modification of the Stokes' function has to maintain the integrity of the basic Stokes' equation in (2.1). Substituting (2.2) into (2.1), the modified Stokes' equation will be:

$$N_i = \frac{R}{4\pi\gamma} \iint_\sigma S_i(\cos\psi)\Delta g d\sigma + \frac{R}{4\pi\gamma} \iint_\sigma W_i(\cos\psi)\Delta g d\sigma \qquad (2.3)$$

Equation (2.3) is rigorously equivalent to (2.1)

A powerful relationship that provides an immediate conversion of an integral over the sphere σ to a series of harmonics is proven in (Jekeli, 1980) and will be used extensively within the text. The relationship reads:

$$\iint_{\sigma} K(\cos\psi)\Delta g_{nm}d\sigma = 2\pi k_n \Delta g_{nm} \tag{2.4}$$

where $K(\cos\psi)$ an arbitrary kernel function

$2\pi k_n$ the eigenvalues of the integral operator in (2.4)

Δg_{nm} the n^{th} degree and m^{th} order spherical harmonic of the surface function Δg.

From (2.4) we obtain

$$\sum_{n=o}^{\infty} \sum_{m=o}^{n} \iint_{\sigma} K(\cos\psi)\Delta g_{nm}d\sigma = \sum_{n=o}^{\infty} \sum_{m=o}^{n} 2\pi k_n \Delta g_{nm}, \text{ or}$$

$$\iint_{\sigma} K(\cos\psi)\Delta g d\sigma = 2\pi \sum_{n=o}^{\infty} k_n \Delta g_n \tag{2.5}$$

Applying (2.5) to (2.3) we easily obtain:

$$N_i = \frac{R}{4\pi\gamma} \iint_{\sigma} S_i(\cos\psi)\Delta g d\sigma + \frac{R}{2\gamma} \sum_{n=o}^{\infty} W_{in}\Delta g_n \tag{2.6}$$

where $2\pi W_{in}$ are the eigenvalues of the second integral operator in (2.3).

Now we are ready to split (2.6) (or equivalently (2.1)) into two components. From (2.6) we take

$$N = \frac{R}{4\pi\gamma} \iint_{\sigma_c} S_i(\cos\psi)\Delta g d\sigma + \frac{R}{4\pi\gamma} \iint_{\sigma-\sigma_c} S_i(\cos\psi)\Delta g d\sigma + \frac{R}{2\gamma} \sum_{n=o}^{\infty} W_{in}\Delta g_n \tag{2.7}$$

Note that the second and the third term in (2.7) are to be computed from a given set of potential coefficients and the first term is the cap contribution.

To bring the second integral to the form of a summation, we write

$$\frac{R}{4\pi\gamma}\iint_{\sigma-\sigma_i} S_i(\cos\psi)\Delta g\,d\sigma = \frac{R}{4\pi\gamma}\iint_{\sigma} \overline{S_i}(\cos\psi)\Delta g\,d\sigma \tag{2.8}$$

$$\text{where } \overline{S_i}(\cos\psi) = \begin{cases} 0 & \text{if } 0 \le \psi \le \psi_c \\ S_i(\cos\psi) & \text{if } \psi_c < \psi \le \pi \end{cases} \tag{2.9}$$

Expanding $\overline{S_i}(\cos\psi)$ in spherical harmonics we have

$$\overline{S_i}(\cos\psi) = \sum_{n=0}^{\infty} \frac{2n+1}{2} Q_{in} P_n(\cos\psi) \tag{2.10}$$

where Q_{in} are the Fourier coefficients of $\overline{S_i}(\cos\psi)$:

$$Q_{in} = \frac{1}{2\pi}\iint_{\sigma} \overline{S_i}(\cos\psi)P_n(\cos\psi)\,d\sigma \tag{2.11}$$

Since $2\pi Q_{in}$ are the eigenvalues of the integral operator of the right-hand side of equation (2.8), equation (2.5) together with (2.8) gives

$$\frac{R}{4\pi\gamma}\iint_{\sigma-\sigma_i} S_i(\cos\psi)\Delta g\,d\sigma = \frac{R}{2\gamma}\sum_{n=0}^{\infty} Q_{in}\Delta g_n \tag{2.12}$$

Substituting (2.12) into (2.7) the final equation for the modified Stokes' function is

$$N_i = \frac{R}{4\pi\gamma}\iint_{\sigma_c} S_i(\cos\psi)\Delta g\,d\sigma + \frac{R}{2\gamma}\sum_{n=0}^{\infty} Q_{in}\Delta g_n + \frac{R}{2\gamma}\sum_{n=0}^{\infty} W_{in}\Delta g_n$$

$$= \frac{R}{4\pi\gamma} \iint_{\sigma_c} S_i(\cos\psi)\Delta g d\sigma + \frac{R}{2\gamma} \sum_{n=0}^{\infty} (Q_{in} + W_{in})\Delta g_n \qquad (2.13)$$

The practical computation of (2.13) is done using $\theta^\circ x\theta^\circ$ terrestrial mean gravity anomalies $\hat{\Delta}g^T$ for the numerical integration and a set of potential coefficients up to degree M as follows:

$$\hat{N}_i = \frac{R}{4\pi\gamma} \iint_{\sigma_c} S_i(\cos\psi)\hat{\Delta}g^T d\sigma + \frac{R}{2\gamma} \sum_{n=0}^{M} (Q_{in} + W_{in})\hat{\Delta}g_n^s \qquad (2.14)$$

To derive expressions for the global RMS undulation error associated with (2.14), we will follow the concepts given in (Christodoulidis, 1976): The global RMS undulation error will have four error components, due to:

1. Erroneous $\hat{\Delta}g^T$ (mean values of $\theta^\circ x\theta^\circ$ blocksize). This error will be called "propagation error".
2. Finite blocksize (i.e. θ° is not infinitely small) used for the Stokes' numerical integration. This error will be called "discretion error".
3. Erroneous potential coefficients. This error will be called "commission error".
4. Limited degree of expansion of the potential coefficients used. This error will be called "ommission error".

Notice that there is an analogy between error sources 1 and 3 and 2 and 4. Errors 1 and 2 are to be interpreted as the errors due to erroneous input data in (2.14) ($\hat{\Delta}g^T$, $\hat{\Delta}g^s$) whereas errors 2 and 4 are to be interpreted as the errors due to the limited degree of expansion of

the terrestrial data ($\hat{\Delta}g_n^T$ are taken only to degree $n = n_T$) and the potential coefficient data ($\hat{\Delta}g_n^s$ are taken only up to degree $n = M$).

Using the rule of thumb for the maximum degree n_T of the terrestrial error degree variances, we have

$$n_T = 180^\circ/\theta^\circ \tag{2.15}$$

where θ° is the blocksize (in degrees) of the mean gravity anomalies used in (2.14).

We then furthermore assume that

$$\Delta g_n^T = \hat{\Delta}g_n^T + \varepsilon_n^T \qquad 0 \leq n \leq n_T \tag{2.16}$$

$$\text{and } M[(\Delta g_n^T)^2] = C_n \qquad n_T < n \tag{2.17}$$

with C_n taken from a model of anomaly error degree variances.

A common model is the Tscherning-Rapp model (Tscherning and Rapp, 1974):

$$C_n = \frac{A(n-1)}{(n-2)(n+B)} S^{n+2} \qquad 3 \leq n < \infty \tag{2.18}$$

with $A = 425.28$ mgal^2; $B = 24$, $S = 0.999617$, $C_2 = 7.5S^4$ mgal^2 and will be used for the numerical applications. The C_n values refer to a sphere of radius equal to the mean earth radius.

Similarly, for the potential coefficient set, we assume:

$$\Delta g_n^s = \hat{\Delta}g_n^s + \varepsilon_n^s \qquad 0 \leq n \leq M \tag{2.19}$$

$$M[(\Delta g_n^s)^2] = C_n \qquad M < n \tag{2.20}$$

Combining (2.13) and (2.14) together with the assumptions (2.16), (2.17) and (2.19), (2.20) we obtain the error when computing the geoid undulation through (2.14):

$$\delta N_i = N_i - \hat{N}_i = \delta N_{i,1} + \delta N_{i,2} + \delta N_{i,3} + \delta N_{i,4} \tag{2.21}$$

with $$\delta N_{i,1} = \frac{R}{4\pi\gamma} \iint_{\sigma_c} S_i(\cos\psi) \sum_{n=0}^{n_T} \varepsilon_n^I d\sigma \tag{2.22}$$

$$\delta N_{i,2} = \frac{R}{4\pi\gamma} \iint_{\sigma_c} S_i(\cos\psi) \sum_{n=n_T+1}^{\infty} \Delta g_n^I d\sigma \tag{2.23}$$

$$\delta N_{i,3} = \frac{R}{2\gamma} \sum_{n=0}^{M} (Q_{in} + W_{in}) \varepsilon_n^s \tag{2.24}$$

$$\delta N_{i,4} = \frac{R}{2\gamma} \sum_{n=M+1}^{\infty} (Q_{in} + W_{in}) \Delta g_n^s \tag{2.25}$$

Using (2.5), the errors $\delta N_{i,1}$, $\delta N_{i,2}$ can be rewritten as:

$$\delta N_{i,1} = \frac{R}{4\pi\gamma} \iint_{\sigma} S_i(\cos\psi) \sum_{n=0}^{n_T} \varepsilon_n^I d\sigma - \frac{R}{4\pi\gamma} \iint_{\sigma-\sigma_c} S_i(\cos\psi) \sum_{n=0}^{n_T} \varepsilon_n^I d\sigma =$$

$$= \frac{R}{4\pi\gamma} \iint_{\sigma} S_i(\cos\psi) \sum_{n=0}^{n_T} \varepsilon_n^I d\sigma - \frac{R}{4\pi\gamma} \iint_{\sigma} \overline{S_i}(\cos\psi) \sum_{n=0}^{n_T} \varepsilon_n^I d\sigma, \text{ or}$$

$$\delta N_{i,1} = \frac{R}{2\gamma} \sum_{n=0}^{n_T} (X_{in} - Q_{in}) \varepsilon_n^I \tag{2.26}$$

Here X_{in} are the Fourier coefficients of $S_i(\cos\psi)$. Similarly,

$$\delta N_{i,2} = \frac{R}{2\gamma} \sum_{n=n_T+1}^{\infty} (X_{in} - Q_{in}) \Delta g_n^I \tag{2.27}$$

According to our discussion above we have the following errors:

Error $\delta N_{i,1}$ is the error due to erroneous terrestrial gravity data (propagation error)

Error $\delta N_{i,2}$ is the error due to discretized data in the numerical integration (discretion error)

Error $\delta N_{i,3}$ is the error due to erroneous potential coefficients (commission error)

Error $\delta N_{i,4}$ is the error due to the limited degree of expansion of the potential coefficients (omission error)

The expected global mean square errors of each error source described above can now be found, using (2.26), (2.27), (2.24), (2.25):

$$\overline{\delta N_i^2}_{,1} = M(\delta N_{i,1}^2) = \left(\frac{R}{2\gamma}\right)^2 \sum_{n=0}^{n_T} (X_{in} - Q_{in})^2 \sigma_n \tag{2.28}$$

$$\overline{\delta N_i^2}_{,2} = M(\delta N_{i,2}^2) = \left(\frac{R}{2\gamma}\right)^2 \sum_{n=n_T+1}^{\infty} (X_{in} - Q_{in})^2 C_n \tag{2.29}$$

$$\overline{\delta N_i^2}_{,3} = M(\delta N_{i,3}^2) = \left(\frac{R}{2\gamma}\right)^2 \sum_{n=0}^{M} (Q_{in} + W_{in})^2 \delta C_n \tag{2.30}$$

$$\overline{\delta N_i^2}_{,4} = M(\delta N_{i,4}^2) = \left(\frac{R}{2\gamma}\right)^2 \sum_{n=M+1}^{\infty} (Q_{in} + W_{in})^2 C_n \tag{2.31}$$

The total global mean square error, assuming uncorrelated error sources is

$$\overline{\delta N_i^2} = \overline{\delta N_i^2}_{,1} + \overline{\delta N_i^2}_{,2} + \overline{\delta N_i^2}_{,3} + \overline{\delta N_i^2}_{,4} \tag{2.32}$$

and the total global root mean square error is from (2.32):

$$\overline{\delta N_i} = (\overline{\delta N_i^2}_{,1} + \overline{\delta N_i^2}_{,2} + \overline{\delta N_i^2}_{,3} + \overline{\delta N_i^2}_{,4})^{1/2} \tag{2.33}$$

We thus have derived general expressions for the geoid undulation computation and it's expected global RMS error when a modification of Stokes' function is attempted. Each of the following four methods, or

even any arbitrary modification of Stokes' function which follows the principal (2.2) can be easily formulated according to (2.14) and (2.28) - (2.31). The derivation has been given step-by-step because of its importance for the error analysis discussion, and for the understanding of the sections 2.2 and 2.3 that follow.

2.2 The Conventional Methods

2.2.1 Stokes' Method

In Stokes' method (i=1) no modification of the Stokes' function is attempted.

In this case:

$$W_1(\cos\psi) = 0 \tag{2.34}$$

which means that all the Fourier coefficients W_{1n} are zero:

$$W_{1n} = 0 \qquad 0 \leq n < \infty \tag{2.35}$$

and from (2.2) if follows that

$$S_1(\cos\psi) = S(\cos\psi) \tag{2.36}$$

The Fourier coefficients of $S_1(\cos\psi)$ can be taken from the expansion of the Stokes' function in spherical harmonics:

$$S_1(\cos\psi) = \sum_{n=2}^{\infty} \frac{2n+1}{n-1} P_n(\cos\psi) \tag{2.37}$$

Expansion (2.37) can be rewritten as

$$S_1(\cos\psi) = \sum_{n=0}^{\infty} \frac{2n+1}{2} X_{1n} P_n(\cos\psi) \tag{2.38}$$

Comparing (2.37) and (2.38) the Fourier coefficients X_{1n} of $S_1(\cos\psi)$ are

given by (cf. Heiskanen and Moritz, 1967, p. 97).

$$X_{1n} = \begin{cases} 0 & 0 \leq n \leq 2 \\ \frac{2}{n-1} & 2 < n < \infty \end{cases} \tag{2.39}$$

Thus, the undulation in Stokes' method is computed according to (2.14) as:

$$\hat{N}_1 = \frac{R}{4\pi\gamma} \iint_{\sigma_c} S(\cos\psi)\hat{\Delta}g^T d\sigma + \frac{R}{2\gamma} \sum_{n=0}^{M} Q_{1n}\hat{\Delta}g_n^s \tag{2.40}$$

with the components of the global mean square error from (2.28) - (2.31) and (2.35), (2.39)

$$\overline{\delta N}_{1,1}^2 = \left(\frac{R}{2\gamma}\right)^2 \sum_{n=0}^{n_T} (X_{1n} - Q_{1n})^2 \sigma_n \qquad \text{(propagation error)} \tag{2.41}$$

$$\overline{\delta N}_{1,2}^2 = \left(\frac{R}{2\gamma}\right)^2 \sum_{n=n_T+1}^{\infty} \left(\frac{2}{n-1} - Q_{1n}\right)^2 \sigma_n \qquad \text{(discretion error)} \tag{2.42}$$

$$\overline{\delta N}_{1,3}^2 = \left(\frac{R}{2\gamma}\right)^2 \sum_{n=0}^{M} Q_{1n}^2 \delta C_n \qquad \text{(commission error)} \tag{2.43}$$

$$\overline{\delta N}_{1,4}^2 = \left(\frac{R}{2\gamma}\right)^2 \sum_{n=M+1}^{\infty} Q_{1n}^2 C_n \qquad \text{(ommission error)} \tag{2.44}$$

The total global RMS error is

$$\overline{\delta N}_1 = (\overline{\delta N}_{1,1}^2 + \overline{\delta N}_{1,2}^2 + \overline{\delta N}_{1,3}^2 + \overline{\delta N}_{1,4}^2)^{1/2} \tag{2.45}$$

The truncation coefficients Q_{1n} can be numerically computed by a subroutine written by Paul (1973) based on an accurate recursive formula.

2.2.2 Meissl's Method

To avoid the discontinuity of the kernel (2.9), Meissl (1971) introduced the following modification:

$$W_2(\cos\psi) = \begin{cases} S_0 & 0 \le \psi \le \psi_0 \\ 0 & \psi_0 < \psi \le \pi \end{cases} \tag{2.46}$$

It follows that

$$S_2(\cos\psi) = \begin{cases} S(\cos\psi) - S_0 & 0 \le \psi \le \psi_0 \\ S(\cos\psi) & \psi_0 < \psi \le \pi \end{cases} \tag{2.47}$$

and

$$\bar{S}_2(\cos\psi) = \begin{cases} 0 & 0 \le \psi \le \psi_0 \\ S_2(\cos\psi) & \psi_0 < \psi \le \pi \end{cases} \tag{2.48}$$

Notice that the kernel $\bar{S}_2(\cos\psi)$ is now a continuous function of the spherical distance ψ everywhere in $0 \le \psi \le \pi$.

We now proceed for the computation of the Fourier coefficients X_{2n}, W_{2n}, Q_{2n}.

Introducing the following recursive formulas for $P_n(y)$, $y = \cos\psi$

$$(n+1)P_{n+1}(y) + nP_{n-1}(y) = (2n+1)yP_n(y) \qquad n \ge 1 \tag{2.49}$$

$$(1-y^2)P_n'(y) = n(P_{n-1}(y) - yP_n(y)) \qquad n \ge 1 \tag{2.50}$$

$$yP_n'(y) - P_{n-1}'(y) = nP_n(y) \qquad n \ge 1 \tag{2.51}$$

$$(2n+1)P_n(y) = P_{n+1}'(y) - P_{n-1}'(y) \qquad n \ge 1 \tag{2.52}$$

(the prime denotes differentiation with respect to the argument y)

and denoting with $y_0 = \cos\psi_0$, we take:

$$W_{2n} = \int_{-1}^{1} W_2(y)P_n(y)dy = \int_{-1}^{1} S_0P_n(y)dy = S_0 \int_{-1}^{1} P_n(y)dy, \text{ or}$$

$$W_{2n} = \begin{cases} 2S_o & n = 0 \\ 0 & n \geq 1 \end{cases} \qquad (2.53)$$

Also $\quad Q_{2n} = \int_{-1}^{1} \bar{S}_2(y)P_n(y)dy = \int_{-1}^{y_o} S_2(y)P_n(y)dy =$

$$= \int_{-1}^{y_o} S(y)P_n(y)dy - S_o\int_{-1}^{y_o} P_n(y)dy \qquad (2.54)$$

From (2.54) and (2.52) we obtain

$$Q_{2n} = Q_{1n} - \begin{cases} \frac{S_o}{2n+1}\,(P_{n+1}(y_o) - P_{n-1}(y_o)) & n \geq 1 \\ S_o(y_o+1) & n = 0 \end{cases} \qquad (2.55)$$

An alternative formula of Q_{2n} can be derived, using (2.55) and (2.49).

Now $\quad P_{n+1}(y) = \frac{(2n+1)yP_n(y) - nP_{n-1}(y)}{n+1} \qquad (2.56)$

Substituting (2.56) into (2.55) we have:

$$Q_{2n} = Q_{1n} + \begin{cases} \frac{S_o}{n+1}\,(P_{n-1}(y_o) - y_oP_n(y_o)) & n \geq 1 \\ -S_o(y_o+1) & n = 0 \end{cases} \qquad (2.57)$$

Note that for n = 0 the Q_{2o} coefficient usually given in the literature (Rapp, 1985a) as

$$Q_{2o} = S_o(1-y_o) \qquad (2.58)$$

corresponds to our $Q_{2o} + W_{2o} = -S_o(y_o+1) + 2S_o = S_o(1-y_o)$

Finally, the X_{2n} coefficients are

$$X_{2n} = \int_{-1}^{1} S_2(y)P_n(y)dy = \int_{-1}^{1} S(y)P_n(y)dy - S_o\int_{-1}^{1} P_n(y)dy \quad \text{or}$$

$$X_{2n} = \begin{cases} -2S_o & n=0 \\ 0 & n=1 \\ \frac{2}{n-1} & n\geq 2 \end{cases} \qquad (2.59)$$

Now we are ready to give the final formulas for Meissl's method. The undulation is computed as

$$\hat{N}_2 = \frac{R}{4\pi\gamma} \iint_{\sigma_c} S_2(\cos\psi)\hat{\Delta}g^T d\sigma + \frac{R}{2\gamma} \sum_{n=0}^{M} Q_{2n}\hat{\Delta}g_n^s \qquad (2.60)$$

with the components of the global mean square error from (2.28) - (2.31) and (2.53), (2.55), (2.59):

$$\overline{\delta N_2^2}_{,1} = \left(\frac{R}{2\gamma}\right)^2 \sum_{n=0}^{n_T} (X_{2n} - Q_{2n})^2 \sigma_n \qquad \text{(propagation error)} \qquad (2.61)$$

$$\overline{\delta N_2^2}_{,1} = \left(\frac{R}{2\gamma}\right)^2 \sum_{n=n_T+1}^{\infty} \left(\frac{2}{n-1} - Q_{2n}\right)^2 C_n \qquad \text{(discretion error)} \qquad (2.62)$$

$$\overline{\delta N_2^2}_{,3} = \left(\frac{R}{2\gamma}\right)^2 \left[\sum_{n=2}^{M} Q_{2n}^2 \delta C_n + (Q_{20} + W_{20})^2 \delta C_0 \right]$$

$$\text{(commission error)} \qquad (2.63)$$

$$\overline{\delta N_2^2}_{,4} = \left(\frac{R}{2\gamma}\right) \sum_{n=M+1}^{\infty} Q_{2n}^2 C_n \qquad \text{(ommission error)} \qquad (2.64)$$

The total global RMS error is

$$\overline{\delta N_2} = (\overline{\delta N_2^2}_{,1} + \overline{\delta N_2^2}_{,2} + \overline{\delta N_2^2}_{,3} + \overline{\delta N_2^2}_{,4})^{1/2} \qquad (2.65)$$

Expressions (2.61), (2.62), (2.63), (2.64) and (2.65) are equivalent to the expressions for the global mean square undulation error of Meissl's method given in (Engelis, et al., 1985a) if we are to start the summations from two instead of zero.

2.3 The New Methods

2.3.1 Molodenskii's Method

We will now present the Molodenskii's modification to the original

Stokes' formula (2.1) (Jekeli, 1980, p. 22). The function of ψ, $W_3(\cos\psi)$ that is to be subtracted from the Stokes' function $S(\cos\psi)$ is

$$W_3(\cos\psi) = \sum_{k=0}^{\bar{n}} \frac{2k+1}{2} W_{3k} P_k(\cos\psi) \tag{2.66}$$

Using (2.2) we take

$$S_3(\cos\psi) = S(\cos\psi) - \sum_{k=0}^{\bar{n}} \frac{2k+1}{2} W_{3k} P_k(\cos\psi) \tag{2.67}$$

The Fourier coefficients X_{3n}, W_{3n}, and Q_{3n} can be immediately computed. Rewritting (2.67) as

$$S_3(\cos\psi) = \sum_{n=0}^{\infty} \frac{2n+1}{2} X_{3n} P_n(\cos\psi) \tag{2.68}$$

with

$$X_{3n} = \begin{cases} -W_{3n} & 0 \leq n \leq 1 \\ \dfrac{2}{n-1} - W_{3n} & 2 \leq n \leq \bar{n} \\ \dfrac{2}{n-1} & \bar{n} < n < \infty \end{cases} \tag{2.69}$$

we obtain the Fourier coefficients X_{3n}.

Furthermore, from (2.66) it is obvious that W_{3n} $(0 \leq n \leq \bar{n})$ are the Fourier coefficients of $W_3(\cos\psi)$. Finally, since

$$\bar{S}_3(\cos\psi) = \begin{cases} 0 & 0 \leq \psi \leq \psi_0 \\ S_3(\cos\psi) & \psi_0 < \psi \leq \pi \end{cases} \tag{2.70}$$

we take $(y = \cos\psi,\ y_0 = \cos\psi_0)$

$$Q_{3n} = \int_{-1}^{1} \bar{S}_3(y) P_n(y)\,dy = \int_{-1}^{y_0} S_3(y) P_n(y)\,dy =$$

$$= \int_{-1}^{y_0} \left(S(y) - \sum_{k=0}^{\bar{n}} \frac{2k+1}{2} W_{3k} P_k(y)\right) P_n(y)\,dy, \text{ or}$$

$$Q_{3n} = Q_{1n} - \sum_{k=o}^{\bar{n}} \frac{2k+1}{2} W_{3k} \int_{-1}^{y_o} P_k(y)P_n(y)dy \qquad (2.71)$$

The definite integrals from -1 to y_o of the product of two Legendre polynomials $P_r(y)\cdot P_n(y)$ are analytically given in (ibid, p. 10).

If

$$e_{rn} = \int_{-1}^{y_o} P_r(y)\cdot P_n(y)dy \qquad r, n \geq 0 \qquad (2.72)$$

Then

$$e_{rn} = \frac{1}{(r-n)(r+n+1)} [nP_r(y_o)P_{n-1}(y_o) - rP_n(y_o)P_{r-1}(y_o) + y_o(r-n)P_n(y_o)P_r(y_o)] \qquad r \neq n \; r, n > 0 \qquad (2.73)$$

Also, $e_{r,o} = \frac{1}{2r+1} [P_{r+1}(y_o)P_{r-1}(y_o)] \qquad r > 0 \qquad (2.74)$

$$e_{o,o} = 1 + y_o \qquad (2.75)$$

$$e_{r,r} = \frac{1}{2r+1} [(2r-1)e_{r-1,r-1} + y_o(P_r^2(y_o) + P_{r-1}^2(y_o)) - 2P_r(y_o)P_{r-1}(y_o)] \qquad r > 0 \qquad (2.76)$$

Formulas (2.73) - (2.76) are very useful for the numerical computation of e_{rn} coefficients and can very easily be programmed. Notice that from (2.72) it holds

$$e_{rn} = e_{nr} \qquad (2.77)$$

Inserting (2.72) into (2.71) we have the truncation coefficients Q_{3n}:

$$Q_{3n} = Q_{1n} - \sum_{k=o}^{\bar{n}} \frac{2k+1}{2} W_{3k}e_{kn} \qquad (2.78)$$

In Molodenskii's method the function $W_3(y)$ is to be defined as the "best" approximation to $S(y)$ in the interval $[-1, y_o]$, by minimizing the

norm of the difference:

$$\int_{-1}^{y_o}[S(y) - W_3(y)]^2 dy \longrightarrow \text{minimum} \tag{2.79}$$

After condition (2.79), the W_{3n} coefficients are computed (without the derivations, which can be found in (ibid, pp. 29-31)), from

$$W_{3n} = \sum_{r=n}^{\bar{n}} \frac{2r+1}{2} u_r h_{rn} \qquad 0 \leq n \leq \bar{n} \tag{2.80}$$

with

$$u_r = \frac{1}{k} \sum_{n=o}^{r} \frac{2n+1}{2} h_{rn} Q_{1n} \qquad 0 \leq r \leq n \tag{2.81}$$

$$h_{rn} = (2n+1)k^{-r} \sum_{i=o}^{p} \binom{p}{i}\binom{q}{i}(1-k)^{i+1} \qquad 0 \leq n < r$$

$$h_{rr} = \frac{2}{2r+1} k^{-r} \qquad r \geq 0 \tag{2.82}$$

$$p = r-n-1, \quad q = r+n, \quad k = \cos^2\frac{\psi_o}{2}$$

It also follows immediately from condition (2.79) that

$$Q_{3n} = 0 \qquad 0 \leq n \leq \bar{n} \tag{2.83}$$

The number $\bar{n}$ is the maximum number of "proper" harmonics that are removed from the Stokes' function (see eq. (2.67)). For reasons that will be explained in Chapter 3, we choose

$$\bar{n} < M \tag{2.84}$$

Then, in Molodenskii's method the undulation is computed as (ibid, eq. (95)):

$$\hat{N}_3 = \frac{R}{4\pi\gamma} \iint_{\sigma_c} S_3(\cos\psi)\hat{\Delta}g^T d\sigma + \frac{R}{2\gamma} \sum_{n=o}^{\bar{n}} W_{3n}\hat{\Delta}g_n^s + \frac{R}{2\gamma} \sum_{n=\bar{n}+1}^{M} Q_{3n}\hat{\Delta}g_n^s \tag{2.85}$$

The components of the global mean square error from (2.28) - (2.31) and (2.69), (2.71), (2.80), and (2.83) are:

$$\overline{\delta N_3^2}_{,1} = \left(\frac{R}{2\gamma}\right)^2 \left[\sum_{n=0}^{\bar{n}} (X_{3n} - W_{3n})^2 \sigma_n + \sum_{n=\bar{n}+1}^{n_T} \left(\frac{2}{n-1} - Q_{3n}\right)^2 \sigma_n \right] \qquad (2.86)$$

(propagation error)

$$\overline{\delta N_3^2}_{,2} = \left(\frac{R}{2\gamma}\right)^2 \sum_{n=n_T+1}^{\infty} \left(\frac{2}{n-1} - Q_{3n}\right)^2 C_n \qquad \text{(discretion error)} \qquad (2.87)$$

$$\overline{\delta N_3^2}_{,3} = \left(\frac{R}{2\gamma}\right)^2 \left[\sum_{n=0}^{\bar{n}} W_{3n}^2 \delta C_n + \sum_{n=\bar{n}+1}^{M} Q_{3n}^2 \delta C_n \right] \qquad \text{(commission error)} \qquad (2.88)$$

$$\overline{\delta N_3^2}_{,4} = \left(\frac{R}{2\gamma}\right)^2 \sum_{n=M+1}^{\infty} Q_{3n}^2 C_n \qquad \text{(ommission error)} \qquad (2.89)$$

The total global RMS error is

$$\overline{\delta N_3} = (\overline{\delta N_3^2}_{,1} + \overline{\delta N_3^2}_{,2} + \overline{\delta N_3^2}_{,3} + \overline{\delta N_3^2}_{,4})^{1/2} \qquad (2.90)$$

2.3.2 Modified Sjöberg's Method

Proceeding as in Molodenskii's method, we have that

$$W_4(\cos\psi) = \sum_{k=0}^{\bar{n}} \frac{2k+1}{2} W_{4k} P_k(\cos\psi) \qquad (2.91)$$

is the function to be subtracted from the Stokes' function $S(\cos\psi)$. Then

$$S_4(\cos\psi) = S(\cos\psi) - \sum_{k=0}^{\bar{n}} \frac{2k+1}{2} W_{4k} P_k(\cos\psi) \qquad (2.92)$$

or $$S_4(\cos\psi) = \sum_{n=0}^{\infty} \frac{2n+1}{2} X_{4n} P_n(\cos\psi) \qquad (2.93)$$

with

$$X_{4n} = \begin{cases} -W_{4n} & 0 \leq n \leq 1 \\ \dfrac{2}{n-1} - W_{4n} & 2 \leq n \leq \bar{n} \\ \dfrac{2}{n-1} & \bar{n} < n < \infty \end{cases} \qquad (2.94)$$

Finally

$$\bar{S}_4(\cos\psi) = \begin{cases} 0 & 0 \leq \psi \leq \psi_0 \\ S_4(\cos\psi) & \psi_0 < \psi \leq \pi \end{cases} \tag{2.95}$$

and

$$Q_{4n} = \int_{-\pi}^{\pi} \bar{S}_4(\cos\psi)P_n(\cos\psi)d\psi = \int_{-1}^{1} \bar{S}_4(y)P_n(y)dy =$$

$$= \int_{-1}^{y_0} S_4(y)P_n(y)dy = \int_{-1}^{y_0}(S(y) - \sum_{k=0}^{\bar{n}} \frac{2k+1}{2} W_{4k}P_k(y))P_n(y)dy \quad \text{or}$$

$$Q_{4n} = Q_{1n} - \sum_{k=0}^{\bar{n}} \frac{2k+1}{2} W_{4k}e_{kn} \tag{2.96}$$

with e_{kn} from (2.73) - (2.76).

Now, in general, $Q_{4n} \neq 0$, $0 \leq n \leq \bar{n}$, but $W_{4n} = 0$ for $\bar{n} < n \leq M$ since we again choose (see Chapter 3) $\bar{n} < M$. Using the general formulation discussed in Section 2.1, we compute the undulation according to (eq. (2.14))

$$\hat{N}_4 = \frac{R}{4\pi\gamma} \iint_{\sigma_c} S_4(\cos\psi)\hat{\Delta}g^T d\sigma + \frac{R}{2\gamma} \sum_{n=0}^{\bar{n}} (Q_{4n} + W_{4n})\hat{\Delta}g_n^s + \frac{R}{2\gamma} \sum_{n=\bar{n}+1}^{M} Q_{4n}\hat{\Delta}g_n^s \tag{2.97}$$

with the components of the global mean square error from (2.28) - (2.31):

$$\overline{\delta N_4^2}_{,1} = \left(\frac{R}{2\gamma}\right)^2 \left[\sum_{n=0}^{\bar{n}} (X_{4n} - Q_{4n})^2\sigma_n + \sum_{n=\bar{n}+1}^{n_T} \left(\frac{2}{n-1} - Q_{4n}\right)^2 \sigma_n\right]$$

(propagation error) (2.98)

$$\overline{\delta N_4^2}_{,2} = \left(\frac{R}{2\gamma}\right)^2 \sum_{n=n_T+1}^{\infty} \left(\frac{2}{n-1} - Q_{4n}\right)^2 C_n \quad \text{(discretion error)} \tag{2.99}$$

$$\overline{\delta N_4^2}_{,3} = \left(\frac{R}{2\gamma}\right)^2 \left[\sum_{n=0}^{\bar{n}} (Q_{4n} + W_{4n})^2 \delta C_n + \sum_{n=\bar{n}+1}^{M} Q_{4n}^2 \delta C_n \right]$$

(commission error) (2.100)

$$\overline{\delta N_4^2}_{,4} = \left(\frac{R}{2\gamma}\right) \sum_{n=M+1}^{\infty} Q_{4n}^2 C_n \qquad \text{(ommision error)} \qquad (2.101)$$

and the total mean square error:

$$\overline{\delta N_4^2} = \overline{\delta N_4^2}_{,1} + \overline{\delta N_4^2}_{,2} + \overline{\delta N_4^2}_{,3} + \overline{\delta N_4^2}_{,4} \qquad (2.102)$$

In Meissl's method care is taken for the kernel $\bar{S}_2(\cos\psi)$ to be continuous at $\psi = \psi_0$; in Molodenskii's method the norm of the approximation of $S(\cos\psi)$ through $W_3(\cos\psi)$ is minimized (eq. (2.79)). In this method, the brilliant idea, due to Sjöberg (1986a) to directly minimize the expression of the mean square error (2.102) is utilized:

$$\overline{\delta N_4^2} \longrightarrow \text{minimum} \qquad (2.103)$$

To minimize (2.102) the partials are to be taken with respect to (up till now) arbitrary coefficients W_{4n}:

$$\frac{\partial(\overline{\delta N_4^2})}{\partial W_{4k}} = 0 \qquad k = 0, 1, \ldots, \bar{n} \qquad (2.104)$$

Notice that the coefficients Q_{4n} are also linear functions of W_{4n} through eq. (2.96). The algebra will be given in Appendix A. We give the final result of the equations (2.104). They are equivalent to the linear system:

$$\sum_{t=0}^{\bar{n}} a_{kt} W_{4t} = h_k; \quad k = 0, 1, \ldots, \bar{n} \qquad (2.105)$$

$$\text{where } a_{kt} = a_{tk} = (\sigma_t + \delta C_k)\delta_{kt} - \frac{2k+1}{2} e_{kt} (\sigma_t + \delta C_t)$$

$$- \frac{2t+1}{2} e_{kt} (\sigma_k + \delta C_k)$$

$$+ \frac{2k+1}{2} \frac{2t+1}{2} \left[\sum_{n=0}^{M} e_{tn}e_{kn}(\sigma_n + \delta C_n) \right.$$

$$\left. + \sum_{n=M+1}^{n_T} e_{tn}e_{kn}(\sigma_n + C_n) + \sum_{n=n_T+1}^{\infty} e_{tn}e_{kn}(C_n + C_n) \right] \qquad (2.106)$$

$$\text{and } h_k = \frac{2k+1}{2} \left[\sum_{n=0}^{M} e_{kn}[Q_{1n}(\sigma_n + \delta C_n) - X_{1n}\sigma_n] \right.$$

$$+ \sum_{n=M+1}^{n_T} e_{kn}[Q_{1n}(\sigma_n + C_n) - X_{1n}\sigma_n]$$

$$\left. + \sum_{n=n_T+1}^{\infty} e_{kn}[Q_{1n}(C_n + C_n) - X_{1n}\sigma_n] \right] + X_{1k}\sigma_k - Q_{1k}(\sigma_k + \delta C_k) \qquad (2.107)$$

Kroenecker's δ_{kt} is defined as $\delta_{kt} = \begin{cases} 0 & k \neq t \\ 1 & k = t \end{cases}$

The computation of W_{4n} coefficients is achieved by inverting the (symmetric) matrix $A = \begin{bmatrix} a_{11} & \cdots & \cdots \\ \vdots & a_{kk} & \vdots \\ \cdots & \cdots & a_{nn} \end{bmatrix}$ and multiplying the result by the vector $H = [h_1 \ \ldots \ h_k \ \ldots \ h_n]^T$:

$$[W_{41} \ W_{42} \ \ldots \ W_{4n}]^T = A^{-1}H \qquad (2.108)$$

Once the W_{4n} coefficients are computed, the X_{4n} coefficients are computed backwards through (2.94), the Q_{4n} through (2.96) and finally the undulation through (2.97) and it's global mean square error components through (2.98) - (2.102).

CHAPTER III

ERROR ANALYSIS

In this chapter the numerical application of the formulas giving the global RMS undulation error for all the four methods will be examined: Formulas (2.41) - (2.44) for Stokes' method; (2.61) - (2.64) for Meissl's method; (2.85) - (2.89) for Molodenskii's method; (2.98) - (2.102) for modified Sjöberg's method. Irrespectively of which method will be the most precise (i.e. will give the smallest global RMS undulation error), all the methods will be considered for the actual geoid computations.

It is clear by examining the global RMS error formulas for all the methods discussed in the previous chapter that we need models for the error anomaly degree variances due to the errors of both the $\theta^{\circ}x\theta^{\circ}$ terrestrial gravity anomalies (σ_n) and the potential coefficients (δC_n) to numerically apply the formulas. Also, the anomaly degree variances (C_n) are required, and they are modeled as discussed before (eq. (2.18)) according to the Tscherning-Rapp model.

The anomaly degree variances are used to compute the ommission error for the degrees $M<n<\infty$ and the discretion error for degree $n_T<n<\infty$. We here list some values of the anomaly degree variances C_n of the Tscherning-Rapp model (Table 1), for high degrees.

Table 1. Anomaly Degree Variances of the Tscherning-Rapp Model ($mgal^2$).

n	$C_n(mgal^2)$
180	1.955
200	1.766
300	1.173
400	0.862
500	0.671
2000	0.098
5000	0.012

Tests using different values of A are later presented in this chapter.

The error anomaly degree variances due to erroneous potential coefficients are taken from the errors $\delta\bar{C}_{nm}$, $\delta\bar{S}_{nm}$ of the fully normalized potential coefficients of the OSU86D solution (Rapp and Cruz, 1986a). The above set of potential coefficients does not contain any zero or first order coefficients, and thus the summation when computing the commission error, will start from 2

$$\delta C_n = \gamma^2(n-1)^2 \sum_{m=0}^{n} (\delta\bar{C}_{nm}^2 + \delta\bar{S}_{nm}^2) \quad 2 \leq n \leq M \tag{3.1}$$

Notice that in writing (3.1) we assume that the errors in the potential coefficients are uncorrelated.

The numerical values of δC_n for some degrees are listed in Table 2.

Table 2. Error Anomaly Degree Variances due to the OSU86D Potential Coefficient Errors (mgal²).

n	δC_n (mgal²)
2	$0.644 \cdot 10^{-6}$
3	$0.745 \cdot 10^{-4}$
4	$0.296 \cdot 10^{-3}$
5	$0.256 \cdot 10^{-2}$
10	$0.568 \cdot 10^{-1}$
20	0.274
100	0.522
150	0.936
180	1.300

For the error anomaly degree variances due to the errors in the $\theta^\circ x\theta^\circ$ terrestrial anomalies, various error models were examined. For all the models we assumed $\hat{\Delta}g_0^I = \hat{\Delta}g^I = 0$, and thus for the computation of the propagation error (eq. (2.28)) the summation will again start from 2.

MODEL A

The error anomaly degree variances are taken from the numerical integration of the error covariance function $C_\varepsilon(\psi)$ of the 6'x10' free-air anomalies in Europe (Weber and Wenzel, 1982).

$$\sigma_n = \frac{2n+1}{\beta_n^2} \int_{\psi=0}^{\psi_{max}} C_\varepsilon(\psi) h(\psi, \psi_{max}) P_n(\cos\psi) \sin\psi d\psi \quad 2 \leq n \leq n_T \qquad (3.2)$$

where:

β_n Pellinen smoothing factors for a spherical cap equivalent to a 6'x10' block

$C_\varepsilon(\psi) = 22e^{-4\psi^\circ} + 3$ mgal² error covariance function

ψ° spherical separation in degrees

ψ_{max} maximum distance of integration = 10°

$d\psi$ step of integration = 1'

$h(\psi,\psi_{max}) = \frac{1}{2}\left[1 + \cos\frac{\pi\psi}{\psi_{max}}\right]$ Hanning smoothing window, to smooth out the side lobes produced by the limited length (10°) of the error covariance function

n_T 1800 maximum degree at the anomaly error degree variances

The above error covariance function implies an error variance $C_\varepsilon(0) = 25$ mgal² and a correlation length $\lambda = 0.°21$. The correlation length λ is defined as:

$$C_\varepsilon(\lambda) = \tfrac{1}{2}C_\varepsilon(0)$$

MODEL B

Another model proposed by Sjöberg (1986b) is based on the following form of the error covariance function:

$$C_\varepsilon(\psi) = c(1-u)\left[\frac{1}{(1-2u\cos\psi+u^2)^{\frac{1}{2}}} - 1 - u\cos\psi\right] \qquad (3.3)$$

where the coefficients u and c are computed by specifying the variance $C_\varepsilon(0)$ and the correlation length λ. Then the error degree variances are given by the closed formula:

$$\sigma_n = c(1-u)u^n \qquad 2 \leq n < \infty \qquad (3.4)$$

For this form three separate sets of $C_\varepsilon(0)$ and λ were tested:

MODEL B.1 $C_\varepsilon(0) = 25$ mgal², $\lambda = 0.°21$ (to comply with MODEL A)

MODEL B.2 $C_\varepsilon(0) = 25$ mgal², $\lambda = 0.°1$

MODEL B.3 $C_\varepsilon(0) = 25$ mgal², $\lambda = 1.°0$

The latter two models (B.2 and B.3) check the sensitivity of the global RMS undulation error with respect to the correlation length of the error covariance function.

MODEL C

In case that we assume uncorrelated errors of "a" mgal between the $\theta^{\circ}x\theta^{\circ}$ anomalies, then the error anomaly degree variances can be given by (Wichiencharoen, 1984):

$$\sigma_n = (2n+1)\frac{a^2}{4\pi}\theta^2 \qquad 2 \leq n \leq n_T \tag{3.5}$$

where θ is the blocksize in radians;

$n_T = 180/\theta^{\circ}$ θ° being the blocksize in degrees. For this model we used $\theta^{\circ} = 2/60$ (2'x2' anomalies).

Notice that the error degree variances given in (3.5) increase linearly with the degree. This does not happen with any of the models A, B.1, B.2, B.3. Numerical values of the error anomaly degree variances implied by models A, B.1, B.2, B.3 and C are listed in Table 3.

Table 3. Error Anomaly Degree Variances (in mgal^2) Implied by Models A, B.1, B.2, B.3, C.

	MODEL				
n	A	B.1	B.2	B.3	C
2	0.034	0.053	0.025	0.257	$3.38\cdot10^{-6}$
3	0.048	0.053	0.025	0.255	$4.73\cdot10^{-6}$
4	0.061	0.053	0.025	0.252	$6.05\cdot10^{-6}$
5	0.073	0.053	0.025	0.250	$7.40\cdot10^{-6}$
10	0.121	0.052	0.025	0.237	$1.42\cdot10^{-5}$
20	0.133	0.051	0.025	0.214	$2.75\cdot10^{-5}$
100	0.034	0.043	0.023	0.093	$1.35\cdot10^{-4}$
1000	0.010	0.006	0.009	$0.837\cdot10^{-5}$	$1.35\cdot10^{-3}$
1500	0.015	0.002	0.006	$0.472\cdot10^{-7}$	$2.02\cdot10^{-3}$
1800	0.037	0.001	0.004	$0.211\cdot10^{-8}$	$2.43\cdot10^{-3}$
5000	———	$0.128\cdot10^{-5}$	$0.162\cdot10^{-3}$	$0.861\cdot10^{-23}$	$6.73\cdot10^{-3}$

For comparison purposes for all the four methods we will initially use Model A. Then, models B.1, B.2, B.3, C will be tested using the

modified Sjöberg's method only.

The choice of $\bar{n}$ (see Chapter 2) to be less than the maximum degree of the potential coefficients used is discussed by Jekeli (1980, p. 33, fig. 10). Using the Molodenskii's method Jekeli showed that one obtains the lowest global RMS undulation error when $\bar{n} < M$. However the above conclusion is based on errorless gravity data:

$$\sigma_n = 0 \qquad 2 \leq n < \infty \tag{3.6}$$

Sjöberg (1986a, p. 14, fig. 2) also shows that the lowest global RMS undulation error is achieved if a "hybrid" solution is used with $\bar{n} = 20$, $M = 180$. Finally, the choice $\bar{n} = M$, in the case of the modified Sjöberg's method with $M = 180$, will require the inversion of a symmetric matrix (see eq. (2.108)) of dimension 180x180 and the computation effort does not pay back in terms of gain in precision, as it will be shown later in this chapter.

Figure 1 shows the global RMS undulation error for all the four methods for capsizes 0°, 1°, ... , 10°. The cases $\bar{n} = M = 20$ are also shown for the Molodenskii's and modified Sjöberg's methods, which for $\psi_o < 4°$ have large (greater than 70 cm) error due to the large ommission error. (For the rest of this discussion, when we use the terms "Molodenskii's method", or "modified Sjöberg's method" we will refer to the cases $\bar{n} = 20$, $M = 180$, unless otherwise stated.)

The gain in precision for all the capsizes when the modified Sjöberg's method is used is clear. This results from the fact that the

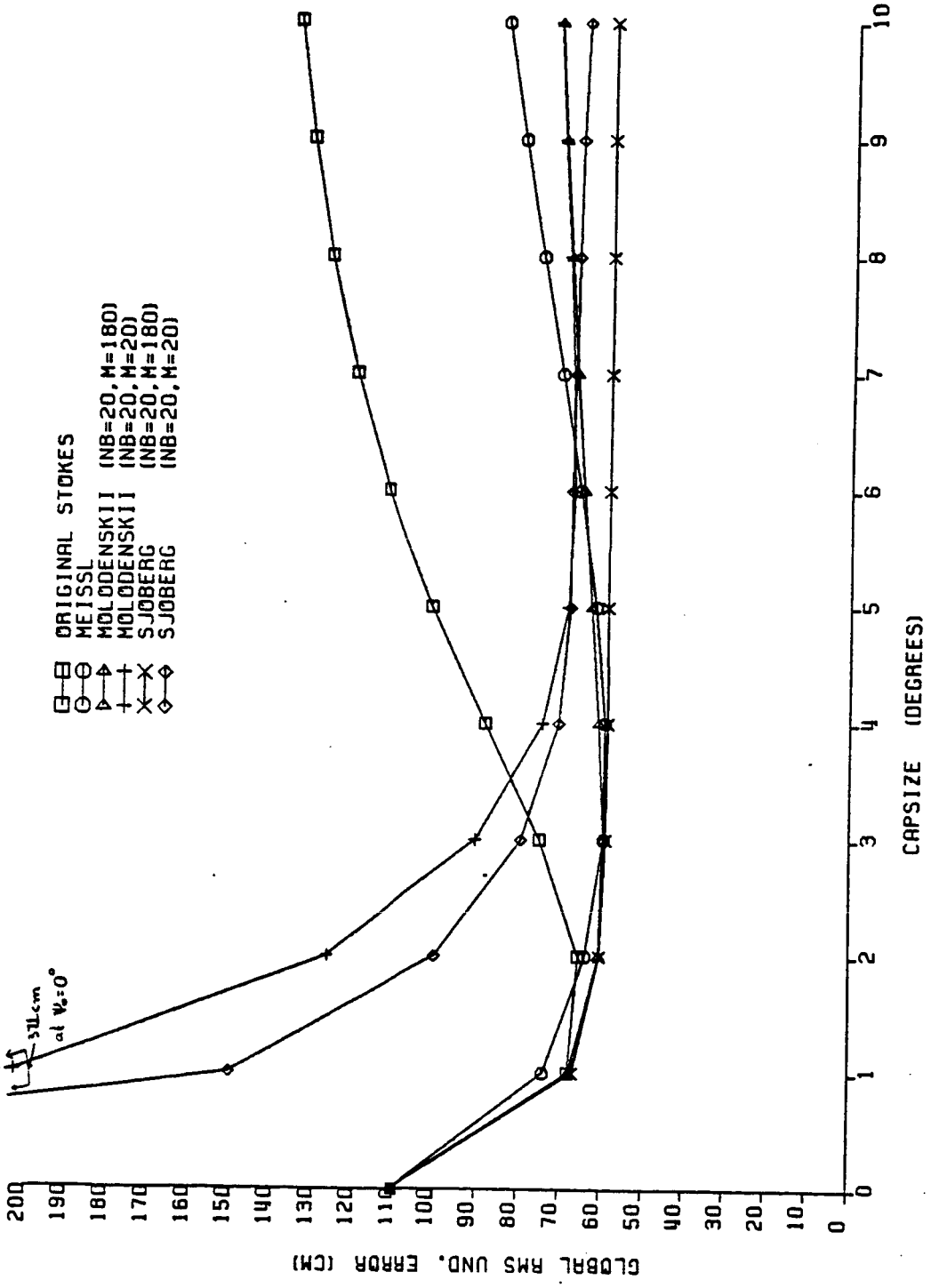

Figure 1. Global RMS Error in Undulation (in cm) for the Four Methods Using Model A for the Terrestrial Anomaly Errors and the OSU86D Potential Coefficient Errors.

modified Sjöberg's method minimizes the global mean square undulation error itself (condition (2.103)). However, this improvement in precision for the capsize of 2° is on the order of 5 cm and may or may not be realized when actual geoid computations will be carried out using the above capsize. For capsizes $0° \leq \psi_0 \leq 3°$ the Molodenskii's method is better than the Meissl's method. For capsizes $3° \leq \psi_0 \leq 6°$ the reverse happens. Then, for capsizes $6° \psi_0 \leq 10°$ the Molodenskii's method takes again the advantage. Stokes' method compares well with the other methods for $0° \leq \psi_0 \leq 2°$. For larger capsizes the global RMS error increases faster for Stokes' method than for any other method. This is due to the fact that the propagation error increases faster for Stokes' method than for any other method as the capsize increases. Notice also from the above diagram that increasing the capsize does not substantially decrease the error in the case of the modified Sjöberg's method, which is welcome when actual geoid computations are performed.

In case that we assume $\sigma_0 = \sigma_1 = \delta C_0 = 0$ (see also Chapter 10), the modified Sjöberg's method results in a singular matrix A to be inverted for $\psi_0 = 0°$. This follows immediately from the orthogonality of the Legendre's polynomials: ($y_0 = \cos 0 = 1$)

$$e_{rn} = \int_{-1}^{1} P_r(y) P_n(y) dy = 0 \qquad r \neq n \tag{3.7}$$

Then the elements of matrix A from eq. (2.106) will be:

$a_{tr} = 0$ for $t \neq r$; $a_{00} = a_{01} = a_{10} = 0$

and matrix A has two rows equal to zero. The value of the global RMS error for this case can be computed using the values of the commission

and omission error of the OSU86D set. (The propagation and the discretion error are zero). Also, matrix A is near-singular for the other nonzero capsizes (see also Colombo's method discussed in (Jekeli, 1980, p. 38), where the condition $\delta N_c = 0$ results in an ill-conditioned system of equations). Further investigation is required that will result in some type of regularization of matrix A. In Sjöberg's method the minimization of $\overline{\delta N_4^2}$ is equivalent to the minimization of the weighted sum of the residuals $V^T PV = \min$ in a traditional least squares adjustment. See also (Wenzel, 1982).

The individual error components of the modified Sjöberg's method are shown in Figure 2, and it can be seen that the major contibution to the error budget comes from the propagation and the commission error which for $\psi_0 = 3^\circ$ are on the order of 45 cm and 40 cm respectively. The omission and the discretion error are very small (less than 8 cm for $\psi_0 \leq 2^\circ$).

We then tested models A-C for the error anomaly degree variances using the modified Sjöberg's method. For these tests and for the rest of this discussion the capsize of 2° has been used, unless otherwise stated. The global RMS undulation errors due to the above models are shown in Table 4:

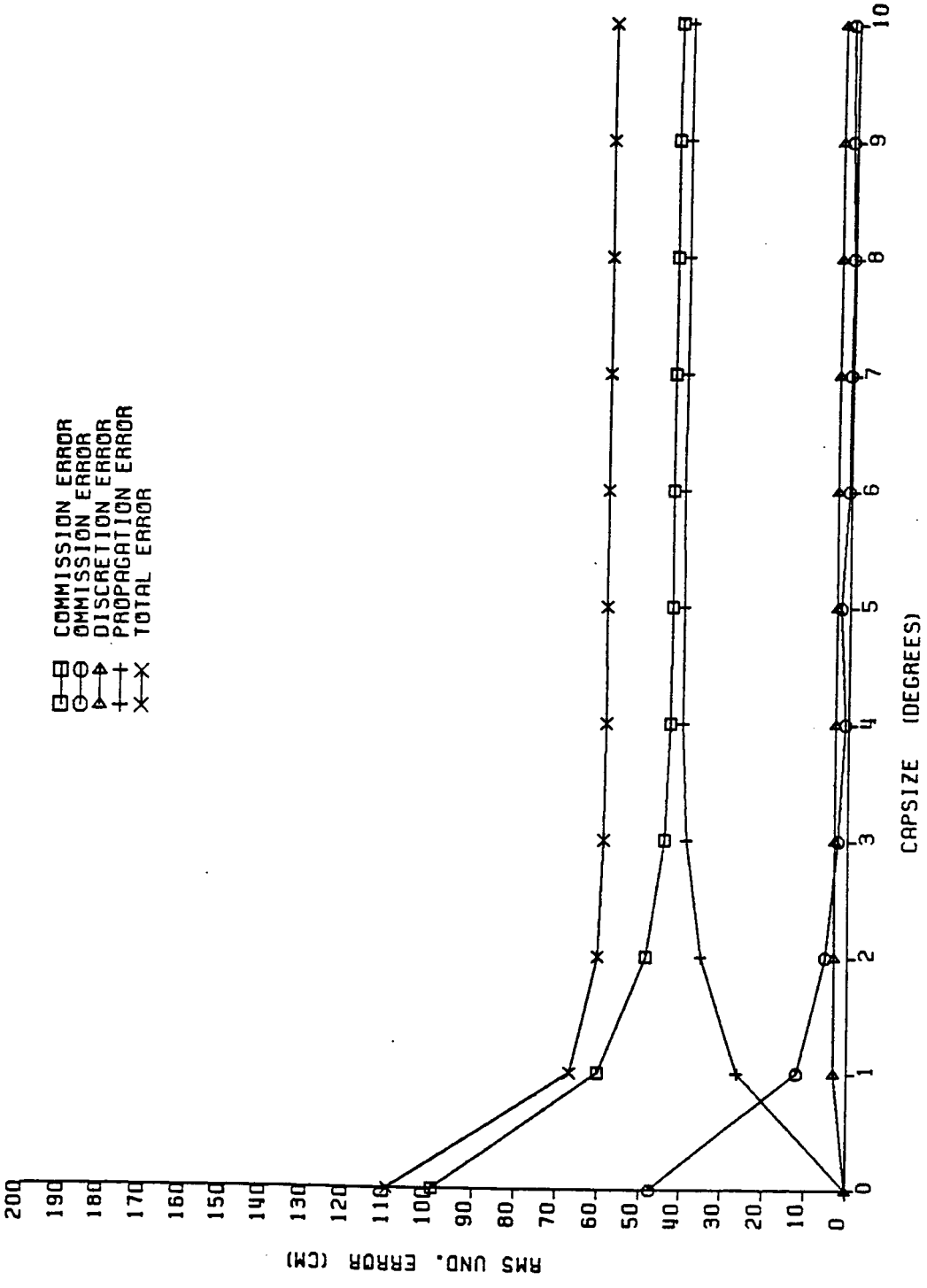

Figure 2. The Various Error Components of the Global RMS Undulation Error (in cm) for the Modified Sjöberg's Method ($\bar{n}$ = 20, M = 180). Model A for the Terrestrial Anomaly Errors and the OSU86D Potential Coefficient Errors Have Been Used.

Table 4. Global RMS Undulation Error (in cm) for the Modified Sjöberg's Method Using Different σ_n-models for Anomaly Errors.

MODEL	$\overline{\delta N}_A$ (cm)
A	60
B.1	58
B.2	53
B.3	72
C	35

We see by comparing model A and B.1 that for the same error variance $C_\varepsilon(0)$ and correlation length λ, the form of the error covariance function does not give any significant difference for the total error budget. But the correlation length plays an important role and it can increase the error from 52.70 cm (λ = 0.°1) to 72.10 cm (λ = 1°). Finally, assuming uncorrelated errors, the total error in undulation is reduced to 35.27 cm which is the most optimistic case.

The choice of the error variance $C_\varepsilon(0)$ is also a very important factor for the modified Sjöberg's method. To demonstrate this we will show results of actual geoid computations in Maui Island (located in the vicinity of Hawaii). Using eq. (2.97) with $\bar{n}$ = 20, M = 180 we computed the geoid undulation for station 7210 in Maui from 2′x2′ terrestrial and altimetric anomalies and the OSU86F set of potential coefficients. For more details see the next chapters. In Table 5 with N_c we denote the first term in (2.97) (cap contribution) and with N_p we denote the last two terms in (2.97) (i.e. contribution from the outer zone). Then $N = N_c + N_p$.

Table 5. Actual Geoid Computations in Maui (Station 7210) with the Modified Sjöberg's Method Using Different Error Variances.

	$C_\varepsilon(0)$ (mgal^2)		
	25	10	625
N_c (m)	17.80	19.17	7.38
N_p (m)	0.86	-0.48	9.43
N (m)	18.66	18.69	16.81

Results of Table 5 are to be compared with the value of 20.49 m for the undulation of the station (See chapter 4). Notice that the smaller the error variance, the larger weight will be given to the terrestrial gravity data. For the pessimistic selection of the $C_\varepsilon(0)$ to be 625 mgal^2, the value of the undulation shows a discrepancy of ~3.50 m with the value of 20.49 m, whereas for the other two selections of $C_\varepsilon(0)$ the discrepancy is ~1.80 m.

Generally, each of the four methods we examine assigns different weights to the terrestrial gravity data and to the potential coefficients. To see this, we can rewrite (2.14) as

$$N_i = \frac{R}{4\pi\gamma}\left[\iint_{\sigma} S_i(\cos\psi)\hat{\Delta}g^T d\sigma - \iint_{\sigma-\sigma_c} S_i(\cos\psi)\hat{\Delta}g^T d\sigma\right] + \frac{R}{2\gamma}\sum_{n=0}^{M}(Q_{in}+W_{in})\hat{\Delta}g^s_n$$

$$= \frac{R}{2\gamma}\left[\sum_{n=0}^{n_T}(X_{in}-Q_{in})\hat{\Delta}g^T_n + \sum_{n=0}^{M}(Q_{in}+W_{in})\hat{\Delta}g^s_n\right]$$

$$= \frac{R}{2\gamma}\left[\sum_{n=0}^{n_T}P_{in}^T\hat{\Delta}g^T_n + \sum_{n=0}^{M}P^s_{in}\hat{\Delta}g^s_n\right] \qquad (3.8)$$

Thus, the weights that are used for the terrestrial data are:

$$\bar{P}^T_{in} = \frac{P^T_{in}}{P^T_{in}+P^s_{in}} = \frac{X_{in}-Q_{in}}{X_{in}+W_{in}} \quad 0\leq n\leq n_T \qquad (3.9)$$

For the potential coefficients they are:

$$\bar{P}_{in}^{s} = \frac{P_{in}^{s}}{P_{in}^{I}+P_{in}^{s}} = 1 - \bar{P}_{in}^{I} = \frac{Q_{in}+W_{in}}{X_{in}+W_{in}} \quad 0 \leq n \leq M \tag{3.10}$$

Equations (3.9) and (3.10), in the case of Stokes' method (i=1), are valid for $n \geq 2$ and for Meissl's method (i=2) for $n \neq 1$, so that the denominators of (3.9) and (3.10) do not become zero. The weights $\bar{P}_{in}^{I}$, $\bar{P}_{in}^{s}$ for Stokes' method and $\bar{P}_{2n}^{I}$, $\bar{P}_{2n}^{s}$ for Meissl's method are determined independently of the errors of $\hat{\Delta}_g^{I}$ and $\hat{\Delta}_g^{s}$. (They are only functions of the capsize ψ_0). For the Molodehskii's method $\bar{P}_{3n}^{I}$ and $\bar{P}_{3n}^{s}$ are determined immediately after the numbers $\bar{n}$ and M are given, but, again, without any refinement that would account for errors in $\hat{\Delta}_g^{I}$, $\hat{\Delta}_g^{s}$. Only the modified Sjöberg's method gives weights that take into account the errors in $\hat{\Delta}_g^{I}$ (through σ_n) and in $\hat{\Delta}_g^{s}$ (through δC_n). This is clearly shown in Table 5. The selection of the proper model for the anomaly degree variances however does not play an important role for the modified Sjöberg's method, since this model is used to model the behavior of the anomaly spherical harmonics of high degrees only ($n > M$ for the omission error and $n > n_T$ for the discretion error). To see this we list in Table 6 the various global RMS undulation errors for the modified Sjöberg's method, when different values of A for the C_n model (see eq. (2.18)) are used:

Table 6. Influence of the A-value of the C_n Model on the Global RMS Error for the Modified Sjöberg's Method.

A (mgal^2)	$\overline{\delta N}_4$ (cm)
80.00	59
425.28	60
10000.00	65

The effect of different S-values (see eq. (2.18)) is expected to be neglibible for δN_4, but separate tests have not been carried out to show this.

We now examine the global RMS undulation error for the Molodenskii's and modified Sjöberg's method in case that a higher degree of expansion M is used for the potential coefficients. Table 7 clearly shows that increasing the degree of expansion from M = 180 to M = 250 the global RMS error remains essentially the same.

Table 7. Global RMS Undulation Error (in cm) for Molodenskii's and Modified Sjöberg's Methods Using Two Different Degrees of Expansions.

	$\overline{\delta N}$ (cm)	
METHOD	M = 180	M = 250
Molodenskii's	61	61
Modified Sjöberg's	60	60

Finally, different values of $\bar{n}$ (number of harmonics in $W_3(\psi)$ and $W_4(\psi)$) influence the global RMS error only in the case of Molodenskii's method as Table 8 shows (M = 180).

Table 8. Global RMS Undulation Error (in cm) for Molodenskii's and Modified Sjöberg's Method Using Various Numbers of Harmonics in $W_i(\psi)$.

$\bar{n}$	$\overline{\delta N_3}$	$\overline{\delta N_4}$
5	63	61
20	61	60
40	62	60
180	71	60

Table 8 shows that the combination $\bar{n}$ = 20, M = 180 gives the smallest global RMS error in the undulation in the case of Molodenskii's method. This result is in analogy with (Jekeli, 1980, p. 33, fig. 10). The improvement we obtain in the case of the modified Sjöberg's method (1 cm) is negligible and the computation effort much larger when we increase $\bar{n}$.

Summarizing, we see that the selection of the σ_n and δC_n models is critical for the modified Sjöberg's method, whereas the C_n model does not play an important role. Although we can have a reasonable δC_n model using eq. (3.1), it is very difficult to have a reasonable σ_n model for the terrestrial gravity anomalies, because for the majority of the cases, either

a) No error estimates are available, or

b) Unrealistic error estimates are given.

Even if reasonable error estimates were available for the given gravity data, the algorithms to compute the error covariance function $C_\varepsilon(\psi)$ and/or the corresponding σ_n model have not yet been developed satisfactorily: The method of computing an error covariance function by comparing two independent data bases for the same region (Weber and Wenzel, 1982) suffers from the fact that two independent data sets are rarely given for the same region since the gravity measurements are usually made once within a broad time period. On the other hand, the empirical error covariance function computation based on actual error estimates will not give a unique solution due to the plus or minus sign of the error estimates.

Finally, the selected σ_n models are only approximate and the assumption that they are valid everywhere on the earth is not rigorously true. Also, the reference surface that is associated with these models has been taken to be the sphere of radius R, or, in a first approximation, the geoid. Changing the radius of the reference surface, by several hundred meters, will cause a small change in the σ_n models and such a change will not significantly affect the error analysis. However from the theoretical point of view, it is critical to associate a surface with the selected models.

CHAPTER IV

LASER STATIONS

The coordinate system that was selected as the consistent coordinate system for defining the laser station coordinates was the SL6 system (Robbins et al., 1985). Although the laser station coordinates were also given in the SL5.1AP system (Smith et al., 1985), we selected the SL6 system as the most recent one. Initially, the geodetic coordinates (ϕ,λ,h) of 46 laser stations referred to the SL6 solution were available from Robbins et al., (1985). The station number, name and occupation of these stations are given in Table 9 (Alfano, 1986). Stations 7907 in Peru and 7929 in Brasil were immediately excluded from the list of the stations that we would finally use for geoid undulation computations due to the lack of local terrestrial gravity information. We thus retained 44 stations whose coordinates had to be transformed from the SL6 reference ellipsoid (a_e = 6378144.11 m; f = 1/298.255) to our adopted reference ellipsoid (we will call it OSU GRS: Ohio State University Geodetic Reference System) with parameters:

$$\begin{aligned} a_e &= 6378136.0 \text{ m} \\ f &= 1/298.257222101 \\ GM &= 398600.440 \text{ km}^3/\text{sec}^3 \\ \omega &= 729115 \cdot 10^{-11} \text{ rad/sec} \end{aligned} \qquad (4.1)$$

The three last parameters in (4.1) are the same as the parameters

Table 9. Laser Stations Occupation

NUMBER	NAME	OCCUPATION
7051	QUILAS	Quincy, California
7109	QUILAS	Quincy, California
7886	QUILAS	Quincy, California
7062	SANDIE	Otay Mountain, San Diego, California
7110	MONLAS	Mount Laguna, California
7082	BEARLK	Bear Lake, Utah
7084	OVRLAS	Owens Valley Radio Observatory, Big Pine, Calif.
7114	OVRLAS	Owens Valley Radio Observatory, Big Pine, Calif.
7085	GOLDLS	Goldstone, California
7115	GOLLAS	Goldstone, California
7086	FTDAVS	McDonald Observatory, Fort Davis, Texas
7885	FORLAS	McDonald Observatory, Fort Davis, Texas
7112	PLALAS	Platteville, Colorado
7887	VANLAS	Vandenberg Air Force Base, California
7888	HOPLAS	Mount Hopkins, Arizona
7921	HOPLAS	Mount Hopkins, Arizona
7894	YUMLAS	Yuma Proving Grounds, Arizona
7063	STALAS	GORF, GSFC, Greenbelt, Maryland
7064	GSFCLS	GORF, GSFC, Greenbelt, Maryland
7100	GSF100	GORF, GSFC, Greenbelt, Maryland
7101	GSF101	GORF, GSFC, Greenbelt, Maryland
7102	GSF102	GORF, GSFC, Greenbelt, Maryland
7103	GSF103	GORF, GSFC, Greenbelt, Maryland
7104	GSF104	GORF, GSFC, Greenbelt, Maryland
7105	GSF105	GORF, GSFC, Greenbelt, Maryland
7069	RAMLAS	Patrick Air Force Base, Florida
7091	HAYLAS	Haystack Observatory, Westford, Massachussets
7120	MUILAS	Lure Observatory, Mount Haleakala, Maui, Hawaii
7210	MAULAS	Lure Observatory, Mount Haleakala, Maui, Hawaii
7090	YARLAS	Yarragadee, Australia
7943	ORRLAS	Orroral Valley, Australia
7067	BDILAS	Bermuda Island
7805	FINLAS	Metsahovi, Finland
7939	MATLAS	Matera, Italy
7835	GRALAS	Grasse, France
7840	RGOLAS	Royal Greenwich Observatory, Great Britain
8833	KOOLAS	Kootwijk Observatory, Apeldoorn, Netherlands
7834	WETLAS	Wettzell, Federal Republic of Germany
7838	SHOLAS	Simosato Hydrographic Observatory, Japan
7061	EASTER	Easter Island, Chile
7068	GRKLAS	Grand Turk Island
7092	KWJLAS	Kwajalein, Marshall Islands
7096	SAMLAS	American Samoa
7121	HUANIL	Huahine, Society Island, French Polynesia
7907	ARELAS	Arequipa, Peru
7929	NATLAS	Natal, Brazil

of the GRS'80 reference ellipsoid. For the transformation of coordinates we followed the scheme (Rapp, 1985c):

$$(\phi,\lambda,h)_{SL6} \longrightarrow (x,y,z) \longrightarrow (\phi,\lambda,h)_{OSU}$$

Provided the orthometric height H of the laser station is available the value of the undulation N_T of the station is the difference

$$N_T = h - H \qquad (4.2)$$

where h is the given ellipsoidal height. The reference point for the ellipsoidal heights of the laser station was given either as a fixed marker on the ground (Bench Mark) or as the intersection of the horizontal and vertical axes of the laser instrument. Accordingly, the reference point for the orthometric height should be the same, so that the value of the undulation computed from equation (4.2) is meaningful and useful for comparisons. In case that the reference point is not the same then discrepancies up to 3.5 m (maximum vertical separation between the Bench Mark and the instrument's axis) can occur. Using the calibration information for the laser stations included in (Noll, 1983) we transformed the orthometric heights to refer either to the fixed marker or to the intersection of the instrument axis so that the orthometric and the ellipsoidal height would have the same reference point. This transformation was not possible for 11 stations because no calibration data (i.e. North-East-Up coordinates of the intersection of the instrument axis with respect to the fixed marker) was available for those stations. For the above 11 stations the orthometric heights were taken from (Alfano, 1986), and they are thought to refer to the intersection of the instrument axes.

In Table 10 we see the coordinates of the stations transformed to the OSU GRS, the orthometric height, the reference point (BM = fixed marker, IA = intersection of the laser instrument axes, UN = unknown) and the undulation computed using eq. (4.2) for the 44 laser stations. There are laser stations very close to each other (see for example the coordinates of the stations 7051, 7109 and 7886 in Quincy, California, in Table 10). It is useful to group those stations under a common name. This is shown in Table 11, where the laser stations with distances less than 100 km are grouped under the same name.

Table 11. Grouping the Laser Stations with Distances Less than 100 km

NAME	STATIONS INCLUDED
QUI	7051,7109,7886
SAN	7062,7110
OVR	7084,7114.
GOL	7085,7115
FTD	7086,7885
HOP	7888,7921
STA	7063,7064,7100,7101,7102,7103,7104,7105
HAW	7120,7210

The distribution of the 44 laser stations is shown in Figure 3 and the distribution of the 11 laser stations with unknown height references is shown in Figure 4. The accuracy of the undulation computed from equation (4.2) has not been rigorously computed, since no accuracies were available for the orthometric heights nor for the ellipsoidal heights.

Table 10. Laser Station Coordinates Referred to the OSU GRS (a_e = 6378136.0 m, f = 1/298.257222101)

NUM	NAME	LATITUDE DD	MM	SS.SSSS	LONGITUDE DD	MM	SS.SSSS	ELL.(M)	ORT.(M)	REF	UND(M)
7051	QUILAS	39	58	24.5651	239	3	37.5530	1060.9132	1083.4800	BM	-22.5668
7109	QUILAS	39	58	29.9961	239	3	18.9490	1107.2592	1129.8520	BM	-22.5928
7886	QUILAS	39	58	30.0121	239	3	18.0180	1110.5048	1129.8000	UN	-19.2952
7062	SANDIE	32	36	2.6526	243	9	32.7810	989.5260	1022.0000	BM	-32.4740
7110	MONLAS	32	53	29.9965	243	34	38.2580	1839.9153	1870.7780	BM	-30.8627
7082	BEARLK	41	56	0.8900	248	34	45.5370	1963.9328	1976.5150	BM	-12.5822
7084	OVRLAS	37	13	55.6502	241	42	15.1130	1179.0608	1203.9580	BM	-24.8972
7114	OVRLAS	37	13	57.2062	241	42	22.2150	1178.9648	1203.8060	BM	-24.8412
7085	GOLDLS	35	25	27.9573	243	6	48.9170	966.3705	996.0500	BM	-29.6795
7115	GOLLAS	35	14	53.8944	243	12	28.9490	1039.5651	1069.1450	BM	-29.5799
7086	FTDAVS	30	40	37.2987	255	59	2.4810	1962.3776	1983.1610	BM	-20.7834
7085	FORLAS	30	40	37.3007	255	59	2.4780	1962.3310	1983.1610	BM	-20.8300
7112	PLALAS	40	10	57.9951	255	16	26.3360	1502.5151	1519.9130	BM	-17.3979
7087	VANLAS	34	33	58.3514	239	29	57.9780	605.2623	636.4000	UN	-31.1377
7088	HOPLAS	31	41	6.3096	249	7	18.5000	2335.6675	2337.8690	UN	-2.2015
7921	HOPLAS	31	41	3.2166	249	7	18.8370	2353.9135	2383.3870	UN	-29.4735
7894	YUMLAS	32	56	20.9285	245	47	48.6070	242.6696	271.3000	UN	-28.6304
7063	STALAS	39	1	13.3561	283	10	19.7950	20.2032	53.1200	BM	-32.9168
7064	GSFCLS	39	1	15.0981	283	10	18.6050	18.1092	51.8260	BM	-33.6368
7100	GSF100	39	1	15.4451	283	10	47.6350	11.1462	43.6440	BM	-32.4978
7101	GSF101	39	1	16.1991	283	10	42.8350	9.3502	42.4330	BM	-33.0828
7102	GSF102	39	1	14.3741	283	10	18.7920	18.9272	51.8150	BM	-32.8878
7103	GSF103	39	1	14.6011	283	10	18.7950	18.8692	51.8030	BM	-32.9338
7104	GSF104	39	1	17.0761	283	10	36.8380	10.9342	43.8760	BM	-32.9418
7105	GSF105	39	1	14.1581	283	10	20.1580	20.1202	53.0530	BM	-32.9328
7069	PAMLAS	28	13	40.6470	279	23	39.2980	-22.6006	6.5290	BM	-29.1296
7091	HAYLAS	42	37	21.6830	288	30	44.3390	92.9496	120.5020	BM	-27.5524
7120	MUILAS	20	42	27.3880	203	44	38.1020	3068.7162	3048.2530	BM	20.4632
7210	MAULAS	20	42	25.9920	203	44	38.6000	3069.2871	3048.7980	IA	20.4891
7090	YARLAS	-29	-2	-47.4048	115	20	48.1071	242.2921	266.5680	BM	-24.2759
7943	ORRLAS	-35	-37	-29.7502	148	57	17.1240	949.8848	929.5000	UN	20.3848
7067	BOILAS	32	21	13.7566	295	20	37.9270	-22.0603	9.7510	BM	-31.8113
7805	FINLAS	60	13	2.2828	24	23	40.2110	79.1806	59.2300	IA	19.9506
7939	MATLAS	40	38	55.7871	16	42	16.6860	536.9066	490.5200	UN	46.3866
7835	GRALAS	43	45	16.8780	6	55	15.8640	1323.9484	1281.1000	UN	42.8484
7040	PGOLAS	50	52	2.5551	0	20	9.8620	76.2630	30.6000	UN	45.5830
8833	KOOLAS	52	10	42.2392	5	48	35.1190	94.4558	49.8000	UN	44.6558
7834	WETLAS	49	8	41.7711	12	52	40.9670	662.0941	614.4400	IA	47.6541
7838	SHOLAS	33	34	39.7155	135	56	13.1890	102.3687	62.4000	UN	39.9687
7061	EASTER	-27	-8	-52.1600	250	36	58.9940	118.6263	120.8810	IA	-2.2547
7068	GRKLAS	21	27	37.7669	288	52	5.0330	-17.6909	24.8440	BM	-42.5349
7092	KWJLAS	9	23	37.6871	167	28	32.4860	33.8970	1.7160	BM	32.1810
7096	SAMLAS	-14	-20	-7.5140	189	16	30.3570	49.9806	15.2950	BM	34.6856
7121	HUANIL	-16	-44	-0.6796	208	57	31.7780	48.2196	37.8680	IA	10.3516

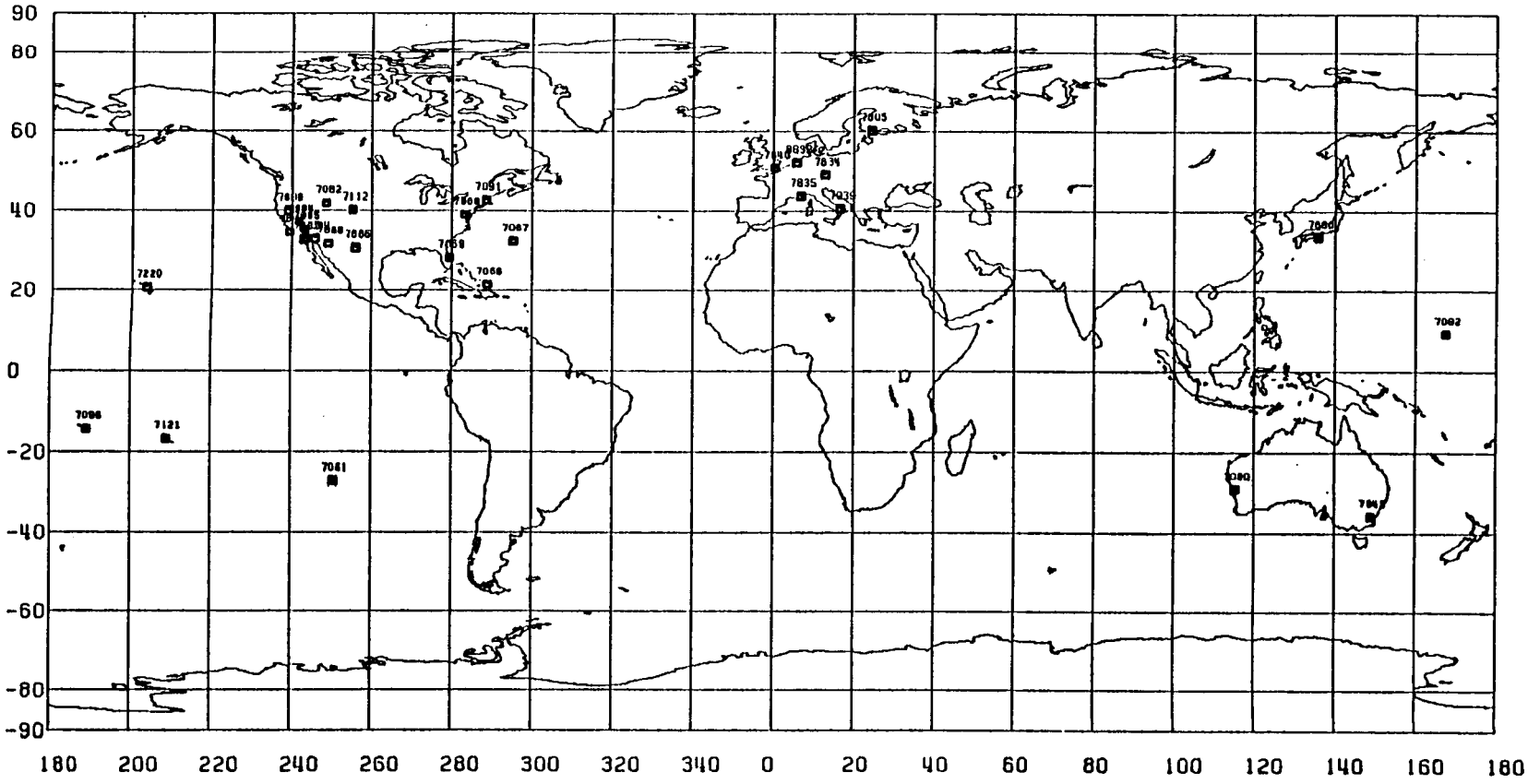

Figure 3. Distribution of the 44 Laser Stations, With Known (33 Stations) and Unknown (11 Stations) Height References.

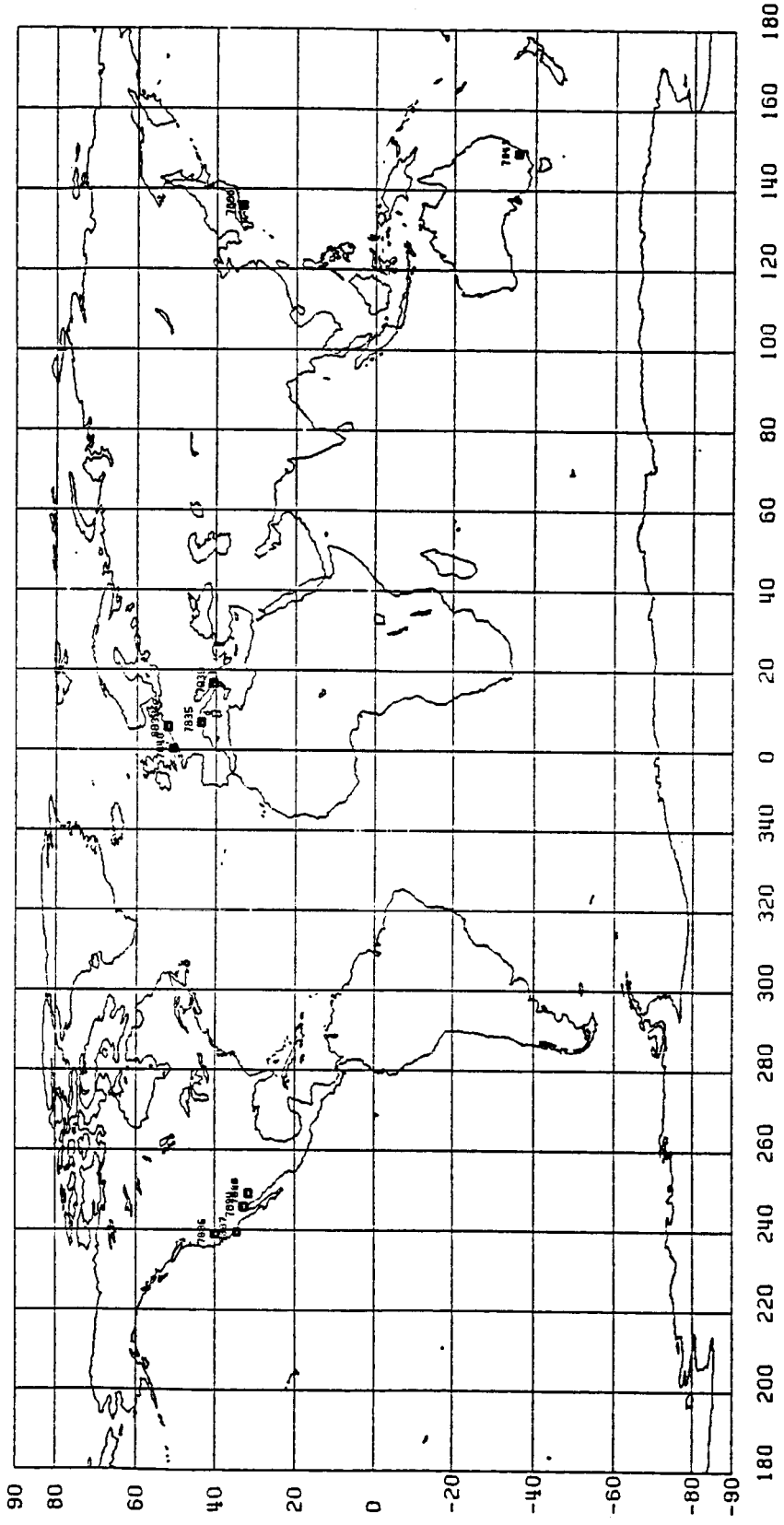

Figure 4. Distribution of the 11 Laser Stations with Unknown Height References.

CHAPTER V

GRAVITY DATA PROCESSING

5.1 Pre-processing of the Data

The terrestrial gravity sources available by region are listed in Table 12 below (Δg = free-air gravity anomaly, $\bar{\Delta g}$ = mean Δg). The third column in Table 12 shows the number of laser stations in the corresponding region.

Table 12. Gravity Sources Available by Region.

REGION	SOURCE	# of LASER STATIONS
UNITED STATES	Point Δg	27
BERMUDA	Point Δg	1
AUSTRALIA	Point Δg	2
EUROPE	6′x10′ $\bar{\Delta g}$	6
JAPAN	10′x10′ $\bar{\Delta g}$	1

The gravity sources in Australia, Europe, and Japan are discussed in (Despotakis, 1986). The point gravity anomalies in the United States, Hawaii and Bermuda have been received in 1983 from the National Geodetic Survey; the 10′x10′ mean anomalies are also described in (Ganeko, 1982); and the 6′x10′ mean anomalies are also described in (Torge et al., 1983). These gravity sources cover only 39 laser stations as Table 12 indicates. For five (7061,7068,7092,7096,7121) oceanic stations the adjusted GEOS-3 and SEASAT oceanic altimeter data (Liang, 1983)

was used. For these stations an approximate geoid undulation was computed from the altimeter sea surface heights using a standard least squares collocation method using procedures similar to (Rapp, 1985b). Numerical details will be given in Chapter 8.

Based on the error analysis results (Chapter 3, Fig. 1) the capsize for the cap contribution computations (first integral term in eq. (2.14)) was selected to be 2°. Thus, within a circle of radius 2° (with the center of the circle at the laser station) sufficient gravity data had to exist. More precisely, within the above circle we had to have full coverage of mean gravity anomalies so that the numerical integration of equation (2.14) would be possible. The gravity anomaly $\hat{\Delta}_g^I$ to be used in (2.14) has to:

a) Refer to the reference formula of normal gravity implied by the constants of the adopted reference ellipsoid (see Chapter 4, eq. (4.1));

b) Be corrected for atmospheric effect;

c) If possible, to be corrected for the terrain efffect. The undulation then has to be corrected for the indirect effect (see Section 5.2).

All the given sources (Table 12) had their free-air anomalies referred to the GRS'67 reference formula. The conversion from this formula to the formula implied by the constants of the OSU GRS will be derived if we take into account that:

$$\Delta g_{1967} = g_{obs} - \gamma_{1967} + \frac{\partial \gamma}{\partial h} h \qquad (5.1)$$

$$\Delta g_{OSU} = g_{obs} - \gamma_{OSU} + \frac{\partial \gamma}{\partial h} h \qquad (5.2)$$

where Δg_{1967}: free-air gravity anomaly referred to the GRS'67
Δg_{OSU} : free-air gravity anomaly referred to the OSU GRS
γ_{1967} : normal gravity on the GRS'67 ellipsoid
γ_{OSU} : normal gravity on the OSU GRS ellipsoid
$\frac{\partial \gamma}{\partial h}$: free-air gradient of the normal gravity
h : elevation of the station

The quantities $\partial\gamma/\partial h \cdot h$ and g_{obs} are the same for both systems. Thus, subtracting (5.1) from (5.2):

$$\Delta g_{OSU} = \Delta g_{1967} + \gamma_{1967} - \gamma_{OSU} \qquad (5.3)$$

Knowing that (International Association of Geodesy, 1971)

$$\gamma_{1967} = 978031.85(1 + a'\sin^2\phi + b'\sin^2 2\phi) \text{ mgal} \qquad (5.4)$$

with $a' = 0.0053024$ and $b' = -0.0000059$,

we can write (Heiskannen and Moritz, 1967, eqs. (2-116) and (2.105a))

$$\gamma_{OSU} = \frac{GM}{ab}\left[1 - \frac{3}{2} m - \frac{3}{14} e'^2 m\right](1 + a'\sin^2\phi + b'\sin^2 2\phi) \qquad (5.5)$$

assuming that a' and b' will be the same as in (5.4) which is correct for the decimal digits we give. We also have:

$$m = \frac{\omega^2 a^2 b}{GM}$$

and a, f, GM, ω from (4.1).

We then obtain

$$\gamma_{OSU} = 978032.83(1 + a'\sin^2\phi + b'\sin^2 2\phi) \text{ mgal} \qquad (5.6)$$

From (5.3), (5.4) and (5.6), we take:

$$\Delta g_{OSU} = \Delta g_{1967} + (978031.85 - 978032.83)(1 + 0.0053024\sin^2\phi - 0.0000059\sin^2 2\phi) \text{ mgal, or}$$

$$\Delta g_{OSU} = \Delta g_{1967} - 0.98 \text{ mgal} \qquad (5.7)$$

Thus, from the anomalies referred to the GRS'67 reference formula, we have to subtract 0.98 mgal, to convert them to the OSU GRS reference formula.

The next step is to apply the atmospheric correction to (5.7) considering the polynomial expansion of the atmospheric correction given in Wichiencharoen (1982a):

$$\delta g_A = 0.8658 - 9.727 \cdot 10^{-5} \cdot H + 3.482 \cdot 10^{-9} \cdot H^2 \qquad (5.8)$$

where H is the elevation of the station, and δg_A, in mgal, is the atmospheric correction computed truncating (5.8) to the second term and giving an approximate value $\bar{H}$ for the elevation of the station. Then the free-air anomalies to be used in equation (2.14) were computed as:

$$\hat{\Delta}_g^I = \Delta g_{OSU} + \delta g_A \qquad (5.9)$$

The above procedure applied to both point and mean Δg given from the various sources listed in Table 12.

To determine the coverage of the gravity anomalies surrounding the laser stations, windows of $\Delta\phi = 5^\circ$ in latitude and $\Delta\lambda$ = INTEGER($5^\circ/\cos\phi$) + 1° in longitude (ϕ: latitude of the laser station) centered at the laser stations were used. Full coverage and mean anomalies (as it was the case with the anomalies surrounding stations 7838 in Japan and 8833, 7834 in Europe) did not require any further process. Insufficient coverage and mean anomalies (as it was the case with the anomalies surrounding stations 7805,7939,7835 and 7840 in Europe) required that we fill-in the gaps. For this purpose we used the OSU86F (Rapp and Cruz, 1986b) potential coefficient set up to degree 360 to compute the

missing $\overline{\Delta g}$ as the point Δg evaluated at the centers of the 6′x10′ empty cells through the formula:

$$\Delta g = \frac{GM}{r^2} \sum_{n=2}^{360} (n-1) \left(\frac{a}{r}\right)^n \sum_{m=0}^{n} (\bar{C}_{nm}\cos m\lambda + \bar{S}_{nm}\sin m\lambda)\bar{P}_{nm}(\sin\bar{\Phi}) \qquad (5.10)$$

where: GM,a : the constants of the OSU GRS given in (4.1)

$\bar{C}_{nm}$,$\bar{S}_{nm}$: the fully normalized potential coefficients of the OSU86F solution; the $\bar{C}_{20}$, $\bar{C}_{40}$ and $\bar{C}_{60}$ refer to the OSU GRS

$\bar{P}_{nm}(\sin\bar{\Phi})$: the fully normalized associated Legendre functions; $\bar{\Phi}$ is the geocentric latitude of the computation point

r : the geocentric radius to the computation point

λ : the longitude of the computation point.

An example of a case with insufficient coverage of the 6′x10′ $\overline{\Delta g}$ is shown in Figure 5 for station 7805 in Finland. The dots represent available 6′x10′ $\overline{\Delta g}$ and the dashes represent fill-in anomalies using the OSU86F field as described above.

The point gravity anomalies surrounding the laser stations in the United States, Hawaii, Bermuda and Australia were transformed to 2′x2′ mean anomalies using interpolation techniques (collocation or weighted average) that are discussed in Section 5.2. For the application of the collocation method using the five closest points it is necessary that the matrix $(C_{ij} + D_{ij})$ is non-singular (see Section 5.2, eq. (5.11)). If the five closest points are very close to each other, which was the case for most of the distributions of the given point anomalies, then the above matrix becomes singular. To avoid this, a thinning procedure was applied to the originally available point anomalies. This procedure was

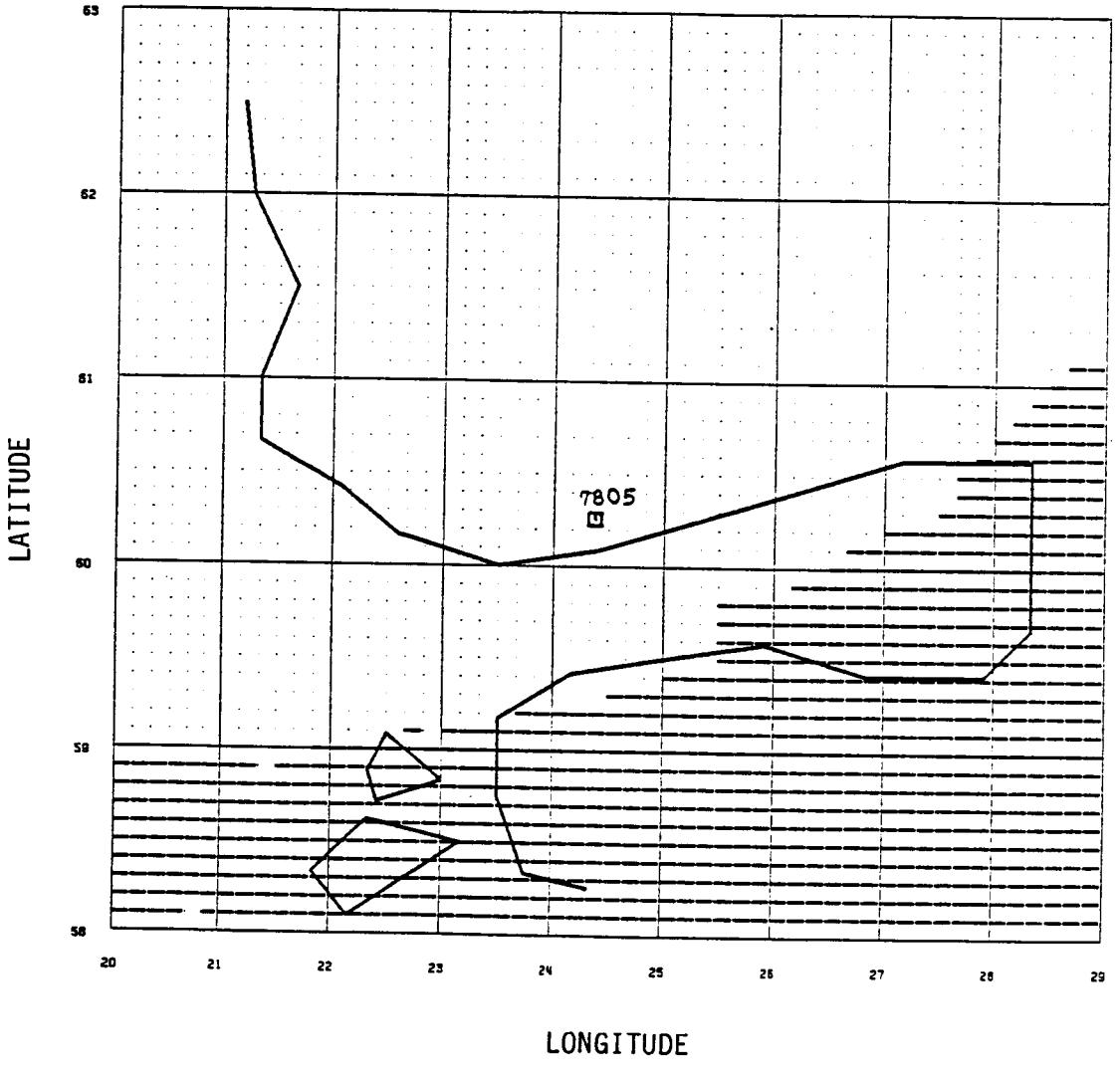

Figure 5. Example of Insufficient Coverage of the 6′x10′ $\overline{\Delta g}$ Surrounding Station 7805 in Finland. Dots Represent Originally Available 6′x10′ $\overline{\Delta g}$ and Dashes Represent Fill-in 6′x10′ $\overline{\Delta g}$ Using the OSU86F Potential Coefficient Set Up to Degree 360.

as follows: For each 2′x2′ cell in which the whole area was subdivided; one value, the one which was closest to the center of the 2′x2′ cell was kept. The thinned data set created this way was then examined to ensure sufficient coverage. If the coverage was sufficient, the prediction of the 2′x2′ $\overline{\Delta g}$ was done as discussed in Section 5.2. An example of such coverage for station 7082 in Bear Lake, Utah is shown on Figure 6. The dots represent the point anomalies of the thinned data set. If the coverage was not sufficient (i.e. areas larger than 1°x1° were completely empty), then

a) For coastal stations or stations on islands the 0.°125 x 0.°125 altimeter anomalies of the world data base described in (Rapp, 1985b) was used to fill-in the empty areas. Examples of this case are shown in Figure 7 for a coastal station (station 7887 in Vandenberg, California) and in Figure 8 for the stations 7120,7210 on the island of Maui. The dots represent point Δg.

b) For continental stations, for which no altimeter anomalies were available, the fill-in anomalies were generated at the centers of the missing 2′x2′ cells using eq. (5.10) as described above. Figure 9 illustrates an example of such a case for stations 7888, and 7921 in Mount Hopkins, Arizona. The dots represent point Δg.

After the fill-in procedures, the 2′x2′ $\overline{\Delta g}$ were predicted as discussed in Section 5.2. The thinning procedure was not applied to the data surrounding station 7067 in Bermuda (see Section 5.3).

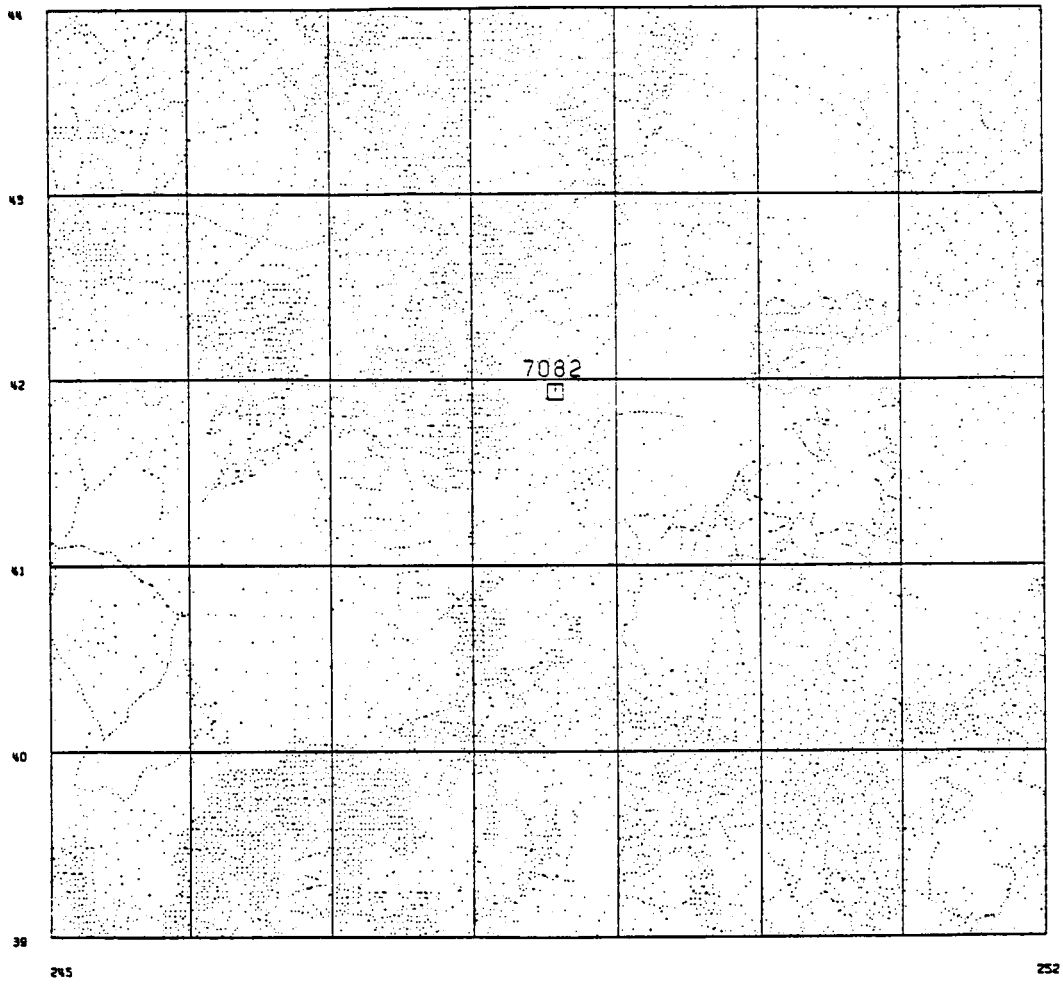

Figure 6. Example of Sufficient Coverage of Point Δg Surrounding Station 7082 in Bear Lake, Utah. The Dots Represent Point Δg.

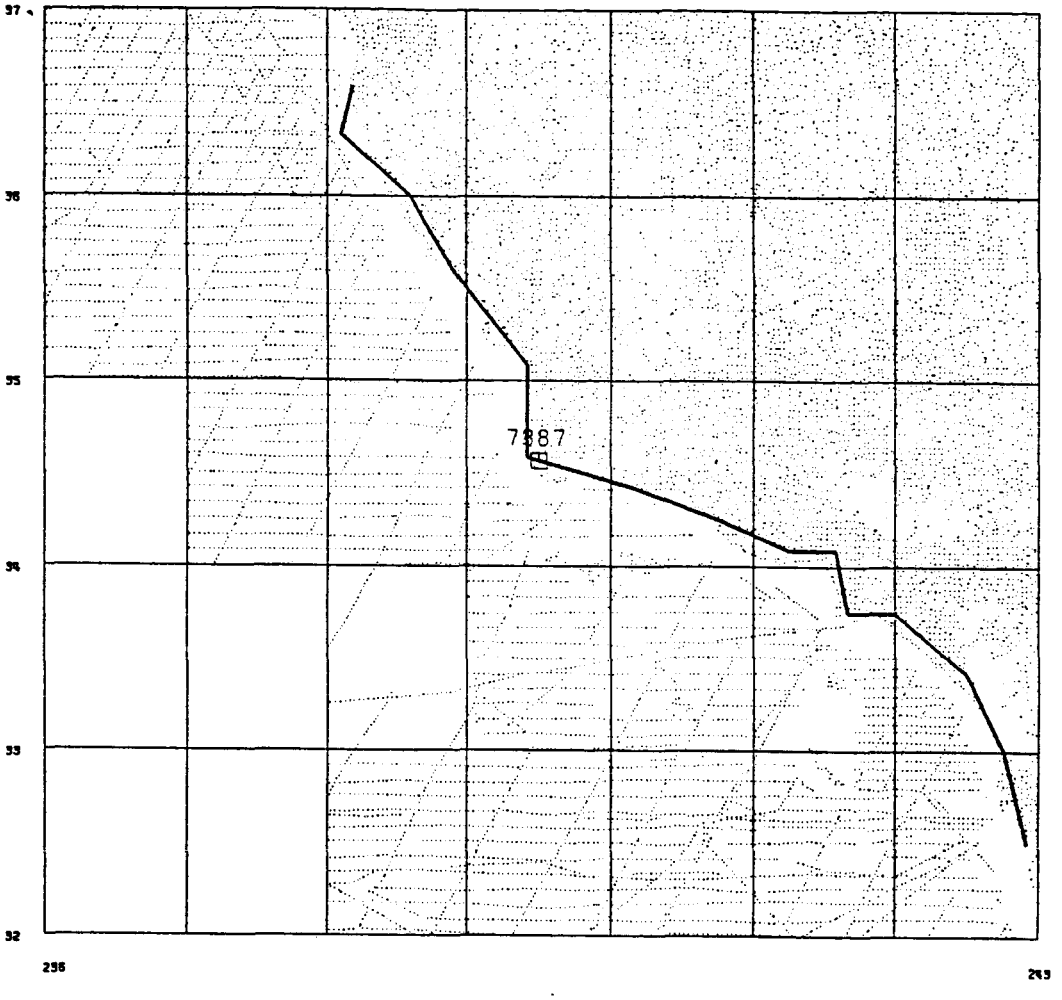

Figure 7. Example of Insufficient Coverage of Point Δg at the Coastline Station 7887 in Vandenberg, California. The Dots Represent Point Δg.

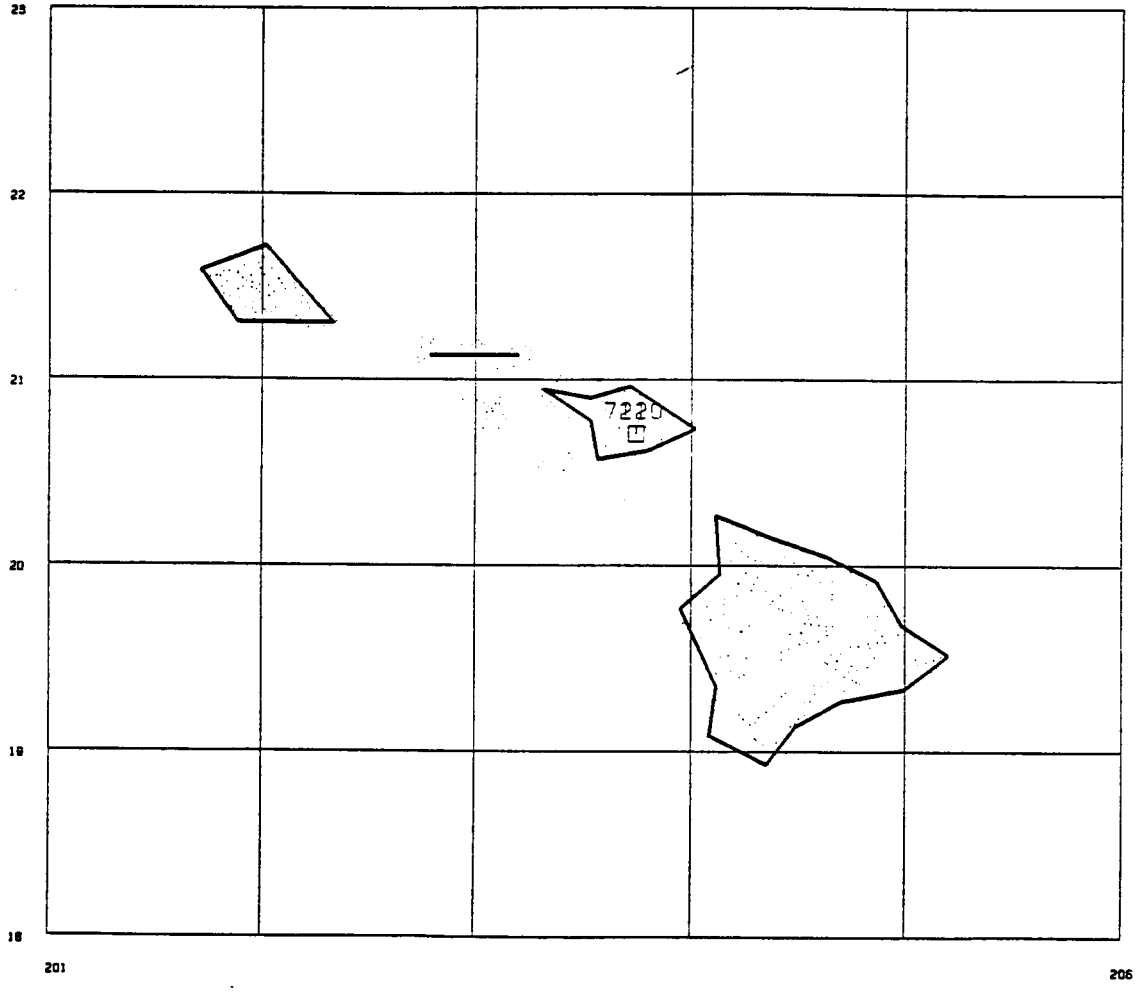

Figure 8. Example of Insufficient Coverage of Point Δg at the Two Stations 7120, 7210 in the Vicinity of Hawaii. The Dots Represent Point Δg.

Figure 9. Example of Insufficient Coverage of Point Δg For the Continental Stations 7888, 7921 on Mount Hopkins, Arizona. The Dots Represent Point Δg.

Some statistics concerning the terrestrial gravity data processing are shown in Table 13. The first column is the number or the name of the region (in case of groups of stations within the same region, see Chapter 4). The second column is the $\Delta\lambda$ dimension selected for each window surrounding the laser station. The third column shows the number of point or mean Δg available for each region before ((1)) and after ((2)) the thinning. If no thinning was applied to the data (e.g. $6'x10'$ $\overline{\Delta g}$ data) this column is left blank ("—"). The fourth column represents the fill-in procedure chosen: A "—" means that no fill-in anomalies were used; "P" means that the fill-in anomalies were taken from the OSU86F potential coefficient set and "A" means that the $0^{\circ}.125$ x $0^{\circ}.125$ altimeter anomalies were used to fill-in the gaps. The fifth column gives the final gridded form (or equivalently: the blocksize of the mean anomalies) in which the original data were transformed to for the numerical integration. The sixth and seventh columns give the variance and the arithmetic mean of the final mean anomalies over the sample area.

For each grid cell the anomaly was computed from (5.10) using the OSU86F potential coefficients up to degree 180 and then the arithmetic mean over the sample area of those anomalies was computed. This mean is shown in column eight. Finally, column nine gives the mean elevation that was used for each particular window for the atmospheric effect computation through equation (5.8).

Table 13. Information Concerning the Terrestrial Gravity Data Processing.

# OR NAME	Δλ (Degs)	# OF Δg OR $\overline{\Delta g}$ (1)	(2)	FILL IN	GRIDDED FORM	VAR [mgal²]	$\bar{X}$ [mgal]	$\bar{X}_P$ [mgal]	$\bar{H}$ [m]
QUI	6	43915	13531	—	2′x2′	1902.29	7.93	6.13	500
SAN	6	62506	10359	P	2′x2′	1231.22	-11.21	- 9.71	500
7082	7	18654	9882	—	2′x2′	1901.87	5.55	16.26	1000
OVR	6	39966	14081	—	2′x2′	2191.67	2.84	2.01	700
GOL	6	52428	14496	—	2′x2′	2288.04	- 6.32	- 5.70	700
FTD	6	12166	5961	—	2′x2′	518.89	- 0.38	4.58	1000
7112	7	26953	11150	—	2′x2′	1353.25	16.75	16.53	1000
7887	7	96744	14345	A	2′x2′	1462.18	-13.6	-14.15	500
HOP	6	13343	5447	P	2′x2′	435.85	- 9.07	- 7.08	1000
7894	6	23765	7296	P	2′x2′	849.12	-10.94	- 7.28	100
STA	6	29561	11705	—	2′x2′	513.82	- 3.21	- 1.09	300
7069	5	43186	5986	A	2′x2′	415.67	5.57	2.79	100
7091	7	31095	10357	A	2′x2′	336.75	0.89	2.84	100
HAW	5	715	458	A	2′x2′	10802.81	25.30	23.79	100
7067	6	15731	—	A	2′x2′	705.18	-11.00	-11.33	0
7805	9	1859	—	P	6′x10′	293.95	-15.95	-15.71	500
7939	7	1886	—	P	6′x10′	2927.86	15.33	15.39	500
7835	6	1747	—	P	6′x10′	2429.60	9.29	8.89	1000
7840	7	1804	—	P	6′x10′	128.03	- 4.16	- 1.87	300
8833	8	2400	—	—	6′x10′	344.54	- 0.68	1.81	100
7834	8	2400	—	—	6′x10′	686.79	21.91	21.32	300
7838	6	1080	—	—	10′x10′	1550.13	22.87	25.42	—
7090	6	11835	4091	A	2′x2′	920.58	-11.85	-12.75	100
7943	6	9804	4730	A	2′x2′	1645.25	14.01	17.33	500

Some blunders (e.g. point anomalies of 1700 mgals) were found for some regions in the western United States, but they were easily removed by applying an editing method (i.e. delete the values of the point anomalies if they are outside certain specified limits). Thus the conclusion is that editing of the data is necessary, especially when we deal with large amounts of data, to avoid any blunders that the data may contain.

5.2 Gravity Predictions

For the transformation of the randomly distributed data points (see Figure 9 for example) into a gridded form of 2′x2′ $\overline{\Delta g}$, predictions of the 2′x2′ $\overline{\Delta g}$ had to be carried out based on the thinned data covering the areas surrounding the laser stations and merged whenever necessary with either the altimeter data or the OSU86F anomalies, as discussed in the previous Section. Two basic types of prediction methods were considered (Cruz, 1983):

a) Collocation method: The 2′x2′ $\overline{\Delta g}$ were computed as the point Δg at the centers of the 2′x2′ cells based on the five closest Δg to the $\overline{\Delta g}$ to be predicted as follows:

$$\hat{\Delta}_g^I = C_{pj}(C_{ij} + D_{ij})^{-1}(\Delta g_i - \overline{\Delta g}) + \overline{\Delta g} \qquad (5.11)$$

where: $\hat{\Delta}_g^I$ is the predicted point value at the center of the 2′x2′ cell (=2′x2′ $\overline{\Delta g}$)

Δg_i is the 5x1 vector of the closest five anomalies to the predicted point

$$\overline{\Delta g} = \sum_{i=1}^{5} \Delta g_i/5$$

D_{ij} is a 5x5 diagonal matrix of the noise of the five data points

$C_{pj} = C_{pj}(\psi)$: 1x5 covariance matrix between the prediction point and the five data points

$C_{ij} = C_{ij}(\psi)$: 5x5 variance covariance matrix between the five data points

ψ: spherical separation.

To compute matrices $C_{pj}(\psi)$ and $C_{ij}(\psi)$ the covariance function based on the Tscherning-Rapp model for the anomaly degree variances (see eq. (2.18)) scaled to reflect the variance of the thinned and/or merged point data with the mean removed was used. Some test computations were carried out using empirical covariance functions but this method is computationally extremely expensive, due to the large number of data involved (see Table 13), and thus was not considered for the final predictions.

b) Bjerhammar method (ibid, p. 15): The 2'x2' $\overline{\Delta g}$ were computed as the point Δg at the centers of the 2'x2' cells based on the five closest Δg to the $\overline{\Delta g}$ to be predicted as follows:

$$\hat{\Delta}_g^T = \sum_{i=1}^{5} \frac{\Delta g_i}{\ell_i} \Big/ \sum_{i=1}^{5} \frac{1}{\ell_i} \qquad (5.12)$$

where: ℓ_i is the distance between the point to be predicted and the data point i (power of the prediction = 1). The predictions were also carried out using the inverse of the square of the distance as a weight (power of prediction = 2):

$$\hat{\Delta}_g^T = \sum_{i=1}^{5} \frac{\Delta g_i}{\ell_i^2} \Big/ \sum_{i=1}^{5} \frac{1}{\ell_i^2} \qquad (5.13)$$

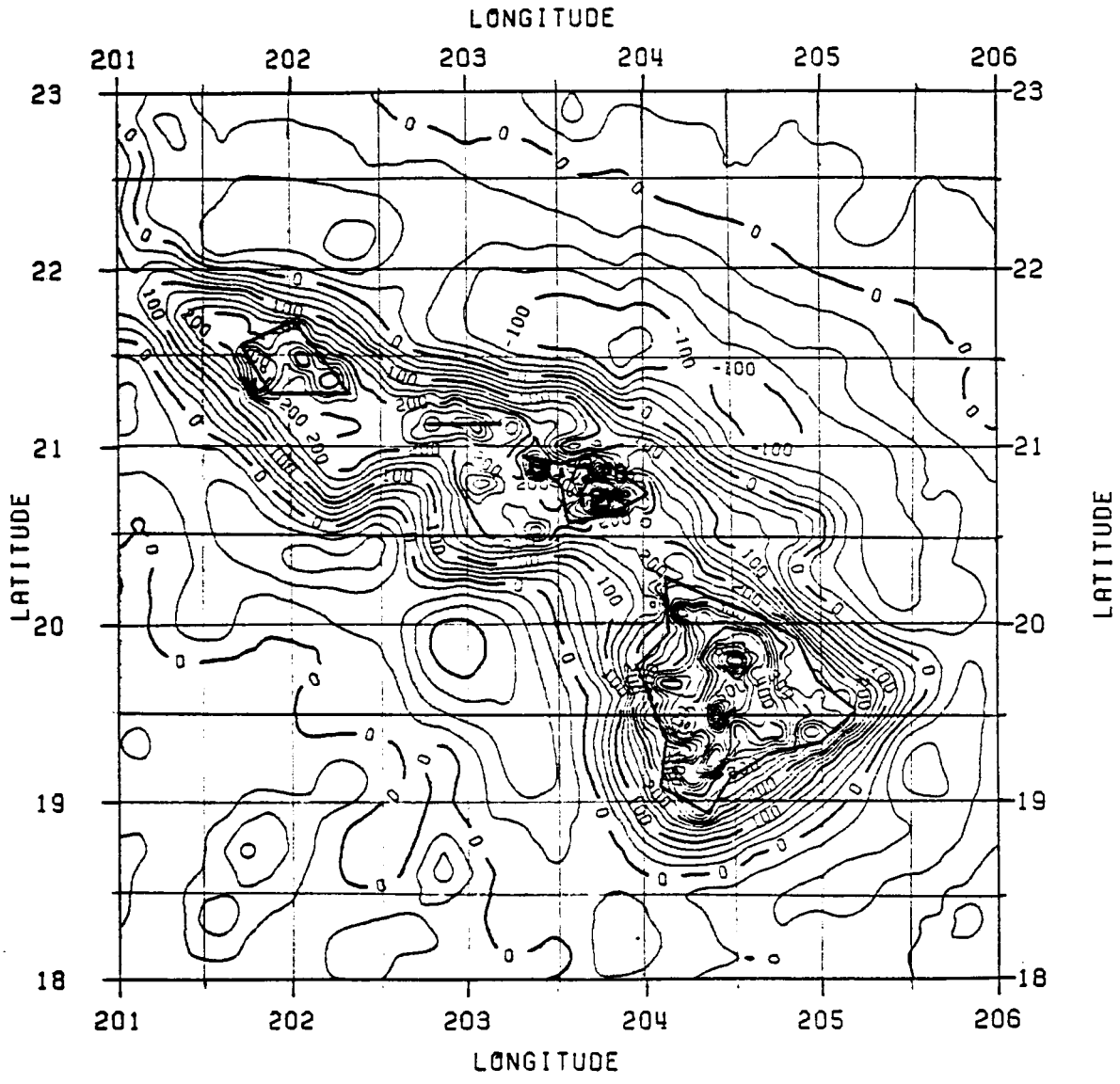

Figure 10. Gravity Predictions in the Vicinity of Hawaii Using the Five Closest Points in A Collocation Method. The Grid Spacing is 2′x2′ and the Contour Interval 25 mgal.

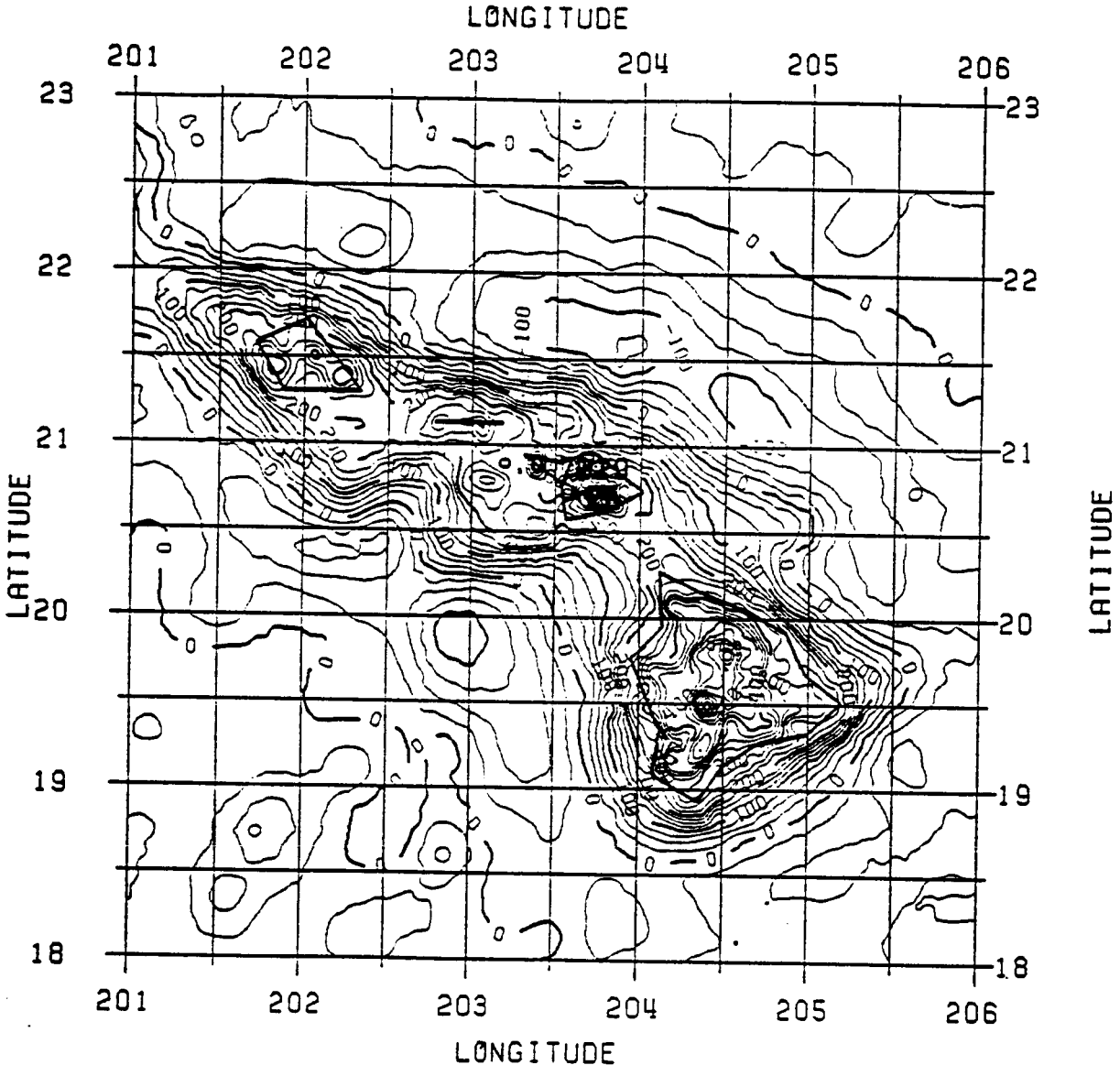

Figure 11. Gravity Predictions in the Vicinity of Hawaii Using the Five Closest Points and the Inverse of the Distance as Weight. The Grid Spacing is 2′x2′ and the Contour Interval 25 mgal.

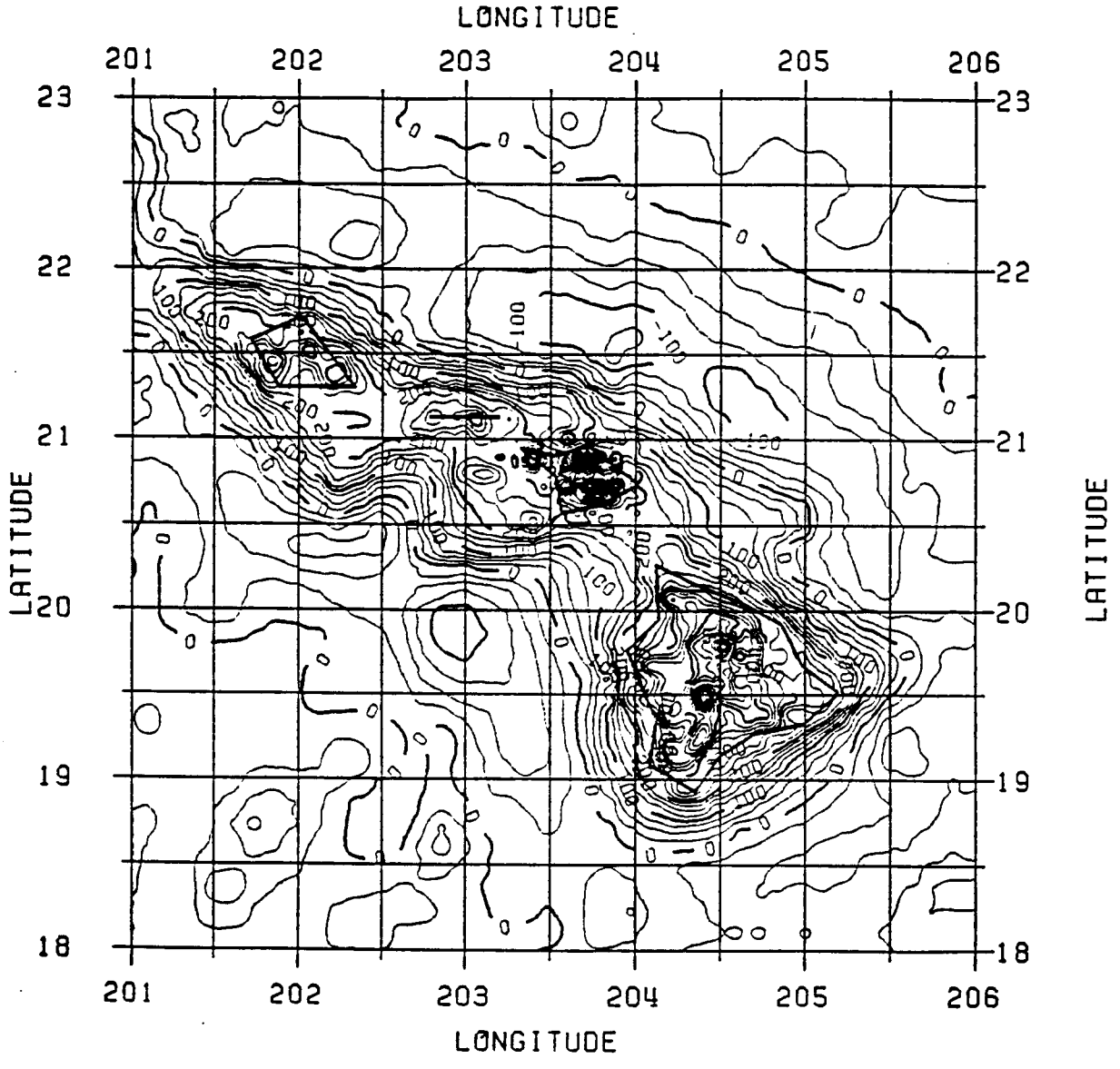

Figure 12. Gravity Predictions in the Vicinity of Hawaii Using the Five Closest Points and the Inverse of the Square of the Distance as Weight. The Grid Spacing is 2'x2' and the Contour Interval 25 mgal.

The following three Figures (10-12) illustrate predictions using the three different formulas discussed above: (5.11), (5.12) and (5.13) respectively, at the laser stations 7120, 7210 in the vicinity of Hawaii. The contour interval is 25 mgal.

On Table 14 we can see the statistics of the differences between the 2′x2′ mean anomalies predicted using the three different methods in the above region.

Table 14. Statistics of the Differences Between the 2′x2′ Mean Anomalies Predicted Using: Equation (5.11) (A), Equation (5.12) (B) and Equation (5.13) (C) for the Vicinity of Hawaii. (See Figures 10, 11, 12). Units are in mgal; Number of 2′x2′ $\overline{\Delta g}$ Compared: 22500.

STATISTICS	C-B	C-A	B-A
Mean Difference	- 0.46	-0.05	0.41
RMS Difference	2.38	0.97	2.18
Standard Deviation Difference	2.34	0.97	2.14
Maximum Difference	18.41	8.32	10.63
Minimum Difference	-10.63	-4.26	-18.41

From the comparisons of Table 14 we can conclude that there is no basic difference between the three different prediction methods. Finally, method b) with power of prediction = 2 (equation (5.13)) was chosen.

5.3 Gravity Predictions in the Bermuda Area

For the transformation of the 15731 available point gravity anomalies surrounding the laser station 7067 in Bermuda island (Figure 13) a different procedure than the one already described for the data surrounding the other laser stations was followed. This procedure used is as follows:

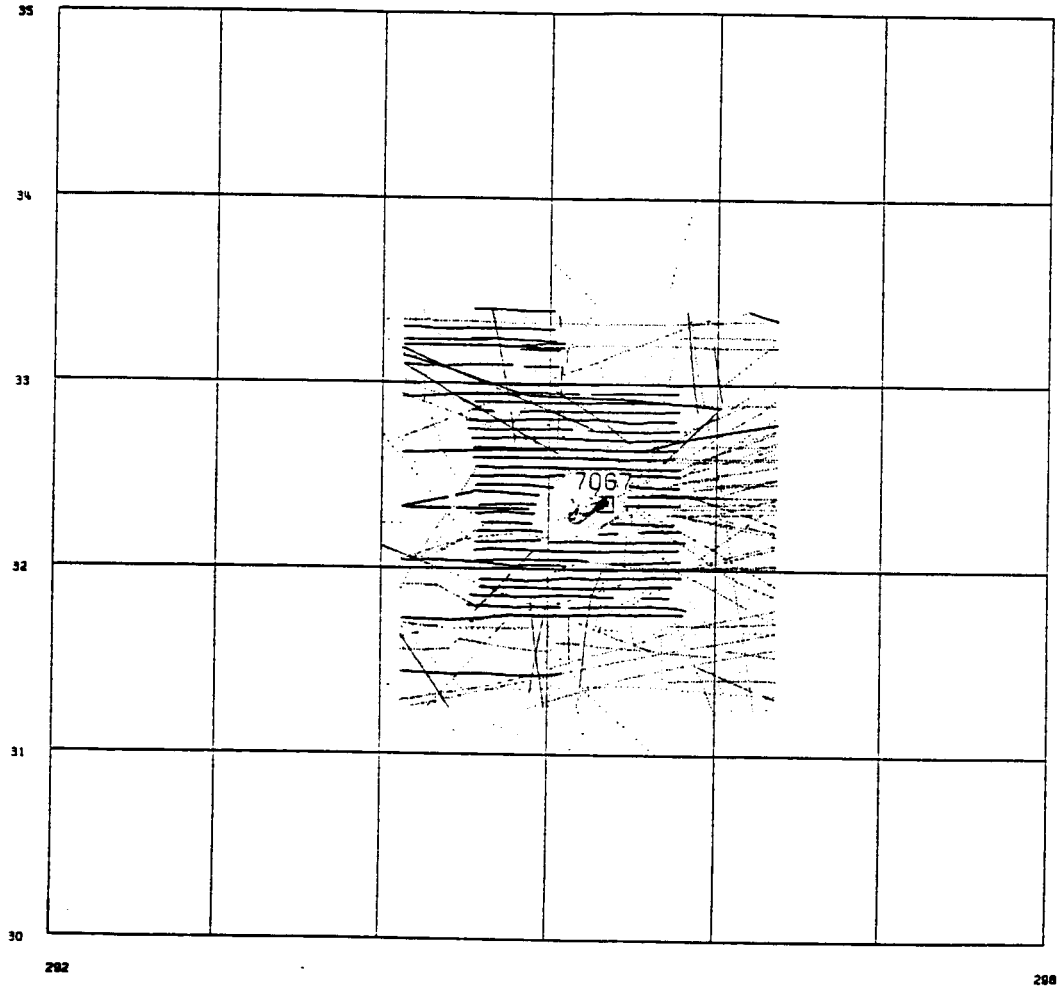

Figure 13. Location of the 15731 Originally Available Point Anomalies at the Laser Station 7067 on the Island of Bermuda. The Dots Represent Known Point Anomalies.

First, the 0°.125 x 0°.125 altimeter anomalies were used to fill-in the empty area bounded by the limits $33°20' < \phi \leq 35°$ and $30° < \phi \leq 31°15'$ in latitude and $292° \leq \lambda < 294°$ and $296°20' \leq \lambda < 298°$ in longitude. Then, the (unthinned) terrestrial point anomalies within the window $31°15' < \phi \leq 33°20'$ and $294° \leq \lambda < 296°20'$ were used together with the 0°.125 x 0°.125 anomalies to produce a merged data set. Applying equation (5.13) to the merged data set we computed 2'x2' anomalies for the whole region ($30° < \phi \leq 35°$, $292° \leq \lambda < 298°$) except for the central window bounded by the limits $32° < \phi \leq 32°.6$ in latitude and $294°.8 \leq \lambda < 295°.6$ in longitude, since the gap that exists within this window (see Figure 13) would give unreliable estimates of the 2'x2' anomalies through equation (5.13).

For this central window the 2'x2' anomalies were computed from the terrestrial point anomalies only if their distance to the five closest points ℓ_i was less than 3' for every i=1,2,3,4,5. If any of the distances ℓ_i, i=1,2,3,4,5 was greater than or equal to 3' then the 2'x2' anomaly was taken from a 2'x2' anomaly data set computed from 10360 Ohio State adjusted GEOS-3/SEASAT altimeter sea surface heights (Liang, 1983) as described in Section 8.4. A total of 35 2'x2' anomalies filled the above gap.

The 2'x2' anomaly data set computed as above was then used for the computation of the geoid undulation of the laser station 7067.

5.4 Terrain Corrections-Indirect Effect

As it already has been mentioned in Section 2.1, the derivation of the Stokes' equation (equation (2.1)) assumes that no masses external to the geoid exist. This is clearly not true for the continents, and thus the masses above the geoid have to either be removed from or shifted to the geoid. This will result in certain corrections to be applied to the computed undulations, known as terrain corrections. For reasons that are discussed in (Heiskannen and Moritz, 1967, pp. 151-152) one of the most advantageous methods to account for these terrain correction computations is the Helmert's second method of condensation (ibid, p. 145): The topography is condensed so as to form a surface layer on the geoid. The masses are shifted along the local vertical and the total mass (of the earth) remains numerically unchanged. This produces an attraction change to the free-air anomalies, TC, a potential change $V_A - V_c$ of the topography which results to an indirect effect on the undulation, δN_I, and a secondary indirect effect on the gravity anomalies ($0.3086 \cdot \delta N_I$) (Wichiencharoen, 1982b). Assuming that the terrain corrections that were given for the point anomalies of the continental United States were computed using the above Helmert's second method of condensation, (i.e. they equal the TC term discussed above), the terrain-corrections and the indirect effects were computed for the continental western United States laser stations as follows: To the point free-air anomalies $\hat{\Delta}_g^I$ of the thinned data sets (see Section 5.1) corrected due to the change of the reference ellipsoid (eq. (5.7)) and the effect of the atmosphere (eq. (5.9)), the terrain correction that was available was added:

$$\hat{\Delta}_{gTC}^I = \hat{\Delta}_g^I + TC \qquad (5.14)$$

where $\hat{\Delta}^I_{gTC}$ is the terrain-corrected anomaly

$\hat{\Delta}^I_g$ is the anomaly of the thinned data sets

TC is the available terrain correction

Then using the thinned data set (corrected for terrain effects through equation (5.14)) the 2′x2′ predictions were carried out as described in Section 5.2. This method has the disadvantage that for the missing 2′x2′ values no rigorous terrain correction is computed but the terrain correction and the value of the free-air anomaly are interpolated as a whole from the 5 terrain-corrected anomalies closest to the missing value. Then to the computed undulations using the terrain-correctd gravity anomalies from equation (5.14) the corresponding indirect effect has to be added. The various models for the indirect effect computation are discussed in (ibid, p. 19). The simplest and computationally fastest but certainly the less accurate model is the model represented by the Grushinsky's formula (ibid, eq. (44)):

$$\delta N_I = \frac{V_A - V_C}{\gamma} = \frac{-\pi G p \bar{h}^2}{\gamma} \qquad (5.15)$$

where δN_I: is the indirect effect on the undulation

V_A : potential of the actual topography

V_C : potential of the condensed topography

G : the Newton's gravitational constant

p : the assumed density of the topographic masses (= 2.67 gr/cm^3)

$\bar{h}$: the mean elevation of the 1°x1° region surrounding the laser station

γ : the mean value of normal gravity (= 979800 mgal)

Table 15 shows the number or the region name of the laser stations of the western United States; the maximum terrain correction and the arithmetic mean of the terrain correction that was computed from the thinned data sets; the mean elevation $\bar{h}$ of the 1°x1° surrounding the laser station; and the indirect effect to be added to equation (2.14) if the anomalies $\hat{\Delta}_g^I$ to be used in the first integral term of (2.14) are taken from (5.14).

Table 15. Information Related to the Terrain Correction and Indirect Effect for the Western United States Laser Stations.

NAME OR NUMBER	TERRAIN CORRECTION (mgal)			
	max	mean	$\bar{h}$(m)	δN_I(m)
QUI	81.5	4.33	1673	−0.16
SAN	75.4	2.64	729	−0.03
7082	57.5	3.72	2012	−0.23
OVR	81.5	5.19	2363	−0.32
GOL	75.4	4.97	674	−0.03
FTD	59.4	0.99	1410	−0.11
7112	82.1	3.91	1520	−0.13
7887	75.7	3.49	100	−0.00
HOP	85.8	1.63	1411	−0.11
7894	74.7	1.97	122	−0.00

The secondary indirect effect on the anomalies (= $0.3086 \cdot \delta N_I$) was neglected.

CHAPTER VI

ELLIPSOIDAL CORRECTIONS

Our derivations for the ellipsoidal corrections for all the four methods given here follow similar lines as in (Rapp, 1981a). A general equation is given for all the four methods, and the ellipsoidal corrections for the traditional methods of Stokes' and Meissl's modification result as two special cases of the above general equation, as it will be shown later in this Chapter.

The general equation (2.3) that is equivalent to the original Stokes' equation (2.1) is the geoid solution of the boundary value problem and is in spherical approximation. Thus the gravity anomaly Δg in (2.3) should be substituted with the spherical part of the anomaly, Δg^o, where (Moritz, 1980, equation (49-21)):

$$\Delta g = \Delta g^o + e^2 \Delta g^1 \tag{6.1}$$

with

$$\Delta g^o = \sum_{n=o}^{\infty} \Delta g_n^o \tag{6.2}$$

$$\Delta g^1 = \sum_{n=o}^{\infty} \Delta g_n^1 \tag{6.3}$$

$$\Delta g_n^o = \frac{n-1}{R} \sum_{m=o}^{n} (A_{nm}\cos m\lambda + B_{nm}\sin m\lambda) P_{nm}(\sin\phi) \tag{6.4}$$

$$\Delta g_n^1 = \frac{1}{R} \sum_{m=o}^{n} (G_{nm}\cos m\lambda + H_{nm}\sin m\lambda) P_{nm}(\sin\phi) \tag{6.5}$$

$$\begin{Bmatrix} G_{nm} \\ H_{nm} \end{Bmatrix} = k_{nm} \begin{Bmatrix} A_{n-2,m} \\ B_{n-2,m} \end{Bmatrix} + \lambda_{nm} \begin{Bmatrix} A_{nm} \\ B_{nm} \end{Bmatrix} + \mu_{nm} \begin{Bmatrix} A_{n+2,m} \\ B_{n+2,m} \end{Bmatrix} \tag{6.6}$$

$$\left.\begin{aligned} k_{nm} &= -\frac{3(n-3)(n-m-1)(n-m)}{2(2n-3)(2n-1)} \\ \lambda_{nm} &= \frac{n^3-3m^2n-9n^2-6m^2-10n+9}{3(2n+3)(2n-1)} \\ \mu_{nm} &= -\frac{(3n+5)(n+m+2)(n+m+1)}{2(2n+5)(2n+3)} \end{aligned}\right\} \tag{6.7}$$

$$\frac{GM}{r}\left(\frac{a}{r}\right)^n \begin{Bmatrix} C_{nm} \\ S_{nm} \end{Bmatrix} = \begin{Bmatrix} A_{nm} + e^2K_{nm} \\ B_{nm} + e^2L_{nm} \end{Bmatrix} \tag{6.8}$$

$$\begin{Bmatrix} K_{nm} \\ L_{nm} \end{Bmatrix} = a_{n-2,m} \begin{Bmatrix} A_{n-2,m} \\ B_{n-2,m} \end{Bmatrix} + b_{nm} \begin{Bmatrix} A_{nm} \\ B_{nm} \end{Bmatrix} + c_{n+2,m} \begin{Bmatrix} A_{n+2,m} \\ B_{n+2,m} \end{Bmatrix} \tag{6.9}$$

$$\left.\begin{aligned} a_{nm} &= -\frac{n(n-m+1)(n-m+2)}{(2n+1)(2n+3)} \\ b_{nm} &= \frac{n^2-3m^2+n}{(2n+3)(2n-1)} \\ c_{nm} &= \frac{(n+1)(n+m)(n+m-1)}{(2n+1)(2n-1)} \end{aligned}\right\} \tag{6.10}$$

The "spherical" undulation from equation (2.3) is (ibid, equation 49-22):

$$N_1^0 = \frac{R}{4\pi\gamma}\iint_\sigma S_1(\cos\psi)\Delta g^0 d\sigma + \frac{R}{4\pi\gamma}\iint_\sigma W_1(\cos\psi)\Delta g^0 d\sigma \tag{6.11}$$

The ellipsoidal form of the equation (2.3) is then (ibid, equation (49-26)):

$$N_1^\xi = N_1^0 + \delta N \tag{6.12}$$

$$\text{with } \delta N = e^2\left(\frac{1}{4} - \frac{3}{4}\sin^2\phi\right)N_o \tag{6.13}$$

N_o is an approximate value of the undulation which can be taken to be the same for all methods, and ϕ is the geodetic latitude of the computation point.

Equation (6.12) can be rewritten using (6.11) and (6.1) as

$$N_i^E = \frac{R}{4\pi\gamma}\iint_\sigma S_i(\cos\psi)(\Delta g - e^2\Delta g^1)d\sigma + \frac{R}{4\pi\gamma}\iint_\sigma W_i(\cos\psi)\Delta g^o d\sigma + \delta N$$

$$= \frac{R}{4\pi\gamma}\iint_{\sigma_c} S_i(\cos\psi)(\Delta g - e^2\Delta g^1)d\sigma + \frac{R}{4\pi\gamma}\iint_{\sigma-\sigma_c} S_i(\cos\psi)\Delta g^o d\sigma$$

$$+ \frac{R}{4\pi\gamma}\iint_\sigma W_i(\cos\psi)\Delta g^o d\sigma + \delta N$$

$$= \frac{R}{4\pi\gamma}\iint_{\sigma_c} S_i(\cos\psi)\Delta g d\sigma + \frac{R}{4\pi\gamma}\iint_{\sigma-\sigma_c} S_i(\cos\psi)\Delta g^o d\sigma + \frac{R}{4\pi\gamma}\iint_\sigma W_i(\cos\psi)\Delta g d\sigma$$

$$+ \delta N - \frac{Re^2}{4\pi\gamma}\iint_{\sigma_c} S_i(\cos\psi)\Delta g^1 d\sigma \qquad (6.14)$$

The first integral term of equation (6.14) is to be computed from the terrestrial gravity data and the next three integral terms and δN will be computed from the given set of potential coefficients.

Thus (6.14) can be rewritten using equation (2.5):

$$N_i^E = \frac{R}{4\pi\gamma}\iint_{\sigma_c} S_i(\cos\psi)\hat{\Delta}_g^I d\sigma + \frac{R}{4\pi\gamma}\iint_\sigma \bar{S}_i(\cos\psi)\Delta g^o d\sigma$$

$$+ \frac{R}{4\pi\gamma}\iint_\sigma W_i(\cos\psi)\Delta g^o d\sigma + \delta N - \frac{Re^2}{4\pi\gamma}\iint_{\sigma_c} S_i(\cos\psi)\Delta g^1 d\sigma$$

$$= \frac{R}{4\pi\gamma}\iint_{\sigma_c} S_i(\cos\psi)\hat{\Delta}_g^I d\sigma + \frac{R}{2\gamma}\sum_{n=o}^{M} Q_{in}\Delta g_n^o + \frac{R}{2\gamma}\sum_{n=o}^{M} W_{in}\Delta g_n^o + \delta N$$

$$- \frac{Re^2}{4\pi\gamma}\iint_{\sigma_c} S_i(\cos\psi)\Delta g^1 d\sigma \qquad (6.15)$$

Choosing $\bar{n} < M$ (see Chapter 3), equation (6.15) can be written:

$$N_i^E = \frac{R}{4\pi\gamma}\iint_{\sigma_c} S_i(\cos\psi)\hat{\Delta}_g^I d\sigma + \frac{R}{2\gamma}\sum_{n=o}^{\bar{n}}(Q_{in}+W_{in})\Delta g_n^o + \frac{R}{2\gamma}\sum_{n=\bar{n}+1}^{M} Q_{in}\Delta g_n^o + \delta N$$

$$- \frac{Re^2}{4\pi\gamma}\iint_{\sigma_c} S_i(\cos\psi)\Delta g^1 d\sigma \qquad (6.16)$$

Note that the harmonics Δg_n^o given by (6.4) will correspond exactly to $\hat{\Delta}g_n^s$ of equation (2.14) if the geocentric latitude $\bar{\phi}$ instead of the geodetic latitude ϕ will be used as an argument for the associated Legendre functions (Rapp, 1981a, equations (25, (26)). In this case, the coefficients

$$\begin{Bmatrix} K_{nm} \\ L_{nm} \end{Bmatrix} = \begin{Bmatrix} 0 \\ 0 \end{Bmatrix} \tag{6.17}$$

and (6.16) can be written ($\bar{n} < M$)

$$\begin{aligned} N_i^\xi = {} & \frac{R}{4\pi\gamma} \iint_{\sigma_c} S_i(\cos\psi)\hat{\Delta}I_g d\sigma + \frac{GM}{2r\gamma} \sum_{n=o}^{\bar{n}} (Q_{in}+W_{in})(n-1)\left(\frac{a}{r}\right)^n \\ & \cdot \sum_{m=o}^{n} (C_{nm}\cos m\lambda + S_{nm}\sin m\lambda) P_{nm}(\sin\bar{\phi}) \\ & + \frac{GM}{2r\gamma} \sum_{n=n+1}^{M} Q_{in}(n-1)\left(\frac{a}{r}\right)^n \sum_{m=o}^{n} (C_{nm}\cos m\lambda + S_{nm}\sin m\lambda) P_{nm}(\sin\bar{\phi}) \\ & + \delta N - \frac{Re^2}{4\pi\gamma} \iint_{\sigma_c} S_i(\cos\psi)\Delta g^1 d\sigma \end{aligned} \tag{6.18}$$

or

$$N_i^\xi = \hat{N}_i^o + \delta N + \delta N_i \tag{6.19}$$

where $\hat{N}_i^o$ is the spherical part of the undulation computed for each of the four methods as already discussed in Chapter 2. Also:

$$\delta N_i = - \frac{Re^2}{4\pi\gamma} \iint_{\sigma_c} S_i(\cos\psi)\Delta g^1 d\sigma \tag{6.20}$$

We now evaluate the integral of equation (6.20)

$$\begin{aligned} \delta N_i &= - \frac{Re^2}{4\pi\gamma} \iint_{\sigma_c} S_i(\cos\psi)\Delta g^1 d\sigma \\ &= - \frac{Re^2}{4\pi\gamma} \left[\iint_{\sigma} S_i(\cos\psi)\Delta g^1 d\sigma - \iint_{\sigma-\sigma_c} S_i(\cos\psi)\Delta g^1 d\sigma \right] \end{aligned}$$

$$= -\frac{Re^2}{4\pi\gamma}\left[\iint_\sigma S_i(\cos\psi)\Delta g^1 d\sigma - \iint_\sigma \bar{S}_i(\cos\psi)\Delta g^1 d\sigma\right]$$

$$= -\frac{Re^2}{4\pi\gamma}\left[2\pi\sum_{n=0}^{M} X_{in}\Delta g_n^1 - 2\pi\sum_{n=0}^{M} Q_{in}\Delta g_n^1\right]$$

$$= -\frac{Re^2}{2\gamma}\sum_{n=0}^{M}(X_{in}-Q_{in})\Delta g_n^1$$

$$= \frac{e^2}{2\gamma}\sum_{n=0}^{M}(Q_{in}-X_{in})\sum_{m=0}^{n}(G_{nm}\cos m\lambda + H_{nm}\sin m\lambda)P_{nm}(\sin\bar{\phi}) \qquad (6.21)$$

Using equation (6.19), (6.20) and (6.21) we can write equation (6.18) as:

$$N_i^E = \frac{R}{4\pi\gamma}\iint_{\sigma_c} S_i(\cos\psi)\hat{\Delta}g^T d\sigma + \frac{GM}{2r\gamma}\sum_{n=0}^{\bar{n}}(Q_{in}+W_{in})(n-1)\left(\frac{a}{r}\right)^n$$

$$\cdot\sum_{m=0}^{n}(C_{nm}\cos m\lambda + S_{nm}\sin m\lambda)P_{nm}(\sin\bar{\phi})$$

$$+\frac{GM}{2r\gamma}\sum_{n=\bar{n}+1}^{M} Q_{in}(n-1)\left(\frac{a}{r}\right)^n\sum_{m=0}^{n}(C_{nm}\cos m\lambda + S_{nm}\sin m\lambda)P_{nm}(\sin\bar{\phi})$$

$$+\frac{e^2}{2\gamma}\sum_{n=0}^{M}(Q_{in}-X_{in})\sum_{m=0}^{n}(G_{nm}\cos m\lambda + H_{nm}\sin m\lambda)P_{nm}(\sin\bar{\phi})$$

$$+ e^2\left(\frac{1}{4} - \frac{3}{4}\sin^2\phi\right)N_o \qquad (6.22)$$

Equation (6.22) is the desired equation of the geoid undulation computation taking into account the ellipsoidal corrections for all the four methods. Notice that the fourth correction term (δN_i) of equation (6.22) arises from the fact that the ellipsoidal effect $e^2\Delta g^1$ has to be removed from the terrestrial anomalies $\hat{\Delta}g^T$, whereas the fifth correction term (δN) arises from the ellipsoidal correction $e^2(1/4-3/4\sin^2\phi)N_o$ to the spherical undulation N_i^S itself. Taking i=1 (Stokes' method) and starting the summation of the second term of the right-hand side in equation (6.22) from 2, we take

$$i=1 \xrightarrow{(6.22)} N_1^{\xi} = \frac{R}{4\pi\gamma} \iint_{\sigma_c} S_1(\cos\psi)\hat{\Delta}g^T d\sigma$$

$$+ \frac{GM}{2r\gamma} \sum_{n=2}^{\bar{n}} (Q_{1n}+W_{1n})(n-1)\left(\frac{a}{r}\right)^n \sum_{m=0}^{n} (C_{nm}\cos m\lambda+S_{nm}\sin m\lambda)P_{nm}(\sin\phi)$$

$$+ \frac{GM}{2r\gamma} \sum_{n=\bar{n}+1}^{M} Q_{1n}(n-1)\left(\frac{a}{r}\right)^n \sum_{m=0}^{n} (C_{nm}\cos m\lambda+S_{nm}\sin m\lambda)P_{nm}(\sin\phi)$$

$$+ \frac{e^2}{2\gamma} \sum_{n=0}^{M} (Q_{1n}-X_{1n}) \sum_{m=0}^{n} (G_{nm}\cos m\lambda+H_{nm}\sin m\lambda)P_{nm}(\sin\phi)$$

$$+ e^2 \left(\frac{1}{4} - \frac{3}{4}\sin^2\phi\right)N_o \qquad (6.23)$$

Taking into account the relationships (2.35), (2.36) and (2.39), we have

$$N_1^{\xi} = \frac{R}{4\pi\gamma} \iint_{\sigma_c} S(\cos\psi)\hat{\Delta}g^T d\sigma$$

$$+ \frac{GM}{2r\gamma} \sum_{n=0}^{M} Q_{1n}(n-1)\left(\frac{a}{r}\right)^n \sum_{m=0}^{n} (C_{nm}\cos m\lambda+S_{nm}\sin m\lambda)P_{nm}(\sin\phi)$$

$$+ \frac{GM}{2\gamma} \sum_{n=0}^{M} (Q_{1n}-X_{1n}) \sum_{m=0}^{n} (G_{nm}\cos m\lambda+H_{nm}\sin m\lambda)P_{nm}(\sin\phi)$$

$$+ e^2 \left(\frac{1}{4} - \frac{3}{4}\sin^2\phi\right)N_o \qquad (6.24)$$

Equation (6.24) is exactly the same as equation (31) derived in (ibid, p. 10845).

Furthermore for i=2 (Meissl's method) and starting the summation of the second term of the right-hand side in equation (6.22) from 2, we take:

$$i=2 \xrightarrow{(6.22)} N_2^{\xi} = \frac{R}{4\pi\gamma} \iint_{\sigma_c} S_2(\cos\psi)\hat{\Delta}g^T d\sigma$$

$$+ \frac{GM}{2r\gamma} \sum_{n=2}^{\bar{n}} (Q_{2n}+W_{2n})(n-1)\left(\frac{a}{r}\right)^n \sum_{m=0}^{n} (C_{nm}\cos m\lambda+S_{nm}\sin m\lambda)P_{nm}(\sin\phi)$$

$$+ \frac{GM}{2r\gamma} \sum_{n=\bar{n}+1}^{M} Q_{2n}(n-1)\left(\frac{a}{r}\right)^n \sum_{m=0}^{n} (C_{nm}\cos m\lambda+S_{nm}\sin m\lambda)P_{nm}(\sin\phi)$$

$$+ \frac{e^2}{2\gamma} \sum_{n=0}^{M} (Q_{2n}-X_{2n}) \sum_{m=0}^{n} (G_{nm}\cos m\lambda+H_{nm}\sin m\lambda)P_{nm}(\sin\Phi)$$

$$+ e^2 \left(\frac{1}{4} - \frac{3}{4}\sin^2\phi\right)N_o \qquad (6.25)$$

Taking into account the relationships (2.47), (2.53), (2.57) and (2.59) we have:

$$N_2^E = \frac{R}{4\pi\gamma} \iint_{\sigma_c} (S(\cos\psi)-S_o)\hat{\Delta}g^T d\sigma$$

$$+ \frac{GM}{2r\gamma} \sum_{n=2}^{M} Q_{2n}(n-1)\left(\frac{a}{r}\right)^n \sum_{m=0}^{n} (C_{nm}\cos m\lambda+S_{nm}\sin m\lambda)P_{nm}(\sin\Phi)$$

$$+ \frac{e^2}{2\gamma} \sum_{n=0}^{M} (Q_{2n}-X_{2n}) \sum_{m=0}^{n} (G_{nm}\cos m\lambda+H_{nm}\sin m\lambda)P_{nm}(\sin\Phi)$$

$$+ e^2 \left(\frac{1}{4} - \frac{3}{4}\sin^2\phi\right)N_o \qquad (6.26)$$

Equation (6.26) is exactly the same as equation (38) derived in (ibid, p. 10846).

The equations for the new methods follow in a similar way for i=3 (Molodenskii's method) and i=4 (modified Sjöberg's method) from the general equation (6.22).

To numerically compute the ellipsoidal corrections the OSU86F potential coefficient set $\{C_{nm}, S_{nm}\}$ up to degree M=36 was used. The numerical evaluation of the term δN was done using an approximation of N_o for all methods taken from

$$N_o = \frac{GM}{r\gamma} \sum_{n=2}^{M} \left(\frac{a}{r}\right)^n \sum_{m=0}^{n} (C_{nm}\cos m\lambda+S_{nm}\sin m\lambda)P_{nm}(\sin\Phi) \qquad (6.27)$$

The numerical evaluation of the term δN_i was done as follows: First, the coefficients $\{A_{nm}, B_{nm}\}$ were computed using equation (6.8) with $\{K_{nm}, L_{nm}\} = \{0, 0\}$ (equation (6.17). Then, the coefficients $\{G_{nm}, H_{nm}\}$ were computed from (6.6) and (6.7). Finally, the term δN_i was computed from equation (6.21) for all the four methods using the Fourier coefficients X_{in}, Q_{in}, W_{in} of each method that have been derived in Chapter 2.

CHAPTER VII

LOCAL AVERAGE CORRECTION

The terrestrial mean anomalies $\hat{\Delta}g^T$ that are used inside the integral of equation (2.14) ($\hat{\Delta}g^T$ + TC in case that terrain corrections have been computed, $\hat{\Delta}g^T$ otherwise), can be expressed as:

$$\hat{\Delta}g^T = \hat{\Delta}g^s + \delta(\Delta g^s) \tag{7.1}$$

where $\hat{\Delta}g^s$ are the mean anomalies implied by the potential coefficient set, used up to degree M

$\delta(\Delta g^s)$ are the errors of the mean anomalies due to the omission and commission errors of the given potential coefficients.

Assuming that the potential coefficients are errorless, the error $\delta(\Delta g^s)$ will be due only to the omission errors (truncation of the given field at degree M). Taking the average over a spherical cap σ_c of both sides of eq. (7.1), we obtain:

$$\frac{1}{S}\iint_{\sigma_c} \hat{\Delta}g^T d\sigma = \frac{1}{S}\iint_{\sigma_c} \hat{\Delta}g^s d\sigma + \frac{1}{S}\iint_{\sigma_c} \delta(\Delta g^s) d\sigma \tag{7.2}$$

For a high degree field (M = 180, or M = 360) the average of the omission errors over a cap of radius on the order of 2° or larger can be realistically considered zero. This can be justified by the fact that the average of a short wavelength signal (as the omission error $\delta(\Delta g^s)$ for a high degree field is) over an area of much longer wavelength

(capsize of 2°) is expected to be zero.

$$\frac{1}{S}\iint_{\sigma_c} \delta(\Delta g^s)d\sigma = 0 \tag{7.3}$$

and from (7.2) and (7.3) we must have:

$$\frac{1}{S}\iint_{\sigma_c} \hat{\Delta}g^T d\sigma - \frac{1}{S}\iint_{\sigma_c} \hat{\Delta}g^s d\sigma = 0 \tag{7.4}$$

Condition (7.4) expresses the fact that the mean over the cap of the terrestrial anomalies should equal to the mean over the cap of the anomalies implied by the potential coefficient set. Of course, if the mean was taken over the whole earth, then, ideally, both terms of the left-hand side of (7.3) would be zero and condition (7.4) would hold (Rapp, 1975):

$$\frac{1}{4\pi}\iint_{\sigma} \hat{\Delta}g^T d\sigma - \frac{1}{4\pi}\iint_{\sigma} \hat{\Delta}g^s d\sigma = 0 - 0 = 0 \tag{7.5}$$

In reality

$$\frac{1}{S}\iint_{\sigma_c} \hat{\Delta}g^T d\sigma - \frac{1}{S}\iint_{\sigma_c} \hat{\Delta}g^s d\sigma = \Delta g_0^I - \Delta g_0^p \neq 0 \tag{7.6}$$

with $$\Delta g_0^I = \frac{1}{S}\iint_{\sigma_c} \hat{\Delta}g^T d\sigma \tag{7.7}$$

and $$\Delta g_0^p = \frac{1}{S}\iint_{\sigma_c} \hat{\Delta}g^p d\sigma \tag{7.8}$$

For a numerical verification of (7.6) see columns 7 and 8 of Table 13, where

$$\bar{x} \equiv \Delta g_0^I \text{ and } \bar{x}_p \equiv \Delta g_0^p$$

If we add to the terrestrial anomalies $\hat{\Delta}g^T$ the difference $\Delta g_0^p - \Delta g_0^I = d$, then condition (7.4) is met:

$$\frac{1}{S}\iint_{\sigma_c}(\hat{\Delta}g^T+d)d\sigma - \frac{1}{S}\iint_{\sigma_c}\hat{\Delta}g^s d\sigma$$

$$= \frac{1}{S}\iint_{\sigma_c}(\hat{\Delta}g^T+\Delta g_0^P-\Delta g_0^I)d\sigma - \frac{1}{S}\iint_{\sigma_c}\hat{\Delta}g^s d\sigma$$

$$= \frac{1}{S}\iint_{\sigma_c}\hat{\Delta}g^T d\sigma + \frac{1}{S}\Delta g_0^P\iint_{\sigma_c}d\sigma - \frac{1}{S}\Delta g_0^I\iint_{\sigma_c}d\sigma - \frac{1}{S}\iint_{\sigma_c}\hat{\Delta}g^s d\sigma$$

$$= \Delta g_0^I + \Delta g_0^P - \Delta g_0^I - \Delta g_0^P = 0$$

The difference $d = \Delta g_0^P - \Delta g_0^I$ is a constant correction to be added to the terrestrial anomalies $\hat{\Delta}g^T$ used to compute the cap contribution. The corresponding effect on the geoid undulation can then analytically be computed as follows:

From equation (2.14) with $\hat{\Delta}g^T + d$ instead of $\hat{\Delta}g^T$ and $\bar{n} < M$ we obtain:

$$N_i = \frac{R}{4\pi\gamma}\iint_{\sigma_c}S_i(\cos\psi)(\hat{\Delta}g^T+d)d\sigma + \frac{R}{2\gamma}\sum_{n=0}^{\bar{n}}(Q_{in}+W_{in})\hat{\Delta}g_n^s$$

$$+ \frac{R}{2\gamma}\sum_{n=\bar{n}+1}^{M}Q_{in}\hat{\Delta}g_n^s$$

$$= \frac{R}{4\pi\gamma}\iint_{\sigma_c}S_i(\cos\psi)\hat{\Delta}g^T d\sigma + \frac{R}{2\gamma}\sum_{n=0}^{\bar{n}}(Q_{in}+W_{in})\hat{\Delta}g_n^s$$

$$+ \frac{R}{2\gamma}\sum_{n=\bar{n}+1}^{M}Q_{in}\hat{\Delta}g_n^s + \frac{R}{4\pi\gamma}\iint_{\sigma_c}S_i(\cos\psi)dd\sigma$$

$$= \hat{N}_i + \delta N_i^? \qquad (7.9)$$

where $\hat{N}_i$ is the geoid undulation computed using each of the four methods as discussed in Chapter 2. The local average correction term is:

$$\delta N_i^? = \frac{R}{4\pi\gamma} \iint_{\sigma_c} S_i(\cos\psi)\,dd\sigma$$

We have:

$$\delta N_i^? = \frac{R}{4\pi\gamma}\, d \iint_{\sigma_c} S_i(\cos\psi)\,d\sigma$$

$$= \frac{R}{4\pi\gamma}\, d \left[\iint_{\sigma} S_i(\cos\psi)\,d\sigma - \iint_{\sigma-\sigma_c} S_i(\cos\psi)\,d\sigma\right]$$

$$= \frac{R}{4\pi\gamma}\, d \left[\iint_{\sigma} S_i(\cos\psi)\,d\sigma - \iint_{\sigma} \bar{S}_i(\cos\psi)\,d\sigma\right] \qquad (7.10)$$

From equation (2.11), for n=0 we take:

$$2\pi Q_{i0} = \iint_{\sigma} \bar{S}_i(\cos\psi) P_0(\cos\psi)\,d\sigma, \text{ or}$$

$$\iint_{\sigma} \bar{S}_i(\cos\psi)\,d\sigma = 2\pi Q_{i0} \qquad (7.11)$$

Similarly, since X_{in} are the Fourier coefficients of $S_i(\cos\psi)$,

$$2\pi X_{i0} = \iint_{\sigma} S_i(\cos\psi) P_0(\cos\psi)\,d\sigma, \text{ or}$$

$$\iint_{\sigma} S_i(\cos\psi)\,d\sigma = 2\pi X_{i0} \qquad (7.12)$$

Substituting (7.11) and (7.12) into (7.10), we obtain:

$$\delta N_i^? = \frac{R}{2\gamma}\, d\,(X_{i0}-Q_{i0}), \text{ or}$$

$$\delta N_i^? = \frac{R}{2\gamma}\,(\Delta g_0^p - \Delta g_0^I)(X_{i0}-Q_{i0}) \qquad (7.13)$$

Equation (7.13) is the general expression for the local average correction, and it can also be used to analytically compute the effect on the undulation due to a constant correction to the gravity data $\hat{\Delta}g^T$ (e.g. a forgotten atmospheric correction).

For each method, equation (7.13) can be reduced as follows:

For i=1 (Stokes' method):

$$\delta N_1^o = \frac{R}{2\gamma} (\Delta g_\delta^p - \Delta g_\delta^I)(X_{1o} - Q_{1o})$$

$$= - \frac{R}{2\gamma} (\Delta g_\delta^p - \Delta g_\delta^I) Q_{1o} \qquad (7.14)$$

For i=2 (Meissl's method)

$$\delta N_2^o = \frac{R}{2\gamma} ((\Delta g_\delta^p - \Delta g_\delta^I)(X_{2o} - Q_{2o})$$

$$= \frac{R}{2\gamma} (\Delta g_\delta^p - \Delta g_\delta^I)(-2S_o - Q_{2o})$$

$$= \frac{R}{2\gamma} (\Delta g_\delta^p - \Delta g_\delta^I)(-W_{2o} - Q_{2o})$$

$$= - \frac{R}{2\gamma} (\Delta g_\delta^p - \Delta g_\delta^I)(Q_{2o} + W_{2o}) \qquad (7.15)$$

For i=3 (Molodenskii's method)

$$\delta N_3^o = \frac{R}{2\gamma} (\Delta g_\delta^p - \Delta g_\delta^I)(X_{3o} - Q_{3o})$$

$$= \frac{R}{2\gamma} (\Delta g_\delta^p - \Delta g_\delta^I)(-W_{3o})$$

$$= - \frac{R}{2\gamma} (\Delta g_\delta^p - \Delta g_\delta^I) W_{3o} \qquad (7.16)$$

And for i=4 (Modified Sjöberg's method)

$$\delta N_4^o = \frac{R}{2\gamma} (\Delta g_\delta^p - \Delta g_\delta^I)(X_{4o} - Q_{4o})$$

$$= \frac{R}{2\gamma} (\Delta g_\delta^p - \Delta g_\delta^I)(-W_{4o} - Q_{4o})$$

$$= - \frac{R}{2\gamma} (\Delta g_\delta^p - \Delta g_\delta^I)(W_{4o} + Q_{4o}) \qquad (7.17)$$

The numerical values of Q_{1o}, $Q_{2o}+W_{2o}$, W_{3o} and $W_{4o}+Q_{4o}$ for $\psi=2^\circ$, $\bar{n}=20$, M=180, error models (3.1) and (3.2) for the potential coefficients and the terrestrial data respectively and model (2.18) for the anomaly degree

variances, are:

$$\left.\begin{aligned} Q_{10} &= -0.075620 \\ Q_{20}+W_{20} &= -0.035852 \\ W_{30} &= -0.053435 \\ Q_{40}+W_{40} &= -0.0583024 \end{aligned}\right\} \qquad (7.18)$$

Then, the corresponding values $a_i = (R/2\gamma)(Q_{in}+W_{in})$ in m/mgal of the corrections $\delta N_i^?$ are ($R = 6371000$ m and $\gamma = 979800$ mgal).

$$\left.\begin{aligned} a_1 &= 0.245854 \text{ m/mgal} \\ a_2 &= 0.116561 \text{ m/mgal} \\ a_3 &= 0.173727 \text{ m/mgal} \\ a_4 &= 0.189550 \text{ m/mgal} \end{aligned}\right\} \qquad (7.19)$$

We can see that Meissl's method is the least sensitive and Stokes' method is the most sensitive to a constant correction. Molodenskii's and modified Sjöberg's methods have sensitivities that are between the Stokes' and Meissl's methods. For the numerical evaluation of $\delta N_i^?$, the values of Δg_δ^P, Δg_δ^I were taken from Table 13.

CHAPTER VIII

NUMERICAL RESULTS AND STATISTICS

8.1 Computational details

As discussed in Chapter 5 the numerical integration of the functions $S_i(\cos\psi)$ was computed using 2′x2′, 6′x10′ and 10′x10′ mean terrestrial $\hat{\Delta}g^T$. The selected capsize was 2° and the functions $S_i(\cos\psi)$ were first tabulated at a spherical interval of 1" out to a spherical distance of 3°. Then the evaluation of $S_i(\cos\psi)$ for each block was done by numerical integration as follows: Each block was subdivided into elements depending on the separation ψ between the computation point (laser station) and the cell. For ψ=4′ the number of subdivisions was 64; for 4′<ψ≤8′ we had 16 subdivisions; for 8′<ψ≤12′ the subdivisions were 4 and for 12′<ψ≤2° the evaluation was made at the center point of the cell (Engelis et al., 1985a). The general equation including ellipsoidal corrections (eq. (6.22)) was applied for all the methods. The outer zone contribution (second and third term in (6.22)) was computed from the OSU86F potential coefficients taken up to degree M=180. Since there is no zero or first degree potential coefficients in the OSU86F field the summations started from 2, although the theoretical formulas developed start their summations from zero. The correct procedure would be to start our summations from zero. The ellipsoidal corrections were computed up to degree M=36 as mentioned in Chapter 6. The models for

the error degree variances of the terrestrial anomalies and the anomalies implied by the potential coefficients are important for the error analysis of the four methods, but they also play a very important role for the modified Sjöberg's method, since for this method the Fourier coefficients X_{4n}, W_{4n} and Q_{4n} are based on them. The model for the anomaly error degree variances of the potential coefficient set was taken from equation (3.1). The models for the terrestrial anomaly error degree variances were selected for each region as Table 16 shows:

Table 16. Models for the Terrestrial Error Anomaly Degree Variances Selected by Region.

Region	Model
UNITED STATES	B.1
BERMUDA	B.1
AUSTRALIA	B.1
EUROPE	A $[\beta_n=\beta_n(6'x10')]$
JAPAN	A $[\beta_n=\beta_n(10'x10')]$

Finally the number $\bar{n}$ of harmonics that were removed from the Stokes' function for the Molodenskii's and the modified Sjöberg's method was taken to be 20 (<M=180). For comparison purposes the point undulation of the laser station was computed using the OSU86F potential coefficients in equation (6.23) with M=360.

8.2 Numerical results

Table 17 shows the results of the undulation computations with the Stokes' method. The first and second columns show the number and the name of the laser stations; the third column shows the reference for the ellipsoidal height of the stations; the next three columns represent the three components of the undulation (see equation (6.22)); cap contribution, NC, potential coefficient contribution (outer zone) NP, and

Table 17. Geoid Undulations of the Laser Stations Using Stokes' Method (Units are in meters).

NUM	NAME	REF	NC	NP	NE	N	OSU86 F	ELL-ORT
7051	QUILAS	BM	2.79	-27.12	-0.01	-24.35	-23.64	-22.57
7109	QUILAS	BM	2.79	-27.13	-0.01	-24.35	-23.65	-22.59
7886	QUILAS	UN	2.79	-27.13	-0.01	-24.35	-23.65	-19.30
7062	SANDIE	BM	-1.41	-33.88	-0.01	-35.30	-34.22	-32.47
7110	MONLAS	BM	-0.33	-33.06	-0.01	-33.39	-32.78	-30.86
7082	BEARLK	BM	1.75	-18.74	0.00	-16.99	-15.16	-12.58
7084	OVRLAS	BM	1.22	-28.63	-0.01	-27.42	-26.29	-24.90
7114	OVRLAS	BM	1.21	-28.62	-0.01	-27.42	-26.30	-24.84
7085	GOLDLS	BM	-1.76	-30.17	-0.01	-31.94	-31.70	-29.68
7115	GOLLAS	BM	-1.85	-30.31	-0.01	-32.16	-31.84	-29.58
7086	FTDAVS	BM	1.51	-23.69	0.01	-22.17	-21.36	-20.78
7085	FORLAS	BM	1.51	-23.69	0.01	-22.17	-21.36	-20.83
7112	PLALAS	BM	2.40	-21.37	0.00	-18.96	-18.28	-17.40
7087	VANLAS	UN	-2.68	-33.43	-0.01	-36.12	-36.47	-31.14
7088	HOPLAS	UN	-2.01	-28.46	0.00	-30.48	-29.48	-2.20
7921	HOPLAS	UN	-2.02	-28.46	0.00	-30.48	-29.48	-29.47
7894	YUMLAS	UN	-4.34	-30.00	-0.01	-34.34	-33.56	-28.63
7063	STALAS	BM	0.04	-33.26	-0.01	-33.23	-33.08	-32.92
7064	GSFCLS	BM	0.04	-33.26	-0.01	-33.23	-33.08	-33.64
7100	GSF100	BM	0.02	-33.26	-0.01	-33.25	-33.09	-32.50
7101	GSF101	BM	0.02	-33.26	-0.01	-33.25	-33.09	-33.08
7102	GSF102	BM	0.04	-33.26	-0.01	-33.23	-33.08	-32.89
7103	GSF103	BM	0.04	-33.26	-0.01	-33.23	-33.08	-32.93
7104	GSF104	BM	0.03	-33.26	-0.01	-33.25	-33.08	-32.94
7105	GSF105	BM	0.04	-33.26	-0.01	-33.23	-33.08	-32.93
7069	RAMLAS	BM	1.02	-30.25	0.01	-29.22	-29.52	-29.13
7091	HAYLAS	BM	0.54	-29.54	-0.02	-29.02	-28.61	-27.55
7120	MUILAS	BM	20.77	-1.83	0.00	18.93	13.02	20.46
7210	MAULAS	IA	20.80	-1.83	0.00	18.96	13.02	20.49
7090	YARLAS	BM	-1.00	-23.77	0.00	-24.77	-25.02	-24.28
7943	ORRLAS	UN	7.47	11.08	0.02	18.57	20.36	20.38
7067	BDILAS	BM	5.69	-37.73	-0.01	-32.05	-35.23	-31.81
7805	FINLAS	IA	-2.54	23.07	-0.01	20.53	20.54	19.95
7939	MATLAS	UN	9.91	36.63	0.01	46.55	45.66	46.39
7835	GRALAS	UN	6.98	44.93	0.02	51.93	51.04	42.85
7840	RGOLAS	UN	-2.46	48.19	0.01	45.75	46.06	45.58
8833	KOOLAS	UN	-0.02	44.14	0.01	44.13	44.80	44.66
7834	WETLAS	IA	4.49	42.17	0.02	46.68	47.02	47.65
7838	SHOLAS	UN	6.85	32.05	0.03	38.93	37.60	39.97

Table 18. Geoid Undulations of the Laser Stations Using Meissl's Method (Units are in meters).

NUM	NAME	REF	NC	NP	NE	N	OSU86 F	ELL-ORT
7051	QUILAS	BM	1.73	-26.07	0.00	-24.34	-23.64	-22.57
7109	QUILAS	BM	1.73	-26.07	0.00	-24.34	-23.65	-22.59
7886	QUILAS	UN	1.73	-26.07	0.00	-24.34	-23.65	-19.30
7062	SANDIE	BM	-0.05	-34.85	0.00	-34.90	-34.22	-32.47
7110	MONLAS	BM	1.18	-34.05	0.00	-32.87	-32.78	-30.86
7082	BEARLK	BM	0.08	-16.44	0.00	-16.36	-15.16	-12.58
7084	OVRLAS	BM	0.92	-28.50	0.00	-27.59	-26.29	-24.90
7114	OVRLAS	BM	0.91	-28.50	0.00	-27.59	-26.30	-24.84
7085	GOLDLS	BM	-1.31	-30.50	0.00	-31.81	-31.70	-29.68
7115	GOLLAS	BM	-1.25	-30.72	0.00	-31.97	-31.84	-29.58
7086	FTDAVS	BM	1.59	-23.23	0.00	-21.64	-21.36	-20.78
7085	FORLAS	BM	1.59	-23.23	0.00	-21.64	-21.36	-20.83
7112	PLALAS	BM	-0.18	-18.60	0.00	-18.77	-18.28	-17.40
7087	VANLAS	UN	-0.73	-35.46	0.00	-36.19	-36.47	-31.14
7088	HOPLAS	UN	-0.80	-29.26	0.00	-30.07	-29.48	-2.20
7921	HOPLAS	UN	-0.81	-29.26	0.00	-30.07	-29.48	-29.47
7894	YUMLAS	UN	-2.14	-31.71	0.00	-33.86	-33.56	-28.63
7063	STALAS	BM	0.86	-33.88	-0.01	-33.03	-33.08	-32.92
7064	GSFCLS	BM	0.86	-33.88	-0.01	-33.03	-33.08	-33.64
7100	GSF100	BM	0.84	-33.88	-0.01	-33.05	-33.09	-32.50
7101	GSF101	BM	0.84	-33.88	-0.01	-33.05	-33.09	-33.08
7102	GSF102	BM	0.86	-33.88	-0.01	-33.03	-33.08	-32.89
7103	GSF103	BM	0.86	-33.88	-0.01	-33.03	-33.08	-32.93
7104	GSF104	BM	0.85	-33.88	-0.01	-33.04	-33.08	-32.94
7105	GSF105	BM	0.86	-33.88	-0.01	-33.03	-33.08	-32.93
7069	RAMLAS	BM	0.50	-30.04	0.00	-29.53	-29.52	-29.13
7091	HAYLAS	BM	0.49	-29.19	-0.01	-28.71	-28.61	-27.55
7120	MUILAS	BM	14.70	3.21	0.00	17.91	13.02	20.46
7210	MAULAS	IA	14.73	3.20	0.00	17.94	13.02	20.49
7090	YARLAS	BM	-0.87	-24.21	0.00	-25.08	-25.02	-24.28
7943	ORRLAS	UN	4.44	14.72	0.01	19.17	20.36	20.38
7067	BDILAS	BM	6.63	-38.72	-0.01	-32.10	-35.23	-31.81
7805	FINLAS	IA	-0.53	21.20	0.00	20.67	20.54	19.95
7939	MATLAS	UN	6.25	40.12	0.00	46.37	45.66	46.39
7835	GRALAS	UN	5.02	46.81	0.01	51.83	51.04	42.85
7840	RGOLAS	UN	-1.53	47.40	0.01	45.88	46.06	45.58
8833	KOOLAS	UN	-0.06	44.55	0.01	44.49	44.80	44.66
7834	WETLAS	IA	2.28	44.65	0.01	46.94	47.02	47.65
7838	SHOLAS	UN	4.79	34.38	0.01	39.18	37.60	39.97

ellispoidal correction NE ($\delta N_1+\delta N$ terms of eq. (6.22)). For the 17 laser stations in the Western United States the NC includes the cap contribution using terrain-corrected gravity anomalies and the indirect effect δN_I (see eq. (5.15)):

$$NC = \frac{R}{4\pi\gamma} \iint_{\sigma_c} (\hat{\Delta}g^T+TC)S(\cos\psi)d\sigma + \delta N_I \qquad (8.1)$$

In Tables 17 through 21 the "NC" column will always be given by (8.1) for the various modifications of the Stokes' function $S_i(\cos\psi)$, unless otherwise stated. The seventh columm (N) is the total undulation computed using the OSU86F set up to M-360 (equation (6.27)). Finally, the last column is the value of the undulation computed from equation (4.2) (Ellipsoidal minus orthometric height). Units are in meters. Tables 18, 19 and 20 show the results for Meissl's, Molodenskii's and modified Sjöberg's methods and their description is identical with the description of Table 17 above.

Table 21 summarizes the results of the four methods by region: The first two columns show the number and name of the laser station; columns three to six show the total undulation computed using the four different methods: Stokes', Meissl's, Molodenskii's and modified Sjöberg's method respectively; the seventh column shows the height reference; the eighth column shows the value of the undulation using the OSU86F set as above and the last column shows the value of the undulation computed from equation (4.2).

Table 19. Geoid Undulations of the Laser Stations Using Molodenskii's Method (Units are in meters).

NUM	NAME	REF	NC	NP	NE	N	OSU86 F	ELL-ORT
7051	QUILAS	BM	2.28	-26.53	-0.01	-24.34	-23.64	-22.57
7109	QUILAS	BM	2.28	-26.53	-0.01	-24.34	-23.65	-22.59
7886	QUILAS	UN	2.28	-26.53	-0.01	-24.34	-23.65	-19.38
7062	SANDIE	BM	-0.65	-34.41	0.00	-35.07	-34.22	-32.47
7110	MONLAS	BM	0.51	-33.68	0.00	-33.18	-32.78	-30.86
7082	BEARLK	BM	0.82	-17.46	0.00	-16.64	-15.16	-12.58
7084	OVRLAS	BM	1.04	-28.55	-0.01	-27.52	-26.29	-24.90
7114	OVRLAS	BM	1.03	-28.55	-0.01	-27.52	-26.30	-24.84
7085	GOLDLS	BM	-1.51	-30.36	-0.01	-31.87	-31.70	-29.68
7115	GOLLAS	BM	-1.51	-30.54	0.00	-32.06	-31.84	-29.58
7086	FTDAVS	BM	1.55	-23.43	0.01	-21.87	-21.36	-20.78
7085	FORLAS	BM	1.55	-23.43	0.01	-21.87	-21.36	-20.83
7112	PLALAS	BM	0.96	-19.82	0.00	-18.86	-18.28	-17.48
7087	VANLAS	UN	-1.59	-34.56	-0.01	-36.16	-36.47	-31.14
7088	HOPLAS	UN	-1.34	-28.91	0.00	-30.25	-29.48	-2.28
7921	HOPLAS	UN	-1.34	-28.91	0.00	-30.25	-29.48	-29.47
7894	YUMLAS	UN	-3.11	-30.96	0.00	-34.07	-33.56	-28.63
7063	STALAS	BM	0.49	-33.68	-0.01	-33.12	-33.08	-32.92
7064	GSFCLS	BM	0.49	-33.68	-0.01	-33.12	-33.08	-33.64
7100	GSF100	BM	0.48	-33.68	-0.01	-33.14	-33.09	-32.58
7101	GSF101	BM	0.48	-33.68	-0.01	-33.14	-33.09	-33.08
7102	GSF102	BM	0.49	-33.68	-0.01	-33.12	-33.08	-32.89
7103	GSF103	BM	0.49	-33.68	-0.01	-33.12	-33.08	-32.93
7104	GSF104	BM	0.48	-33.68	-0.01	-33.13	-33.08	-32.94
7105	GSF105	BM	0.49	-33.68	-0.01	-33.12	-33.08	-32.93
7069	RAMLAS	BM	0.73	-30.13	0.01	-29.39	-29.52	-29.13
7091	HAYLAS	BM	0.51	-29.34	-0.01	-28.85	-28.61	-27.55
7120	MUILAS	BM	17.36	1.00	0.00	18.36	13.02	20.46
7210	MAULAS	IA	17.48	1.00	0.00	18.39	13.02	20.49
7090	YARLAS	BM	-0.83	-24.01	0.00	-24.84	-25.02	-24.28
7943	ORRLAS	UN	5.77	13.12	0.01	18.91	20.36	20.38
7067	BDILAS	BM	6.21	-38.28	-0.01	-32.08	-35.23	-31.81
7805	FINLAS	IA	-1.42	22.03	-0.01	20.60	20.54	19.95
7939	MATLAS	UN	7.86	38.59	0.00	46.45	45.66	46.39
7835	GRALAS	UN	5.87	45.99	0.01	51.87	51.04	42.85
7840	RGOLAS	UN	-1.94	47.75	0.01	45.81	46.06	45.59
8833	KOOLAS	UN	-0.05	44.37	0.00	44.32	44.80	44.66
7834	WETLAS	IA	3.26	43.55	0.01	46.82	47.02	47.65
7838	SHOLAS	UN	5.70	33.35	0.02	39.07	37.60	39.97

Table 20. Geoid Undulations of the Laser Stations Using Modified Sjöberg's Method (Units are in meters).

NUM	NAME	REF	NC	NP	NE	N	OSU86 F	ELL-ORT
7051	QUILAS	BM	2.35	-26.60	-0.01	-24.26	-23.64	-22.57
7109	QUILAS	BM	2.35	-26.61	-0.01	-24.27	-23.65	-22.59
7886	QUILAS	UN	2.35	-26.61	-0.01	-24.26	-23.65	-19.38
7062	SANDIE	BM	-0.83	-34.28	0.00	-35.04	-34.22	-32.47
7110	MONLAS	BM	0.32	-33.37	0.00	-33.06	-32.78	-30.86
7082	BEARLK	BM	1.17	-17.77	0.00	-16.60	-15.16	-12.58
7084	OVRLAS	BM	0.86	-28.43	-0.01	-27.57	-26.29	-24.90
7114	OVRLAS	BM	0.85	-28.42	-0.01	-27.58	-26.30	-24.84
7085	GOLDLS	BM	-1.58	-30.32	-0.01	-31.91	-31.70	-29.68
7115	GOLLAS	BM	-1.59	-30.49	0.00	-32.08	-31.84	-29.58
7086	FTDAVS	BM	1.54	-23.45	0.01	-21.90	-21.36	-20.78
7085	FORLAS	BM	1.54	-23.45	0.01	-21.90	-21.36	-20.83
7112	PLALAS	BM	1.23	-20.18	0.00	-18.95	-18.28	-17.48
7087	VANLAS	UN	-1.87	-34.26	-0.01	-36.14	-36.47	-31.14
7088	HOPLAS	UN	-1.54	-28.78	0.00	-30.32	-29.48	-2.28
7921	HOPLAS	UN	-1.54	-28.78	0.00	-30.32	-29.48	-29.47
7894	YUMLAS	UN	-3.23	-30.86	0.00	-34.09	-33.56	-28.63
7063	STALAS	BM	0.40	-33.58	-0.01	-33.11	-33.08	-32.92
7064	GSFCLS	BM	0.40	-33.58	-0.01	-33.18	-33.08	-33.64
7100	GSF100	BM	0.39	-33.58	-0.01	-33.13	-33.09	-32.58
7101	GSF101	BM	0.39	-33.58	-0.01	-33.12	-33.09	-33.08
7102	GSF102	BM	0.40	-33.58	-0.01	-33.18	-33.08	-32.89
7103	GSF103	BM	0.40	-33.58	-0.01	-33.18	-33.08	-32.93
7104	GSF104	BM	0.39	-33.58	-0.01	-33.12	-33.08	-32.94
7105	GSF105	BM	0.40	-33.58	-0.01	-33.11	-33.08	-32.93
7069	RAMLAS	BM	0.85	-30.18	0.01	-29.33	-29.52	-29.13
7091	HAYLAS	BM	0.45	-29.36	-0.01	-28.92	-28.61	-27.55
7120	MUILAS	BM	17.77	0.86	0.00	18.63	13.02	20.46
7210	MAULAS	IA	17.80	0.86	0.00	18.66	13.02	20.49
7090	YARLAS	BM	-0.97	-23.91	0.00	-24.88	-25.02	-24.28
7943	ORRLAS	UN	5.90	12.94	0.01	18.85	20.36	20.38
7067	BDILAS	BM	5.99	-37.95	-0.01	-31.97	-35.23	-31.81
7805	FINLAS	IA	-1.80	22.72	-0.01	20.91	20.54	19.95
7939	MATLAS	UN	7.91	37.84	0.01	45.76	45.66	46.39
7835	GRALAS	UN	5.90	45.64	0.01	51.55	51.04	42.85
7840	RGOLAS	UN	-1.94	47.89	0.01	45.96	46.06	45.58
8833	KOOLAS	UN	0.00	44.21	0.01	44.22	44.80	44.66
7834	WETLAS	IA	3.62	42.73	0.02	46.37	47.02	47.65
7838	SHOLAS	UN	5.99	32.61	0.02	38.63	37.60	39.97

Table 21. Total Geoid Undulations of the Laser Stations Using All the Four Methods (Units are in meters).

NUM	NAME	STOKES	MEISSL	MOLOD.	SJOB.	REF	OSU86F	ELL-ORT
			WEST UNITED STATES					
7051	QUILAS	-24.35	-24.34	-24.34	-24.26	BM	-23.64	-22.57
7109	QUILAS	-24.35	-24.34	-24.34	-24.27	BM	-23.65	-22.59
7886	QUILAS	-24.35	-24.34	-24.34	-24.26	UN	-23.65	-19.30
7062	SANDIE	-35.30	-34.90	-35.07	-35.04	BM	-34.22	-32.47
7110	MONLAS	-33.39	-32.87	-33.10	-33.06	BM	-32.78	-30.86
7082	BEARLK	-16.99	-16.36	-16.64	-16.60	BM	-15.16	-12.58
7084	OVRLAS	-27.42	-27.59	-27.52	-27.57	BM	-26.29	-24.90
7114	OVRLAS	-27.42	-27.59	-27.52	-27.58	BM	-26.30	-24.84
7085	GOLDLS	-31.94	-31.81	-31.87	-31.91	BM	-31.70	-29.68
7115	GOLLAS	-32.16	-31.97	-32.06	-32.08	BM	-31.84	-29.58
7086	FTDAVS	-22.17	-21.64	-21.87	-21.90	BM	-21.36	-20.78
7885	FORLAS	-22.17	-21.64	-21.87	-21.90	BM	-21.36	-20.83
7112	PLALAS	-18.96	-19.77	-18.86	-18.95	BM	-18.28	-17.40
7887	VANLAS	-36.12	-36.19	-36.16	-36.14	UN	-36.47	-31.14
7888	HOPLAS	-30.48	-30.07	-30.25	-30.32	UN	-29.48	-2.20
7921	HOPLAS	-30.48	-30.07	-30.25	-30.32	UN	-29.48	-29.47
7894	YUMLAS	-34.34	-33.86	-34.07	-34.09	UN	-33.56	-28.63
			EAST UNITED STATES					
7063	STALAS	-33.23	-33.03	-33.12	-33.11	BM	-33.08	-32.92
7064	GSFCLS	-33.23	-33.03	-33.12	-33.10	BM	-33.08	-33.64
7100	GSF100	-33.25	-33.05	-33.14	-33.13	BM	-33.09	-32.50
7101	GSF101	-33.25	-33.05	-33.14	-33.12	BM	-33.09	-33.08
7102	GSF102	-33.23	-33.03	-33.12	-33.10	BM	-33.08	-32.89
7103	GSF103	-33.23	-33.03	-33.12	-33.10	BM	-33.08	-32.93
7104	GSF104	-33.25	-33.04	-33.13	-33.12	BM	-33.08	-32.94
7105	GSF105	-33.23	-33.03	-33.12	-33.11	BM	-33.08	-32.93
7069	RAMLAS	-29.22	-29.53	-29.39	-29.33	BM	-29.52	-29.13
7091	HAYLAS	-29.02	-28.71	-28.85	-28.92	BM	-28.61	-27.55
			HAWAII					
7120	MUILAS	18.93	17.91	18.36	18.63	BM	13.02	20.46
7210	MAULAS	18.96	17.94	18.39	18.66	IA	13.02	20.49
			AUSTRALIA					
7090	YARLAS	-24.77	-25.08	-24.84	-24.88	BM	-25.02	-24.28
7943	ORRLAS	18.57	19.17	18.91	18.85	UN	20.36	20.38
			BERMUDA					
7067	BDILAS	-32.05	-32.10	-32.08	-31.97	BM	-35.23	-31.81
			EUROPE					
7805	FINLAS	20.53	20.67	20.60	20.91	IA	20.54	19.95
7939	MATLAS	46.55	46.37	46.45	45.76	UN	45.66	46.39
7835	GRALAS	51.93	51.83	51.87	51.55	UN	51.04	42.85
7840	RGOLAS	45.75	45.88	45.81	45.96	UN	46.06	45.58
8833	KOOLAS	44.13	44.49	44.32	44.22	UN	44.80	44.66
7834	WETLAS	46.68	46.94	46.82	46.37	IA	47.02	47.65
			JAPAN					
7838	SHOLAS	38.93	39.18	39.07	38.63	UN	37.60	39.97

In Tables 22 and 23 the undulations for the western United States laser stations computed using terrain-corrected (NC from (8.1)) and uncorrected gravity data with the modified Sjöberg's method are shown. In Table 24 the total geoid undulation of the laser stations using the local average correction discussed in Chapter 7 for all the four methods are shown. The magnitude of this effect is 1-2 m. It would be helpful to have a table of residuals between the undulations computed using all the four methods and the undulations computed from equation (4.2). These residuals were computed only for the 28 laser stations with known height references. Table 25 shows the number and name of the laser stations, the differences N_i-(h-H) where N_i are given in Table 21 for all the four methods and h-H is the undulation computed from eq. (4.2), the height references and the residuals between the undulations computed from the OSU86F set (M=360) and the h-H value.

The corresponding table of residuals when the local average correction is included is shown in Table 26. The statistics of the residuals between the terrain-corrected N_{TC} and the uncorrected N_{UN} using the modified Sjöberg's method and the N_T = h-H value are shown in Table 27 for the 12 laser stations in the western United States (corresponded values in Tables 22 and 23).

In Table 28 the statistics of the residuals of the Table 25 are shown (undulations computed using all four methods vs. the N_T value) and in Table 29 the corresponded statistics including the local average correction are shown.

Table 22. Geoid Undulations of the 17 Laser Stations in the Western United States Using Modified Sjöberg's Method and Terrain-corrected Gravity Anomalies (Units are in meters).

NUM	NAME	REF	NC	NP	NE	N	OSU86 F	ELL-ORT
7051	QUILAS	BM	2.35	-26.60	-0.01	-24.26	-23.64	-22.57
7109	QUILAS	BM	2.35	-26.61	-0.01	-24.27	-23.65	-22.59
7886	QUILAS	UN	2.35	-26.61	-0.01	-24.26	-23.65	-19.30
7062	SANDIE	BM	-0.83	-34.20	0.00	-35.04	-34.22	-32.47
7110	MONLAS	BM	0.32	-33.37	0.00	-33.06	-32.78	-30.86
7082	BEARLK	BM	1.17	-17.77	0.00	-16.60	-15.16	-12.58
7084	OVRLAS	BM	0.86	-28.43	-0.01	-27.57	-26.29	-24.90
7114	OVRLAS	BM	0.85	-28.42	-0.01	-27.58	-26.30	-24.84
7085	GOLDLS	BM	-1.58	-30.32	-0.01	-31.91	-31.70	-29.68
7115	GOLLAS	BM	-1.59	-30.49	0.00	-32.08	-31.84	-29.58
7086	FTDAVS	BM	1.54	-23.45	0.01	-21.90	-21.36	-20.78
7885	FORLAS	BM	1.54	-23.45	0.01	-21.90	-21.36	-20.83
7112	PLALAS	BM	1.23	-20.18	0.00	-18.95	-18.28	-17.40
7887	VANLAS	UN	-1.87	-34.26	-0.01	-36.14	-36.47	-31.14
7888	HOPLAS	UN	-1.54	-28.78	0.00	-30.32	-29.48	-2.20
7921	HOPLAS	UN	-1.54	-28.78	0.00	-30.32	-29.48	-29.47
7894	YUMLAS	UN	-3.23	-30.86	0.00	-34.09	-33.56	-28.63

Table 23. Geoid Undulations of the 17 Laser Stations in the Western United States Using Modified Sjöberg's Method and Uncorrected Gravity Anomalies (Units are in meters).

NUM	NAME	REF	NC	NP	NE	N	OSU86 F	ELL-ORT
7051	QUILAS	BM	1.77	-26.60	-0.01	-24.84	-23.64	-22.57
7109	QUILAS	BM	1.77	-26.61	-0.01	-24.84	-23.65	-22.59
7886	QUILAS	UN	1.77	-26.61	-0.01	-24.84	-23.65	-19.30
7062	SANDIE	BM	-1.22	-34.20	0.00	-35.43	-34.22	-32.47
7110	MONLAS	BM	-0.07	-33.37	0.00	-33.45	-32.78	-30.86
7082	BEARLK	BM	0.87	-17.77	0.00	-16.90	-15.16	-12.58
7084	OVRLAS	BM	-0.16	-28.43	-0.01	-28.59	-26.29	-24.90
7114	OVRLAS	BM	-0.17	-28.42	-0.01	-28.60	-26.30	-24.84
7085	GOLDLS	BM	-2.21	-30.32	-0.01	-32.54	-31.70	-29.68
7115	GOLLAS	BM	-2.16	-30.49	0.00	-32.65	-31.84	-29.58
7086	FTDAVS	BM	1.32	-23.45	0.01	-22.12	-21.36	-20.78
7885	FORLAS	BM	1.32	-23.45	0.01	-22.12	-21.36	-20.83
7112	PLALAS	BM	1.05	-20.18	0.00	-19.13	-18.28	-17.40
7887	VANLAS	UN	-2.13	-34.26	-0.01	-36.40	-36.47	-31.14
7888	HOPLAS	UN	-1.65	-28.78	0.00	-30.43	-29.48	-2.20
7921	HOPLAS	UN	-1.65	-28.78	0.00	-30.43	-29.48	-29.47
7894	YUMLAS	UN	-3.39	-30.86	0.00	-34.25	-33.56	-28.63

Table 24. Total Geoid Undulations of the Laser Stations Using All the Four Methods and the Local Average Correction (Units are in meters).

NUM	NAME	STOKES	MEISSL	MOLOD.	SJOB.	REF	OSU86F	ELL-ORT
			WEST UNITED STATES					
7051	QUILAS	-24.79	-24.55	-24.65	-24.60	BM	-23.64	-22.57
7109	QUILAS	-24.79	-24.55	-24.65	-24.61	BM	-23.65	-22.59
7886	QUILAS	-24.79	-24.55	-24.65	-24.60	UN	-23.65	-19.30
7062	SANDIE	-34.93	-34.73	-34.81	-34.76	BM	-34.22	-32.47
7110	MONLAS	-33.02	-32.70	-32.84	-32.78	BM	-32.78	-30.86
7082	BEARLK	-14.36	-15.11	-14.78	-14.57	BM	-15.16	-12.58
7084	OVRLAS	-27.62	-27.69	-27.66	-27.73	BM	-26.29	-24.90
7114	OVRLAS	-27.62	-27.69	-27.66	-27.74	BM	-26.30	-24.84
7085	GOLDLS	-31.79	-31.74	-31.76	-31.79	BM	-31.70	-29.68
7115	GOLLAS	-32.01	-31.90	-31.95	-31.96	BM	-31.84	-29.58
7086	FTDAVS	-20.95	-21.06	-21.01	-20.96	BM	-21.36	-20.78
7085	FORLAS	-20.95	-21.06	-21.01	-20.96	BM	-21.36	-20.83
7112	PLALAS	-19.01	-18.80	-18.90	-18.99	BM	-18.28	-17.40
7087	VANLAS	-36.26	-36.25	-36.26	-36.24	UN	-36.47	-31.14
7088	HOPLAS	-29.99	-29.84	-29.90	-29.94	UN	-29.48	-2.20
7921	HOPLAS	-29.99	-29.84	-29.90	-29.94	UN	-29.48	-29.47
7894	YUMLAS	-33.44	-33.43	-33.43	-33.40	UN	-33.56	-28.63
			EAST UNITED STATES					
7063	STALAS	-32.71	-32.78	-32.75	-32.71	BM	-33.08	-32.92
7064	GSFCLS	-32.71	-32.78	-32.75	-32.70	BM	-33.08	-33.64
7100	GSF100	-32.73	-32.80	-32.77	-32.73	BM	-33.09	-32.50
7101	GSF101	-32.73	-32.80	-32.77	-32.72	BM	-33.09	-33.08
7102	GSF102	-32.71	-32.78	-32.75	-32.70	BM	-33.08	-32.89
7103	GSF103	-32.71	-32.78	-32.75	-32.70	BM	-33.08	-32.93
7104	GSF104	-32.73	-32.79	-32.76	-32.72	BM	-33.08	-32.94
7105	GSF105	-32.71	-32.78	-32.75	-32.71	BM	-33.08	-32.93
7069	RAMLAS	-29.90	-29.85	-29.87	-29.86	BM	-29.52	-29.13
7091	HAYLAS	-28.54	-28.48	-28.51	-28.55	BM	-28.61	-27.55
			HAWAII					
7120	MUILAS	18.56	17.73	18.10	18.34	BM	13.02	20.46
7210	MAULAS	18.59	17.76	18.13	18.37	IA	13.02	20.49
			AUSTRALIA					
7090	YARLAS	-24.99	-25.18	-25.00	-25.05	BM	-25.02	-24.28
7943	ORRLAS	19.39	19.56	19.49	19.48	UN	20.36	20.38
			BERMUDA					
7067	BDILAS	-32.13	-32.14	-32.11	-32.03	BM	-35.23	-31.81
			EUROPE					
7805	FINLAS	20.59	20.70	20.64	20.96	IA	20.54	19.95
7939	MATLAS	46.56	46.38	46.46	45.77	UN	45.66	46.39
7835	GRALAS	51.83	51.78	51.80	51.47	UN	51.04	42.85
7840	RGOLAS	46.31	46.15	46.21	46.39	UN	46.06	45.58
8833	KOOLAS	44.74	44.78	44.75	44.69	UN	44.80	44.66
7834	WETLAS	46.53	46.87	46.72	46.26	IA	47.02	47.65
			JAPAN					
7836	SHOLAS	39.56	39.48	39.51	39.11	UN	37.60	39.97

Table 25. Differences Between the Undulations Computed Using All the Four Methods (and the OSU86F set) and the N_T Value (Units are in meters). Number of Stations: 28.

NUM	NAME	STOKES	MEISSL	MOLOD.	SJOB.	REF	OSU86F
7051	QUILAS	-1.78	-1.77	-1.77	-1.69	BM	-1.07
7109	QUILAS	-1.76	-1.75	-1.75	-1.68	BM	-1.06
7062	SANDIE	-2.83	-2.43	-2.60	-2.57	BM	-1.75
7110	MONLAS	-2.53	-2.01	-2.24	-2.20	BM	-1.92
7082	BEARLK	-4.41	-3.78	-4.06	-4.02	BM	-2.58
7084	OVRLAS	-2.52	-2.69	-2.62	-2.67	BM	-1.39
7114	OVRLAS	-2.58	-2.75	-2.68	-2.74	BM	-1.46
7085	GOLDLS	-2.26	-2.13	-2.19	-2.23	BM	-2.02
7115	GOLLAS	-2.58	-2.39	-2.48	-2.50	BM	-2.26
7086	FTDAVS	-1.39	-0.86	-1.09	-1.12	BM	-0.58
7885	FORLAS	-1.34	-0.81	-1.04	-1.07	BM	-0.53
7112	PLALAS	-1.56	-1.37	-1.46	-1.55	BM	-0.88
7063	STALAS	-0.31	-0.11	-0.20	-0.19	BM	-0.16
7064	GSFCLS	0.41	0.61	0.52	0.54	BM	0.56
7100	GSF100	-0.75	-0.55	-0.64	-0.63	BM	-0.59
7101	GSF101	-0.17	0.03	-0.06	-0.04	BM	-0.01
7102	GSF102	-0.34	-0.14	-0.23	-0.21	BM	-0.19
7103	GSF103	-0.30	-0.10	-0.19	-0.17	BM	-0.15
7104	GSF104	-0.31	-0.10	-0.19	-0.18	BM	-0.14
7105	GSF105	-0.30	-0.10	-0.19	-0.18	BM	-0.15
7069	RAMLAS	-0.09	-0.40	-0.26	-0.20	BM	-0.39
7091	HAYLAS	-1.47	-1.16	-1.30	-1.37	BM	-1.06
7120	MUILAS	-1.53	-2.55	-2.10	-1.83	BM	-7.44
7210	MAULAS	-1.53	-2.55	-2.10	-1.83	IA	-7.47
7090	YARLAS	-0.49	-0.80	-0.56	-0.60	BM	-0.74
7067	BDILAS	-0.24	-0.29	-0.27	-0.16	BM	-3.42
7805	FINLAS	0.58	0.72	0.65	0.96	IA	0.59
7834	WETLAS	-0.97	-0.71	-0.83	-1.28	IA	-0.63

Table 26. Differences Between the Undulations Computed Using All the Four Methods (and the OSU86F set) with the Local Average Correction and the N_T Value (Units are in meters). Number of Stations: 28.

NUM	NAME	STOKES	MEISSL	MOLOD.	SJOB.	REF	OSU86F
7051	QUILAS	-2.22	-1.98	-2.08	-2.03	BM	-1.07
7109	QUILAS	-2.20	-1.96	-2.06	-2.02	BM	-1.06
7062	SANDIE	-2.46	-2.26	-2.34	-2.29	BM	-1.75
7110	MONLAS	-2.16	-1.84	-1.98	-1.92	BM	-1.92
7082	BEARLK	-1.78	-2.53	-2.20	-1.99	BM	-2.58
7084	OVRLAS	-2.72	-2.79	-2.76	-2.83	BM	-1.39
7114	OVRLAS	-2.78	-2.85	-2.82	-2.90	BM	-1.46
7085	GOLDLS	-2.11	-2.06	-2.08	-2.11	BM	-2.02
7115	GOLLAS	-2.43	-2.32	-2.37	-2.38	BM	-2.26
7086	FTDAVS	-0.17	-0.28	-0.23	-0.18	BM	-0.58
7885	FORLAS	-0.12	-0.23	-0.18	-0.13	BM	-0.53
7112	PLALAS	-1.61	-1.40	-1.50	-1.59	BM	-0.88
7063	STALAS	0.21	0.14	0.17	0.21	BM	-0.16
7064	GSFCLS	0.93	0.86	0.89	0.94	BM	0.56
7100	GSF100	-0.23	-0.30	-0.27	-0.23	BM	-0.59
7101	GSF101	0.35	0.28	0.31	0.36	BM	-0.01
7102	GSF102	0.18	0.11	0.14	0.19	BM	-0.19
7103	GSF103	0.22	0.15	0.18	0.23	BM	-0.15
7104	GSF104	0.21	0.15	0.18	0.22	BM	-0.14
7105	GSF105	0.22	0.15	0.18	0.22	BM	-0.15
7069	RAMLAS	-0.77	-0.72	-0.74	-0.73	BM	-0.39
7091	HAYLAS	-0.99	-0.93	-0.96	-1.00	BM	-1.06
7120	MUILAS	-1.90	-2.73	-2.36	-2.12	BM	-7.44
7210	MAULAS	-1.90	-2.73	-2.36	-2.12	IA	-7.47
7090	YARLAS	-0.71	-0.90	-0.72	-0.77	BM	-0.74
7067	BDILAS	-0.32	-0.33	-0.33	-0.22	BM	-3.42
7805	FINLAS	0.64	0.75	0.69	1.01	IA	0.59
7834	WETLAS	-1.12	-0.78	-0.93	-1.39	IA	-0.63

Table 27. Statistics of the Differences Between the Terrain-corrected N_{TC} and Uncorrected N_{UN} Undulations and the N_T Value Using the Modified Sjöberg's Method for Stations in the Western United States (Units are in meters). Number of Stations: 12.

STATISTICS	$N_{TC}-N_T$	$N_{UN}-N_T$
Mean Difference	-2.17	-2.68
RMS Difference	2.31	2.83
Standard Deviation Difference	0.79	0.92
Minimum Difference	-4.02	-4.32
Maximum Difference	-1.07	-1.29

Table 28. Statistics of the Differences Between the Undulations Computed Using All the Four Methods N_i (and the OSU86F Field) and the N_T Value (Units are in meters). Number of Stations: 28.

STATISTICS	N_1-N_T	N_2-N_T	N_3-N_T	N_4-N_T	N_R-N_T	N_R-N_T*
Mean Difference	-1.27	-1.18	-1.21	-1.21	-1.39	-0.92
RMS Difference	1.70	1.65	1.66	1.65	2.36	1.44
Standard Dev. Diff.	1.13	1.15	1.14	1.12	1.91	1.10
Minimum Difference	-4.41	-3.78	-4.06	-4.02	-7.47	-3.42
Maximum Difference	0.58	0.72	0.65	0.96	0.59	0.59

*excluding stations 7120, 7210

Table 29. Statistics of the Differences Between the Undulation Computed Using All the Four Methods N_i' Including the Local Average Correction and the N_T Value (Units are in meters). Number of Stations: 28.

STATISTICS	$N_1'-N_T$	$N_2'-N_T$	$N_3'-N_T$	$N_4'-N_T$
Mean Difference	-1.00	-1.06	-1.03	-1.03
RMS Difference	1.52	1.58	1.54	1.53
Standard Deviation Difference	1.14	1.17	1.15	1.17
Minimum Difference	-2.78	-2.85	-2.82	-2.90
Maximum Difference	0.93	0.86	0.89	1.01

8.3 Discussion of the results

Comparing the terrain-corrected vs. the uncorrected undulations for 12 stations in the western United States (Table 27) we see that the terrain-corrected undulations have better agreement with the N_T value

than the uncorrected undulations: The mean and the RMS difference with the N_T value reduced by ~50 cm when terrain-corrected data was used. The standard deviation of the difference also decreased by ~20 cm when the terrain corrections were taken into account. When we compare the four methods with the N_T value for all the 28 stations for which we have known height references the standard deviation of the difference is ~1.10 m (Table 28). From the same Table we can see that the standard deviation of the difference between the undulations computed using the OSU86F set and the N_T values is 1.91 m. If we are to exclude the two laser stations 7120, 7210 in Maui that show large discrepancies, then the standard deviation of the difference drops to 1.10 m. If we examine Table 25 we see that there are systematic differences for the undulations of the 12 Western United States stations and the N_T value on the order of 2 m. To further investigate these systematic differences the 15′x15′ mean anomalies in the northern United States and Canada (Lachapelle et al., 1982) were used to compute geoid undulations for the above stations. The statistics of the residuals between the values of the undulations using the above data set and the N_T value are shown in Table 30 for all four methods. For the same 12 stations the corresponding statistics using the 2′x2′ anomalies (Table 12) are shown in Table 31. We can see that the systematic differences are also present when the 15′x15′ anomalies are used. However, the standard deviation of the difference decreased from 79 cm (2′x2′ data) to 65 cm (15′x15′ data) which is surprising since one would expect better accuracy when the 2′x2′ data are used instead of the 15′x15′ data. The explanation may be that the 15′ averaging procedure was

Table 30. Statistics of the Differences Between the Undulations Computed Using the 15′x15′ Anomalies and the N_T Value for the 12 Western U.S. Laser Stations. The Modified Sjöberg's Method Has Been Used (Units are in meters).

STATISTICS	N_1-N_T	N_2-N_T	N_3-N_T	N_4-N_T
Mean Difference	-1.99	-1.72	-1.83	-1.82
RMS Difference	2.10	1.83	1.93	1.95
Standard Deviation Difference	0.65	0.65	0.61	0.72
Minimum Difference	-2.88	-2.66	-2.64	-2.69
Maximum Difference	-1.04	-0.73	-0.87	-0.62

Table 31. Statistics of the Differences Between the Undulations Computation Using the 2′x2′ Anomalies (and the OSU86F Field) and the N_T Value for the 12 Western U.S. Laser Stations. The Modified Sjöberg's Method Has Been Used (Units are in meters).

STATISTICS	N_1-N_T	N_2-N_T	N_3-N_T	N_4-N_T	N_R-N_T
Mean Difference	-2.29	-2.06	-2.17	-2.17	-1.46
RMS Difference	2.43	2.21	2.31	2.31	1.59
Standard Dev. Diff.	0.81	0.81	0.79	0.79	0.63
Minimum Difference	-4.41	-3.78	-4.06	-4.02	-0.53
Maximum Difference	-1.34	-0.81	-1.04	-1.07	-2.58

better than the 2′ averaging procedure. The undulations computed from the OSU86F set for the above 12 stations give statistics similar to the undulations computed from the 15′x15′ data when compared to the N_T value. This is an expected result, since the 15′x15′ data was used for the computation of the OSU86F set. The cause of the above systematic differences was not found and further studies are needed to investigate why these systematic differences are present.

The application of the local average correction improves the statistics as it can be seen by comparing Tables 28 and 29. Note the

improvement (compare Tables 25 and 26) of about 2 meters of the undulation of station 7082 in Bear Lake, Utah when the local average correction was used with respect to the N_T value.

Furthermore, there is an excellent internal agreement between the undulations computed using all the four methods. The standard deviations of the differences between the undulations computed using two different methods is on the order of 20 cm. When the undulations computed using all the four methods are compared to the undulations computed using the OSU86F set they have a standard deviation difference of about 1.5 m. The largest differences between the various methods and the OSU86F set occur for the 2 laser stations on Maui (~5 m) and for the Bermuda station (~3 m). The gravimetric undulations for the above cases are closer to the N_T values than the undulations computed from the OSU86F set.

Using a set of 14070 point free-air gravity anomlies by Watts (private communication, 1987) in the vicinity of Hawaii the geoid undulation of the laser station 7210 was computed to be as follows: 18.64 m, 17.95 m, 18.26 m and 18.50 m for the Stokes', Meissl's, Molodenskii's and modified Sjöberg's method respectively. We can see that the above results agree within ~20 cm with the gravimetric values of the undulations of Tables 21 and 24. From the gravity data sent by Watts 8.43 mgal were subtracted to account for a systematic difference that was detected within the 5°x5° computation area in the vicinity of

Hawaii between the Watt's set and the anomalies implied by the OSU86F set.

8.4 Altimeter Geoid Undulation Computations in Bermuda Area

An alternative method to compute geoid undulations is the method of the least squares collocation. This method was applied to the 10360 Ohio State adjusted GEOS-3/SEASAT altimeter sea surface heights (Liang, 1983) covering the Bermuda region ($33°.5 \leq \phi < 31°.63$, $294°.5 \leq \lambda < 295°.87$, laser station number 7067). The above altimeter data was referred to an equatorial radius of 6378137 m. To refer the altimeter data to the equatorial radius of our adopted reference ellipsoid (see Chapter 4, equation (4.1)) we added 1 meter to all the sea surface heights that were selected for the collocation method. We then used the collocation method to compute the undulation at the laser station 7067 with the following specifications:

a) The whole area (1°.37 x 1°.37) was subdivided into 49 0°.20 x 0°.20 sub-areas so that a maximum of 300 points were used for each area by the collocation method. For the predictions near the edges of each 0°.20 x 0°.20 area, a border of 0°.20 was specified.

b) The covariance function used between degrees 2 and 180 was the one implied by the anomaly error degree variances of the potential coefficient solution of Rapp (1981b); between degrees 180 to ∞ the Tscherning-Rapp (1974) model (see eq. (2.18)) was used for the anomaly degree variances.

c) The reference field up to 180 was removed from the data using the solution of Rapp (1981b).

d) The predictions of the undulations were done at the intersections of the points of a grid of 2′x2′. The value of the undulation for the laser station 7067 was then computed using the four closest grid points by bi-linear interpolation with respect to the latitude and the longitude.

The value of the undulation computed from the above collocation method was -32.11 m. The accuracy of the undulation predictions at the four closest grid points was ±0.28 m.

Using the results of the collocation method and the modified Sjöberg's method two geoid maps (Figures 14 and 15) were produced in the Bermuda region ($31°.63 < \phi \leq 33°$, $294°.5 < \lambda \leq 295°.87$). The corresponding map of the differences between the gravimetric and the altimetric geoid (Figure 14 - Figure 15) is shown in Figure 16. The mean difference of the 1764 undulations computed at the 2′ grid intersections in the above region minus the corresponding altimetric undulations was -0.63 m; the RMS difference was 0.78 m and the standard deviation of the difference was 0.47 m.

The laser station 7067 has been also used for the calibration of the altimeter satellites (Kolenkiewicz et al., 1982). Using the four laser supported calibration passes of SEASAT at the time of closest approach to the laser station the geoid undulation has been computed for these

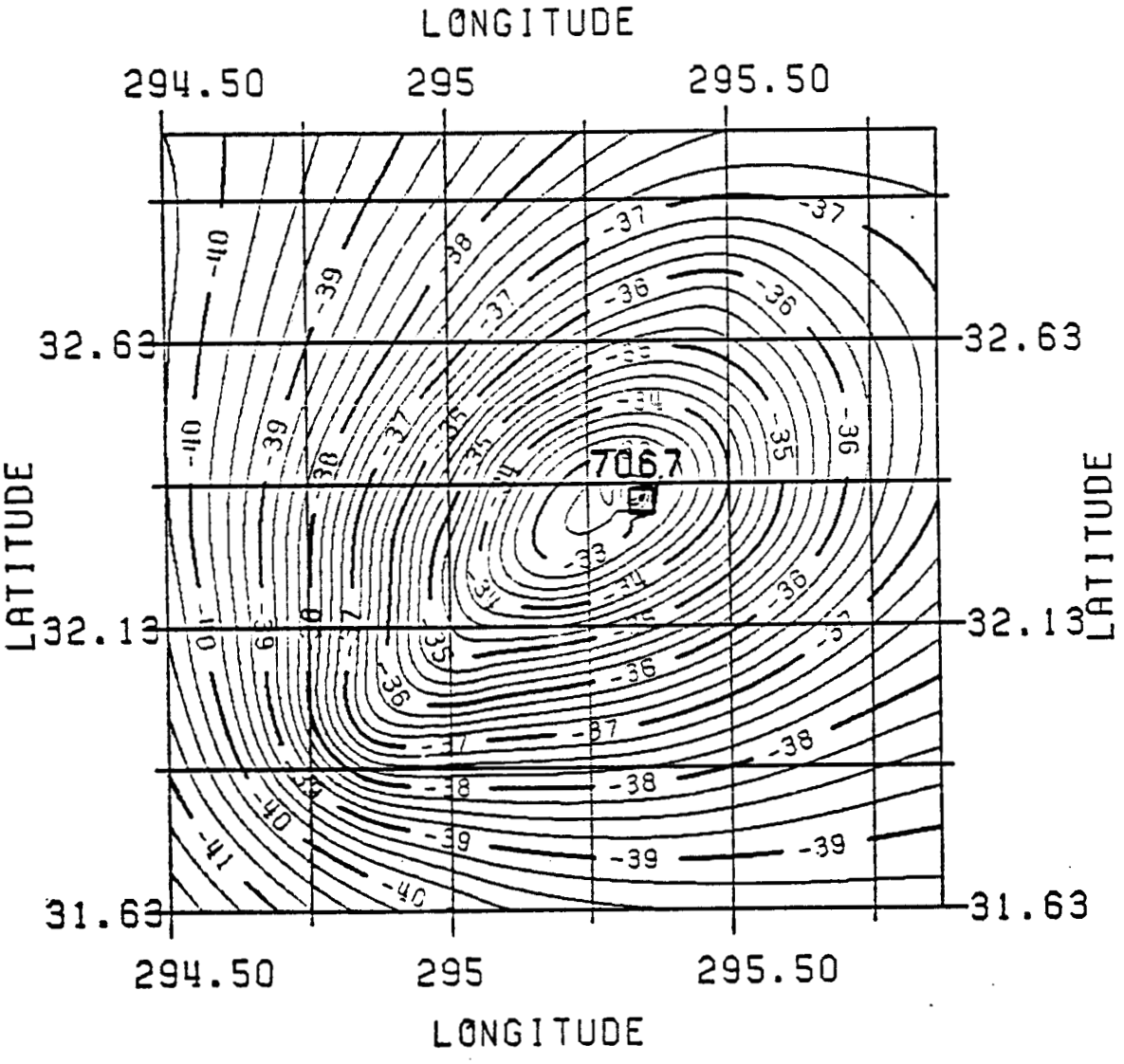

Figure 14. Gravimetric Geoid Using Modified Sjöberg's Method for the Laser Station 7067 in the Bermuda Area (C.I. = 25 cm); 2′x2′ Grid Computed.

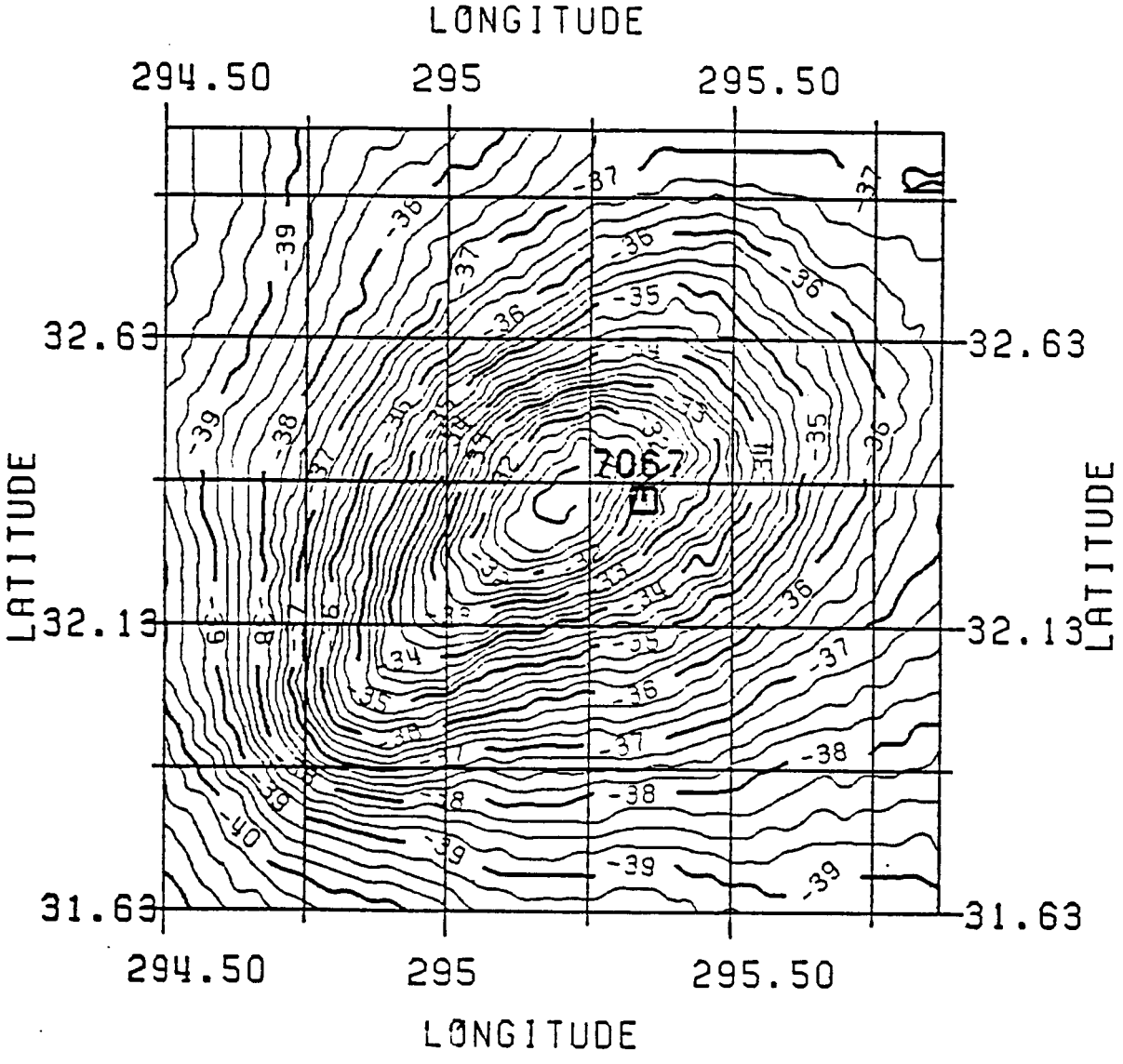

Figure 15. Geoid Computed Using GEOS-3/SEASAT Altimeter Data for the Laser Station 7067 in the Bermuda Area (C.I. = 25 cm); 2′x2′ Grid Computed.

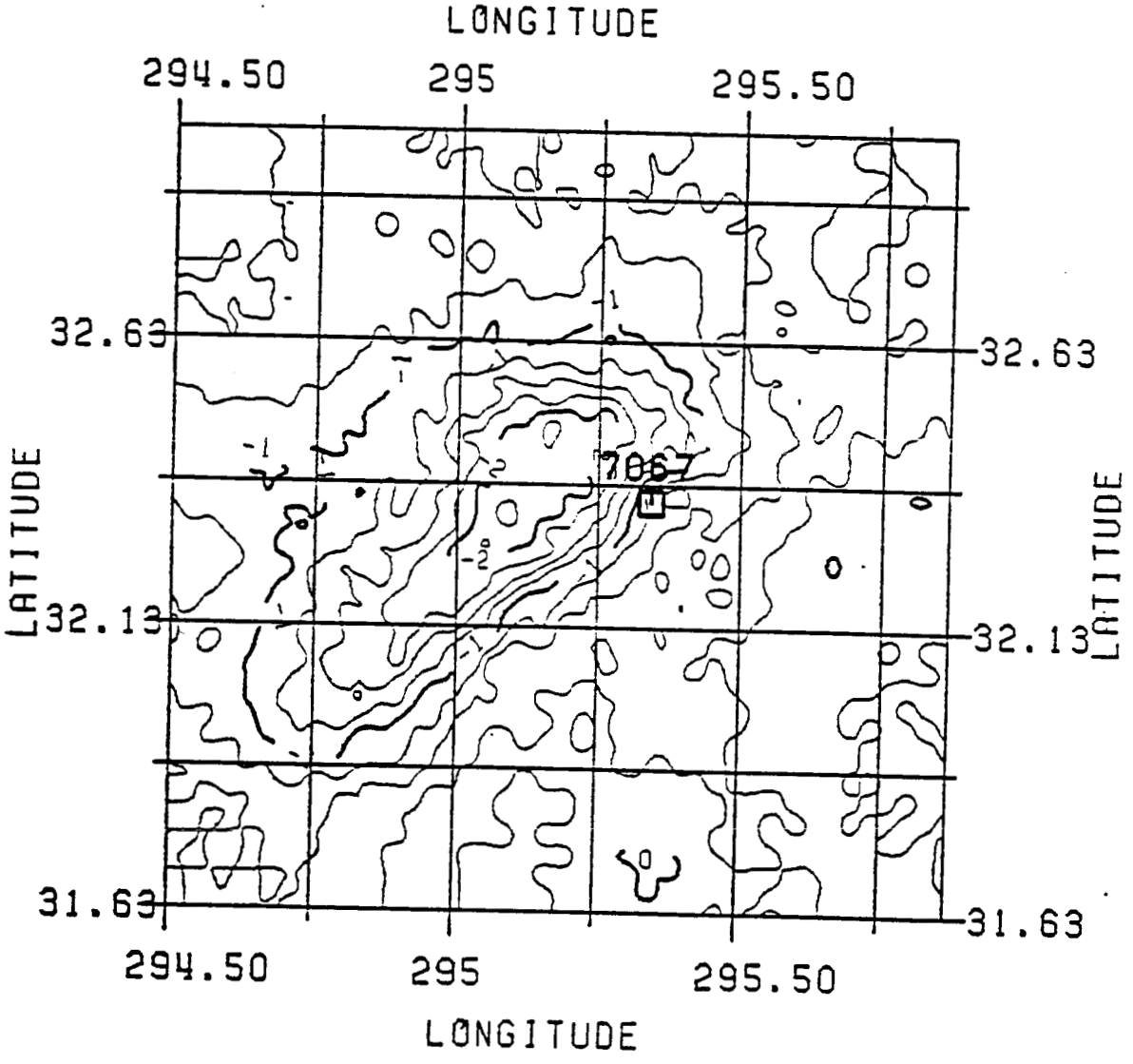

Figure 16. Map of the Differences Between the Gravimetric and the Altimeter Geoid in the Bermuda Area (Figure 14 - Figure 15); C.I. = 25 cm.

passes by Kolenkiewicz et al. (1987), as follows: To the raw altimeter data corrections due to tides, dry troposphere, wet troposphere, ionosphere, center of gravity, sea state bias and height acceleration were applied. Then for the above four closest passes the geoid undulation was obtained from the corrected altimetric observations and the tracking data by smoothing the offshore altimeter data across land (ibid., Table 5). Table 32 summarizes the results obtained from the above SEASAT calibration for the four passes: The first columm gives the date of pass, the second column gives the latitude, the third column gives the geoid undulation which refers to an equatorial radius of 6378137 m and the last column gives the geoid undulation which refers to our adopted equatorial radius of 6378136 m and is obtained by adding 1 meter to column three.

Table 32. Geoid Undulations in meters for the Four SEASAT Passes at the Time of Closest Approach to the Laser Station 7067 in Bermuda (Kolenkiewicz et al., 1987).

Date of Pass 1978	Latitude	Undulation (a_e=6378137 m)	Undulation (a_e=6378136 m)
Sept. 13	32°.3520	-32.89	-31.89
Sept. 16	32°.3553	-32.84	-31.84
Sept. 22	32°.3615	-32.69	-31.69
Oct. 1	32°.3653	-32.62	-31.62

The accuracy that is associated with the above computations (ibid., p. 27) is ±12 cm. To obtain a unique value for the undulation of the laser station (ϕ = 32°.3538) we can linearly interpolate this value with respect to the latitude from the first two values of the undulation (a_e = 6378136 m) of Table 32. This interpolated value of the undulation at the laser

station is then -31.86 m.

Summarizing the geoid undulation computations for the laser station 7067 in Bermuda we have: The gravimetric undulations using all the four methods (Table 21) are: -32.05 m, -32.10 m, -32.08 m, and -31.97 m for the Stokes', Meissl's, Molodenskii's and modified Sjöberg's methods respectively; the "ellipsoidal minus orthometric" value of the undulation is -31.81 m; the value computed from the Ohio State GEOS-3/SEASAT altimeter data is -32.11 m; and the value resulted from the SEASAT calibration is -31.86 m. Thus the results for the Bermuda laser station undulation show a very good agreement on the order of 30 cm using all the different methods. This is clearly due to the sufficient coverage of terrestrial gravity anomalies and GEOS-3/SEASAT altimeter sea surface heights in the Bermuda region.

Finally note that the deviation of the sea surface from the geoid, known as Sea Surface Topography (SST) plays an important role in the above computations and is separately discussed in Appendix B.

8.5 Altimeter Geoid Undulation Computations for the Five Laser Stations in the Western Atlantic and Pacific Using Collocation

Finally, the collocation method applied to the adjusted GEOS-3/SEASAT surface heights as before was used to compute geoid undulations on islands in the Western Atlantic and the Pacific since no terrestrial gravity data was available for the above stations. For each laser station a window of $\Delta\phi = 0^{\circ}.25$ in latitude and $\Delta\lambda = 0^{\circ}.25$ in

longitude centered at the laser station with a border of 0°.25 was used. Again the maximum of data points used was 300. The predictions of the undulations were done at the intersections of the points of a grid of 3′x3′. The value of the undulation was then computed using the four closest grid points by bi-linear interpolation with respect to the latitude and the longitude. Figure 18 shows the undulation map derived from 54 adjusted GEOS-3/SEASAT altimeter data (whose distribution is shown in Figure 17) for the laser station 7061 on Easter Island, Chile. Table 33 shows the laser station number; the number of adjusted GEOS-3/SEASAT altimeter data that were used in the predictions for each oceanic station; the undulation N_{ALT} computed from the OSU86F set taken up to degree 360; and the differences $N_{ALT}-N_T$ and $N_{POT}-N_T$.

In Table 34 we can see the statistics of the differences $N_{ALT}-N_T$ and $N_{pot}-N_T$ for the five oceanic stations. The results using the collocation method showed better agreement with the N_T value than the OSU86F set. The standard deviation of the difference in the first case is 0.79 m and in the second case is 1.25 m. Also the mean difference in the first case is by 1.85 m smaller than in the second case. The better agreements with the N_T values using the collocation method than using the OSU86F set can be explained as follows: Within the collocation method used here all the available altimeter sea surface heights in a 0°.75 x 0°.75 area were taken into account, whereas for the OSU86F solution 0°.5 x 0°.5 mean anomalies derived form the above sea surface heights were used, where clearly some loss of the high frequency information has taken place.

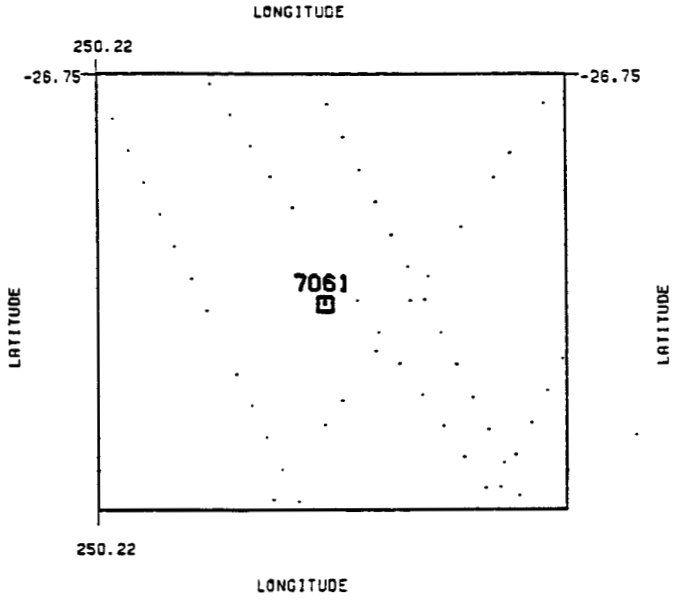

Figure 17. Distribution of the 54 Adjusted GEOS-3/SEASAT Altimeter Data Surrounding the Laser Station 7061 in Easter Island, Chile ($\Delta\phi=\Delta\lambda=0^{\circ}.75$).

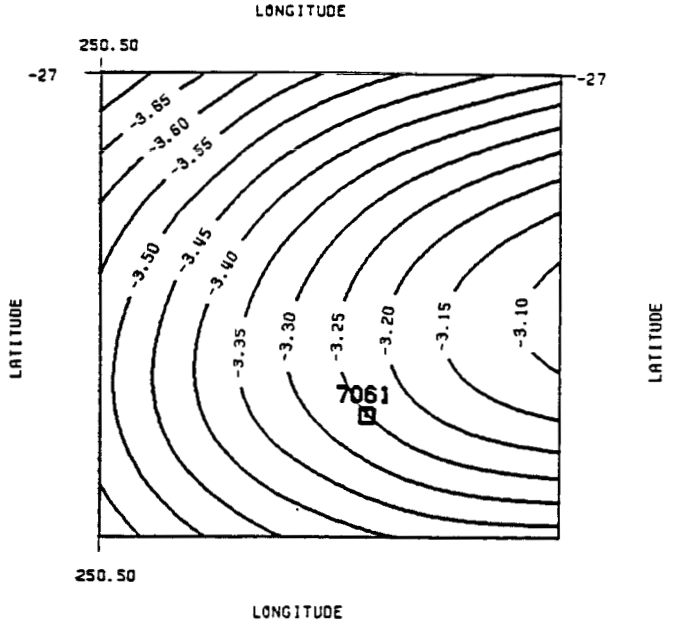

Figure 18. Geoid Undulation Map Based on the Altimeter Data of Fig. 17. C.I. = 5 cm ($\Delta\phi=\Delta\lambda=0^{\circ}.20$).

Finally, the effect of the Sea Surface Topography is separately discussed in Appendix B.

Table 33. Geoid Undulations Computed Using the Collocation Method (N_{ALT}), Based on Adjusted GEOS-3/SEASAT Altimeter Data and from the OSU86F Field, for the Five Oceanic Laser Stations (Units are in meters).

STATION	DATA	N_{ALT}	N_{POT}	N_T	$N_{ALT}-N_T$	$N_{POT}-N_T$
7061	54	- 3.26	- 3.35	- 2.25	-1.01	-1.10
7068	299	-42.63	-44.81	-42.53	-0.10	-2.28
7092	127	31.77	29.72	32.18	-0.41	-2.46
7096	40	33.36	30.45	34.69	-1.33	-4.24
7121	96	8.00	5.96	10.35	-2.35	-4.39

Table 34. Statistics of the Differences $N_{ALT}-N_T$ and $N_{POT}-N_T$ for the Five Oceanic Stations (Units are in meters).

STATISTICS	$N_{ALT}-N_T$	$N_{POT}-N_T$
Mean Difference	-1.04	-2.89
RMS Difference	1.30	2.04
Standard Deviation Difference	0.79	1.25
Minimum Difference	-2.35	-4.39
Maximum Difference	-0.10	-1.10

CHAPTER IX

SUMMARY AND CONCLUSIONS

The geoid undulations for 39 laser stations distributed around the world have been computed using the classical Stokes' and Meissl's methods and the new methods of Molodenskii's and modified Sjöberg's. The high frequency information for the undulation was taken from gravity data within a cap of radius 2° and the low frequency information was taken from a set of potential coefficients (OSU86F). Using the ellipsoidal heights of the laser stations available from the SL6 satellite dynamic solution and the orthometric heights H, available from spirit leveling, the values of the geoid undulation N_T=h-H was obtained and served as a mean for comparisons.

The theoretical improvement in the accuracy of the geoid undulation computations using the modified Sjöberg's method was on the order of 10 cm (Figure 1) which is well below the noise of the actual data used and thus this theoretical improvement was not realized in practice. No method was clearly better than the others. However, all the four methods gave internally consistent results on the order of 30 cm and for most of the regions (Australia, Europe, Bermuda, eastern United States) there was an agreement of ~60 cm or better between the undulations computed from the four methods and the N_T value (see Table

25). For some regions where local high variation of the gravity field occurs (e.g. Maui, (stations 7120,7210), Bermuda (station 7067)) the OSU86F field gives high discrepancies as compared to the N_T values. The "worst" situation was in Maui, where the OSU86F value of the undulation differs from the N_T value by about 7 meters (Table 25). This large difference can be explained by the fact that the OSU86F, being a limited expansion to degree 360 cannot represent the very high frequency signal of some regions of high variation of the gravity field. Such regions are the islands of Maui and Bermuda. The effect of the terrain was taken into account for the 17 laser stations in the Western United States where the terrain was considered to be rough. The effect of this correction was on the order of 60 cm (Table 27). For most of the laser stations no terrain corrections and/or height information was available and thus the computed value of the undulation will be systematically low. This is clearly the situation for the two stations in Hawaii, where the difference between the computed undulations using the four methods and the N_T value is ~2 m (see Table 25). The ellipsoidal corrections for the four methods were derived in a uniform formulation. Using the OSU86F set up to degree 36 those corrections were computed and they were very small in magnitude (maximum: 3 cm which is in good agreement with the results obtained in (Rapp, 1981b, Table 1)). Consequently, they could be neglected in the total undulation computation. A very important correction due to inconsistencies between the local terrestrial anomalies and the anomalies implied from the geopotential set within the same region of a 2° cap, called the "local average correction" was applied to all the computed undulations. The

effect of this correction reached 2 m for station 7082 in Bear Lake, Utah (compare Tables 25,26) and it improved the results with respect to the N_T value by about 30 cm for 28 laser stations that were used for the comparisons (Tables 28,29). It seems that this correction has to always be applied when geoid undulations are computed by a combination of terrestrial data and potential coefficient information. Very good agreement (~30 cm) was achieved between the gravimetric undulations using the four methods, the altimetric undulation, the undulation obtained from the calibration of SEASAT (Kolenkiewicz, 1987) and the N_T value for the station 7067 in Bermuda (see discussion at the end of Section 8.4).

The collocation method using Ohio State adjusted GEOS-3/SEASAT altimeter data for five oceanic stations resulted in values of the undulation consistent with the N_T value on the order of 70 cm (Table 34).

Using the low of propagation of errors the accuracy of the computed geoid undulations for each of the 44 laser stations could be computed from the errors in the gravity data surrounding the laser station, the accuracy of the given potential coefficients and from various models that could represent the omission and discretion errors. These accuracies were not computed individually for each laser station although global error models were considered in the error analysis of the various methods in Chapter 3. The global RMS undulation error from Chapter 3 for the capsize of 2° was computed to be approximately

60 cm for all the four methods (Figure 1). Finally, the accuracies of the altimetric undulations for all the five oceanic laser stations using the collocation method were computed to be ~20 cm.

CHAPTER X

RECOMMENDATIONS FOR FUTURE STUDIES

It is very critical for the future applications of the modified Sjöberg's method that error degree variance models of the terrestrial data which will represent the actual local behavior of the error estimates of those data should be developed. The modification of the Stokes' function for the modified Sjöberg's method is essentially based on the above error models and if the models are properly chosen this method will give the smallest possible error in the geoid undulation computations. A Monte-Carlo method modeling the empirical error covariance function could be suggested. Then, the error degree variances can be obtained by integration of the error covariance function.

The anomaly error degree variances implied by a geopotential model would certainly be different if a full variance-covariance matrix of the potential coefficients could be available. This would again influence the modified Sjöberg's method but the exact effect was not tested.

Another important investigation for precise undulation computations can be the effect of the zero and first degree term of the error anomaly degree variances of the terrestrial data and the zero degree term of the

error degree variances of the potential coefficient data (σ_0, σ_1 and δC_0 respectively, following the notation of the introduction) on the computation of the W_{4n} coefficients in the modified Sjöberg's method. Although the theory was given by equation (2.106) and (2.107), for the numerical applications we assumed $\sigma_0=\delta C_0=\sigma_1=0$. It seems that the stability of the solution (2.108) will be increased by admitting zero and first degree term for the above error degree variances, although this was not checked. The local average correction should be more extensively checked using actual geoid computations. Gravimetric geoid undulation computations in Doppler or GPS stations including and excluding the zero order correction could give a definite answer whether this correction should be applied or not. However, the answer reached here is that this correction has to always be applied.

Finally, the collocation method of computing undulations using the randomly distributed point gravity data surrounding the laser stations could be applied and the results could be compared with the ones given here using the integral formulas.

REFERENCES

Alfano, D. NASA Directory of Station Locations, Flight Dynamics Division, Goddard Space Flight Center, Greenbelt, Maryland, 1986.

Christodoulidis, D., On the Realization of a 10 cm Relative Oceanic Geoid, Report No. 247, Department of Geodetic Science and Surveying, The Ohio State University, Columbus, Ohio, 1976.

Cruz, J., Experiences with Altimeter Data Gridding, Report No. 347, Department of Geodetic Science and Surveying, The Ohio State University, Columbus, Ohio, 1983.

Despotakis, V., The Development of the June 1986 1°x1° and the August 1986 30′x30′ Terrestrial Mean Free-Air Anomaly Data Bases, Internal Report, Department of Geodetic Science and Surveying, The Ohio State University, Columbus, Ohio, 1986.

Engelis, T., R.H. Rapp and Y. Bock, Measuring Orthometric Height Differences with GPS and Gravity Data, manuscripta geodaetica, Vol. 10, No. 3, pp. 187-194, 1985a.

Engelis, T., Global Ocean Circulation from Seasat Altimeter Data, Marine Geodesy, Vol. 9, No. 1, pp. 45-69, 1985b.

Ganeko, Y., 10′x10′ Detailed Gravimetric Geoid Around Japan, presented to the General Meeting of I.A.G., Tokyo, May 1982.

Heiskanen, W. and H. Moritz, Physical Geodesy, W.H. Freeman and Co., San Francisco, 1967.

International Association of Geodesy, Geodetic Reference System 1967, Special Publication of Bulletin Geodesique, Paris, 1971

Jekeli, C., Reducing the Error of Geoid Undulation Computations by Modifying Stokes Function, Report No. 301, Department of Geodetic Science and Surveying, The Ohio State University, Columbus, Ohio, 1980.

Kolenkiewicz, R. and C.F. Martin, Seasat Altimeter Height Calibration, J. Geoph. Res., Vol. 87, No. C5, pp. 3189-3197, 1982.

Kolenkiewicz, R. and C.F. Martin, Analysis of Differences Between NSWC and GSFC Geoid Heights Determined from Seasat Altimeter Data, unpublished report, 1987.

Lachapelle, G. and A. Mainville, Disturbing Potential Components Software at the Geodetic Survey of Canada, Department of Energy, Mines and Resources, Ottawa, Canada, 1982.

Levitus, S., Climatological Atlas of the World Ocean, NOAA, Geophysical Fluid Dynamics Laboratory, Professional Paper 13, Rockville, MD, 1982.

Liang, C.K., The Adjustment and Combination of Geos-3 and Seasat Altimeter Data, Report No. 346, Department of Geodetic Science and Surveying, The Ohio State University, Columbus, Ohio, 1983.

Marsh, G.J., F.J. Lerch, B.H. Putney, D.C. Christodoulidis, T.L. Felsentreger, B.V. Sanchez, D.E. Smith, S.M. Klosko, T.V. Martin, E.C. Pavlis, J.W. Robbins, R.G. Williamson, O.L. Colombo, N.L. Chandler, K.E. Rachlin, G.B. Patel, S. Bhati and D.S. Chinn, An Improved Model of the Earth's Gravitational Field (GEM-T1), Goddard Space Flight Center, Greenbelt, MD, 1986.

Meissl, P., Preparations for the Numerical Evaluation of Second Order Molodensky-type Formulas, Report No. 163, Department of Geodetic Science and Surveying, The Ohio State University, Columbus, 1971.

Moritz, H., Advanced Physical Geodesy, Herbert Wichmann Verlag, Karlsruhe, 1980.

Noll, C.E., Crustal Dynamics Project--Survey Information Produced by the Data Information System on 02/23/83, NASA, Goddard Space Flight Center, Greenbelt Maryland, 1983.

Paul, M.K., A Method of Evaluating the Truncation Error Coefficient for Geoidal Height, Bulletin Geodesique, No. 110, pp. 413-425, 1973.

Rapp, R.H., and R. Rummel, Methods for the Computation of Detailed Geoids and Their Accuracy, Report No. 233, Department of Geodetic Science and Surveying, The Ohio State University, Columbus, Ohio, 1975.

Rapp, R.H., Ellipsoidal Corrections for Geoid Undulation Computations Using Gravity Anomalies in a Cap, J. Geophys. Res., Vol. 86, No. B11, pp. 10843-10848, 1981a.

Rapp, R.H., The Earth's Gravity Field to Degree and Order 180 Using SEASAT Altimeter Data, Terrestrial Gravity Data, and Other Data, Report No. 322, Department of Geodetic Science and Surveying, The Ohio State University, Columbus, Ohio, 1981b.

Rapp, R.H., Advanced Gravimetric Geodesy, Class Notes, Department of Geodetic Science and Surveying, The Ohio State University, Columbus, Ohio, 1985a.

Rapp, R.H., Detailed Gravity Anomalies and Sea Surface Heights Derived from GEOS-3/SEASAT Altimeter Data, Report No. 365, Department of Geodetic Science and Surveying, The Ohio State University, Columbus, Ohio, 1985b.

Rapp, R.H., Advanced Geometric Geodesy, Class Notes, Department of Geodetic Science and Surveying, The Ohio State University, Columbus, Ohio, 1985c.

Rapp, R.H., and J. Cruz, The Representation of the Earth's Gravitational Potential in a Spherical Harmonic Expansion to Degree 250, Report No. 372, Department of Geodetic Science and Surveying, The Ohio State University, Columbus, Ohio, 1986a.

Rapp, R.H., and J. Cruz, Spherical Harmonic Expansions of the Earth's Gravitational Potential to Degree 360 Using 30′ Mean Anomalies, Report No. 376, Department of Geodetic Science and Surveying, The Ohio State University, Columbus, Ohio, 1986b.

Robbins, J.W., and S.M. Klosko, TOPEX Apriori Station Coordinates, Goddard Space Flight Center, Greenbelt, Maryland, 1985.

Sjöberg, L.E., Comparison of Some Methods of Modifying Stokes' Formula, Proceedings of the International Symposium on the Definition of the Geoid, Florence, 1986a.

Sjöberg, L.E., A Comparison of the Modified Stokes' Formula and Hotine's Formula in Physical Geodesy, Report No. 4, Department of Geodesy, The Royal Institute of Technology, Stockholm, 1986b.

Smith, D.E., D.C. Christodoulidis, R. Kolenkiewicz, P.J. Dunn, S.M. Klosko, M.H. Torrence, S. Fricke, and S. Blackwell, A Global Geodetic Reference France from LAGEOS Ranging (SL5.1AP), J. Geophys. Res., Vol. 90, No. B11, pp. 9221-9233, 1985.

Torge, W., G. Weber, and H.G. Wenzel, 6′x10′ Free-Air Gravity Anomalies of Europe Including Marine Areas, presented to the XVIII IU 66 General Assembly, Hamburg 15.-27.8.1983.

Tscherning, C.C., and R.H. Rapp, Closed Covariance Expressions for Gravity Anomalies, Geoid Undulation and Deflections of the Vertical Implied by Anomaly Degree Variance Models, AFCRL-TR-0231, AD 786 417, Report No. 208, Department of Geodetic Science and Surveying, The Ohio State University, Columbus, Ohio, 1974.

Weber, G., and H.G., Wenzel, Estimation of Error Properties In: Validation of Seasat-1 Altimetry Using Ground Truth in the North Sea Region, Deutsche Geodaetische Kommission B 263, Frankfurt, 1982.

Wenzel, H.G., Geoid Computation by Least Squares Spectral Combination Using Integral Kernels, Institut für Theoretische Geodäsie, Universität Hannover, D 3000 Hannover 1, 1982.

Wichiencharoen, C., Fortran Programs for Computing Geoid Undulations From Potential Coefficients and Gravity Anomalies, Internal Report of the Department of Geodetic Science and Surveying, The Ohio State University, Columbus, Ohio, 1982a.

Wichiencharoen, C., The Indirect Effects on the Computation of Geoid Undulations, Report No. 336, Department of Geodetic and Surveying, The Ohio State University, Columbus, Ohio, 1982b.

Wichiencharoen, C., A Comparison of Gravimetric Undulations Computed by the Modified Molodensky Truncation Method and the Method of Least Squares Spectral Combination by Optimal Integral Kernels, Bulletin Geodesique, Vol. 58, No. 4, pp. 494-517, 1984.

APPENDIX A

Proof of equations (2.105), (2.106) and (2.107):

The expression of the global mean square error combining equations (2.98), (2.99), (2.100), (2.101) and (2.102) is:

$$\overline{\delta N_4^2} = \left(\frac{R}{2\gamma}\right)^2 \left[\sum_{n=0}^{\bar{n}} (X_{4n}-Q_{4n})^2\sigma_n + \sum_{n=\bar{n}+1}^{n_T} \left(\frac{2}{n-1} - Q_{4n}\right)^2 \sigma_n \right.$$

$$+ \sum_{n=n_T+1}^{\infty} \left(\frac{2}{n-1} - Q_{4n}\right)^2 C_n + \sum_{n=0}^{\bar{n}} (Q_{4n}+W_{4n})^2 \delta C_n$$

$$\left. + \sum_{n=\bar{n}+1}^{M} Q_{4n}^2 \delta C_n + \sum_{n=M+1}^{\infty} Q_{4n}^2 C_n \right] \qquad (A.1)$$

For convenience, let us use the substitutions

$$\left.\begin{aligned} X_{4n} &= X_n \\ Q_{4n} &= Q_n \\ W_{4n} &= W_n \end{aligned}\right\} \qquad (A.2) \qquad\qquad \frac{R}{2\gamma} = c \qquad (A.3)$$

The minimization of $\overline{\delta N_4^2}$ expressed in (2.103) is equivalent to the conditions

$$\frac{\partial(\overline{\delta N_4^2})}{\partial W_k} = 0, \quad k=0,1, \ldots ,\bar{n} \qquad (A.4)$$

where, from (A.1) and (A,2), (A.3):

$$\overline{\delta N_4^2} = c^2 \left[\sum_{n=0}^{\bar{n}} (X_n-Q_n)^2\sigma_n + \sum_{n=\bar{n}+1}^{n_T} \left(\frac{2}{n-1} - Q_n\right)^2 \sigma_n + \sum_{n=n_T+1}^{\infty} \left(\frac{2}{n-1} - Q_n\right)^2 C_n \right.$$

$$\left. + \sum_{n=0}^{\bar{n}} (Q_n+W_n)^2 \delta C_n + \sum_{n=\bar{n}+1}^{M} Q_n^2 \delta C_n + \sum_{n=M+1}^{\infty} Q_n^2 C_n \right] \qquad (A.5)$$

Denoting with Σ_1, Σ_2, Σ_3, Σ_4, Σ_5 and Σ_6 the summations in (A.5) and taking into account eq. (2.96), we have:

$$\left.\begin{aligned}
\Sigma_1 &= \sum_{n=0}^{\bar{n}} (X_n - Q_n)^2 \sigma_n = \sum_{n=0}^{\bar{n}} \left(X_n - Q_{1n} + \sum_{r=0}^{\bar{n}} \frac{2r+1}{2} W_r e_{rn}\right)^2 \sigma_n \\
\Sigma_2 &= \sum_{n=\bar{n}+1}^{n_T} \left(\frac{2}{n-1} - Q_n\right)^2 \sigma_n = \sum_{n=\bar{n}+1}^{n_T} \left(\frac{2}{n-1} - Q_{1n} + \sum_{r=0}^{\bar{n}} \frac{2r+1}{2} W_r e_{rn}\right)^2 \sigma_n \\
\Sigma_3 &= \sum_{n=n_T+1}^{\infty} \left(\frac{2}{n-1} - Q_n\right)^2 C_n = \sum_{n=n_T+1}^{\infty} \left(\frac{2}{n-1} - Q_{1n} + \sum_{r=0}^{\bar{n}} \frac{2r+1}{2} W_r e_{rn}\right) \delta C_n \\
\Sigma_4 &= \sum_{n=0}^{\bar{n}} (Q_n + W_n)^2 \delta C_n = \sum_{n=0}^{\bar{n}} \left(Q_{1n} - \sum_{r=0}^{\bar{n}} \frac{2r+1}{2} W_r e_{rn}\right)^2 \delta C_n \\
\Sigma_5 &= \sum_{n=\bar{n}+1}^{M} Q_n^2 \delta C_n = \sum_{n=\bar{n}+1}^{M} \left(Q_{1n} - \sum_{r=0}^{\bar{n}} \frac{2r+1}{2} W_r e_{rn}\right)^2 \delta C_n \\
\Sigma_6 &= \sum_{n=M+1}^{\infty} Q_n^2 C_n = \sum_{n=M+1}^{\infty} \left(Q_{1n} - \sum_{r=0}^{\bar{n}} \frac{2r+1}{2} W_r e_{rn}\right) C_n
\end{aligned}\right\} \quad (A.6)$$

Thus, condition (A.4) can be written

$$\begin{aligned}
\frac{\partial(\overline{\delta N_4^2})}{\partial W_k} &= \frac{\partial[c^2(\Sigma_1+\Sigma_2+\Sigma_3+\Sigma_4+\Sigma_5+\Sigma_6)]}{\partial W_k} \\
&= \frac{c^2 \partial(\Sigma_1+\Sigma_2+\Sigma_3+\Sigma_4+\Sigma_5+\Sigma_6)}{\partial W_4} \\
&= c^2\left[\frac{\partial\Sigma_1}{\partial W_k} + \frac{\partial\Sigma_2}{\partial W_k} + \frac{\partial\Sigma_3}{\partial W_k} + \frac{\partial\Sigma_4}{\partial W_k} + \frac{\partial\Sigma_5}{\partial W_k} + \frac{\partial\Sigma_6}{\partial W_k}\right] = 0,
\end{aligned}$$

or, since $c^2 \neq 0$

$$\frac{\partial\Sigma_1}{\partial W_k} + \frac{\partial\Sigma_2}{\partial W_k} + \frac{\partial\Sigma_3}{\partial W_k} + \frac{\partial\Sigma_4}{\partial W_k} + \frac{\partial\Sigma_5}{\partial W_k} + \frac{\partial\Sigma_6}{\partial W_k} = 0, \quad K=0,1, \ldots,\bar{n} \qquad (A.7)$$

Using the obvious relationships

$$\left.\begin{aligned}
\frac{\partial(X_n)}{\partial W_k} &= -\delta_{kn}, \quad k=0,1, \ldots,\bar{n} \\
\frac{\partial(Q_n)}{\partial W_k} &= -\frac{2k+1}{2} e_{kn}, \quad k=0,1, \ldots,\bar{n}
\end{aligned}\right\} \quad (A.8)$$

where δ_{kn} is the Kroenecker's δ: $\delta_{kn} = \begin{cases} 0 & k \neq n \\ 1 & k=n \end{cases}$, we evaluate the partials (A.7) from (A.6), one by one:

$$\frac{\partial \Sigma_1}{\partial W_k} = 2 \sum_{n=o}^{\bar{n}} \left(X_n - Q_{1n} + \sum_{r=o}^{\bar{n}} \frac{2r+1}{2} W_r e_{rn}\right)\left(-\delta_{kn} + \frac{2k+1}{2} e_{kn}\right)\sigma_n \qquad (A.9)$$

$$\frac{\partial \Sigma_2}{\partial W_k} = 2 \sum_{n=\bar{n}+1}^{n_T} \left(\frac{2}{n-1} - Q_{1n} + \sum_{r=o}^{\bar{n}} \frac{2r+1}{2} W_r e_{rn}\right)\left(\frac{2k+1}{2} e_{kn}\right)\sigma_n \qquad (A.10)$$

$$\frac{\partial \Sigma_3}{\partial W_k} = 2 \sum_{n=n_T+1}^{\infty} \left(\frac{2}{n-1} - Q_{1n} + \sum_{r=o}^{\bar{n}} \frac{2r+1}{2} W_r e_{rn}\right)\left(\frac{2k+1}{2} e_{kn}\right)C_n \qquad (A.11)$$

$$\frac{\partial \Sigma_4}{\partial W_k} = 2 \sum_{n=o}^{\bar{n}} \left(Q_{1n} - \sum_{r=o}^{\bar{n}} \frac{2r+1}{2} W_r e_{rn} + W_n\right)\left(-\frac{2k+1}{2} e_{kn} + \delta C_n\right) \qquad (A.12)$$

$$\frac{\partial \Sigma_5}{\partial W_k} = 2 \sum_{n=\bar{n}+1}^{M} \left(Q_{1n} - \sum_{r=o}^{\bar{n}} \frac{2r+1}{2} W_r e_{rn}\right)\left(-\frac{2k+1}{2} e_{kn}\right)\delta C_n \qquad (A.13)$$

$$\frac{\partial \Sigma_6}{\partial W_k} = 2 \sum_{n=M+1}^{\infty} \left(Q_{1n} - \sum_{r=o}^{\bar{n}} \frac{2r+1}{2} W_r e_{rn}\right)\left(-\frac{2k+1}{2} e_{kn}\right)C_n \qquad (A.14)$$

where, for (A.9) - (A.14) K=0,1, . . . ,$\bar{n}$.

Taking into acount that

$$\sum_{n=o}^{\bar{n}} (-X_n \delta_{kn})\sigma_n = \sum_{n=o}^{\bar{n}} W_n \delta_{kn} \sigma_n - \sum_{n=2}^{\bar{n}} \frac{2}{n-1} \delta_{kn} \sigma_n \qquad (A.15)$$

and

$$\sum_{n=o}^{\bar{n}} X_n \frac{2k+1}{2} e_{kn}\sigma_n = -\sum_{n=o}^{\bar{n}} W_n \frac{2k+1}{2} e_{kn}\sigma_n + \sum_{n=2}^{\bar{n}} \frac{2}{n-1} \frac{2k+1}{2} e_{kn}\sigma_n$$

$$= -\frac{2k+1}{2} \sum_{n=o}^{\bar{n}} W_n e_{kn}\sigma_n + \frac{2k+1}{2} \sum_{n=2}^{\bar{n}} \frac{2}{n-1} e_{kn}\sigma_n \qquad (A.16)$$

the partials (A.9) - (A.14) can be written:

$$\frac{1}{2}\frac{\partial \Sigma_1}{\partial W_k} = \sum_{n=o}^{\bar{n}} W_n \delta_{kn}\sigma_n - \sum_{n=2}^{\bar{n}} \frac{2}{n-1} \delta_{kn}\sigma_n + \frac{2k+1}{2} \sum_{n=2}^{\bar{n}} \frac{2}{n-1} e_{kn}\sigma_n$$

$$- \frac{2k+1}{2} \sum_{n=o}^{\bar{n}} W_n e_{kn}\sigma_n + \sum_{n=o}^{\bar{n}} Q_{1n}\delta_{kn}\sigma_n - \frac{2k+1}{2} \sum_{n=o}^{\bar{n}} Q_{1n} e_{kn}\sigma_n$$

$$+ \frac{2k+1}{2} \sum_{n=o}^{\bar{n}} \sum_{r=o}^{\bar{n}} \frac{2r+1}{2} W_r e_{rn} e_{kn}\sigma_n - \sum_{n=o}^{\bar{n}} \sum_{r=o}^{\bar{n}} \frac{2r+1}{2} W_r e_{rn}\delta_{kn}\sigma_n \qquad (A.17)$$

$$\frac{1}{2}\frac{\partial \Sigma_2}{\partial W_k} = \frac{2k+1}{2} \sum_{n=\bar{n}+1}^{n_T} \frac{2}{n-1} e_{kn}\sigma_n - \frac{2k+1}{2} \sum_{n=\bar{n}+1}^{n_T} Q_{1n} e_{kn}\sigma_n$$

$$+ \frac{2k+1}{2} \sum_{n=\bar{n}+1}^{n_T} \sum_{r=0}^{\bar{n}} \frac{2r+1}{2} W_r e_{rn} e_{kn} \delta_n \tag{A.18}$$

$$\frac{1}{2} \frac{\partial \Sigma_3}{\partial W_k} = \frac{2k+1}{2} \sum_{n=n_T+1}^{\infty} \frac{2}{n-1} e_{kn} C_n - \frac{2k+1}{2} \sum_{n=\bar{n}+1}^{n_T} Q_{1n} e_{kn} C_n$$

$$+ \frac{2k+1}{2} \sum_{n=n_T+1}^{\infty} \sum_{r=0}^{\bar{n}} W_r e_{rn} C_n \tag{A.19}$$

$$\frac{1}{2} \frac{\partial \Sigma_4}{\partial W_k} = - \frac{2k+1}{2} \sum_{n=0}^{\bar{n}} Q_{1n} e_{kn} \delta C_n + \sum_{n=0}^{\bar{n}} Q_{1n} \delta_{kn} \delta C_n$$

$$+ \frac{2k+1}{2} \sum_{n=0}^{\bar{n}} \sum_{r=0}^{\bar{n}} \frac{2r+1}{2} W_r e_{rn} e_{kn} \delta C_n$$

$$- \sum_{r=0}^{\bar{n}} \sum_{r=0}^{\bar{n}} \frac{2r+1}{2} W_r e_{rn} \delta_{kn} \delta C_n - \frac{2k+1}{2} \sum_{n=0}^{\bar{n}} e_{kn} W_n \delta_{kn} + \sum_{n=0}^{\bar{n}} W_n \delta_{kn} \delta C_n \tag{A.20}$$

$$\frac{1}{2} \frac{\partial \Sigma_5}{\partial W_k} = - \frac{2k+1}{2} \sum_{n=\bar{n}+1}^{M} Q_{1n} e_{kn} \delta C_n + \frac{2k+1}{2} \sum_{n=\bar{n}+1}^{M} \sum_{r=0}^{\bar{n}} W_r e_{rn} e_{kn} \delta C_n \tag{A.21}$$

$$\frac{1}{2} \frac{\partial \Sigma_6}{\partial W_k} = - \frac{2k+1}{2} \sum_{n=M+1}^{\infty} Q_{1n} e_{kn} C_n + \frac{2k+1}{2} \sum_{n=M+1}^{\infty} W_r e_{rn} e_{kn} C_n \tag{A.22}$$

Using condition (A.7) and adding (A.17) - (A.22), we obtain

$$\sum_{n=0}^{\bar{n}} W_n \delta_{kn} (\sigma_n + \delta C_n) - \frac{2k+1}{2} \sum_{n=0}^{\bar{n}} W_n e_{kn} (\sigma_n + \delta C_n)$$

$$- \sum_{n=0}^{\bar{n}} \sum_{r=0}^{\bar{n}} \frac{2r+1}{2} W_r e_{rn} \delta_{kn} (\sigma_n + \delta C_n)$$

$$+ \frac{2k+1}{2} \Bigg[\sum_{n=0}^{M} \sum_{r=0}^{\bar{n}} \frac{2r+1}{2} W_r e_{rn} e_{kn} (\sigma_n + \delta C_n)$$

$$+ \sum_{n=M+1}^{n_T} \sum_{r=0}^{\bar{n}} \frac{2r+1}{2} W_r e_{rn} e_{kn} (\sigma_n + C_n)$$

$$+ \sum_{n=n_T+1}^{\infty} \sum_{r=0}^{\bar{n}} \frac{2r+1}{2} W_r e_{rn} e_{kn} (C_n + C_n) \Bigg]$$

$$- \frac{2k+1}{2} \sum_{n=0}^{M} Q_{1n} e_{kn} (\sigma_n + \delta C_n) - \frac{2k+1}{2} \sum_{n=M+1}^{n_T} Q_{1n} e_{kn} (\sigma_n + C_n)$$

$$- \frac{2k+1}{2} \sum_{n=n_T+1}^{\infty} Q_{1n} e_{kn} (C_n + C_n)$$

$$+ \frac{2k+1}{2} \sum_{n=2}^{n_T} \frac{2}{n-1} e_{kn} \sigma_n + \frac{2k+1}{2} \sum_{n=n_T+1}^{\infty} \frac{2}{n-1} e_{kn} C_n$$

$$-\sum_{n=2}^{\bar{n}} \frac{2}{n-1}\,\delta_{kn}\sigma_n + \sum_{n=0}^{\bar{n}} Q_{1n}\delta_{kn}\delta C_n + \sum_{n=0}^{\bar{n}} Q_{1n}\delta_{kn}\sigma_n = 0,\ k=0,1,\ \ldots\ ,\bar{n} \qquad (A.23)$$

The third term of the left hand side of eq. (A.23) can be written:

$$\sum_{n=0}^{\bar{n}} \sum_{r=0}^{\bar{n}} \frac{2r+1}{2}\, W_r e_{rn}\delta_{kn}(\sigma_n+\delta C_n) = \sum_{r=0}^{\bar{n}} \frac{2r+1}{2}\, W_r e_{rk}(\sigma_k+\delta C_k) \qquad (A.24)$$

Using (A.24) into (A.23) we obtain after collecting the common factors of W_n:

$$\sum_{t=0}^{\bar{n}} \Big[(\sigma_t+\delta C_t)\delta_{kt} - \frac{2k+1}{2}\, e_{kt}(\sigma_t+\delta C_t) - \frac{2t+1}{2}\, e_{kt}(\sigma_k+\delta C_k)$$

$$+ \frac{2k+1}{2}\,\frac{2t+1}{2} \Big[\sum_{n=0}^{M} e_{tn}e_{kn}(\sigma_n+\delta C_n) + \sum_{n=M+1}^{n_T} e_{tn}e_{kn}(\sigma_n+C_n)$$

$$+ \sum_{n=n_T+1}^{\infty} e_{tn}e_{kn}(C_n+C_n) \Big] \Big] W_t$$

$$= \frac{2k+1}{2} \Big[\sum_{n=0}^{M} Q_{1n}e_{kn}(\sigma_n+\delta C_n) + \sum_{n=M+1}^{n_T} Q_{1n}e_{kn}(\sigma_n+C_n)$$

$$+ \sum_{n=n_T+1}^{\infty} Q_{1n}e_{kn}(C_n+C_n) \Big]$$

$$- \frac{2k+1}{2} \sum_{n=2}^{n_T} e_{kn}\sigma_n - \frac{2k+1}{2} \sum_{n=n_T+1}^{\infty} \frac{2}{n-1}\, e_{kn}C_n + X_{1k}\sigma_k - Q_{1k}(\sigma_k+\delta C_k)$$

$$k=0,1,\ \ldots\ ,\bar{n} \qquad (A.25)$$

where X_{1k} are given by (2.39).

It is now obvious that equations (A.25) are equivalent to the linear system

$$\sum_{t=0}^{\bar{n}} a_{kt}W_t = h_k \quad k=0,1,\ \ldots\ ,\bar{n} \qquad (A.26)$$

with $a_{kt} = a_{tk} = (\sigma_t+\delta C_t)\delta_{kt} - \frac{2k+1}{2}\, e_{kt}(\sigma_t+\delta C_t) - \frac{2t+1}{2}\, e_{kt}(\sigma_k+\delta C_k)$

$$+ \frac{2k+1}{2}\,\frac{2t+1}{2} \Big[\sum_{n=0}^{M} e_{tn}e_{kn}(\sigma_n+\delta C_n) + \sum_{n=M+1}^{n_T} e_{tn}e_{kn}(\sigma_n+C_n)$$

$$+ \sum_{n=n_T+1}^{\infty} e_{tn} e_{kn} (C_n + C_n) \Big] \qquad (A.27)$$

and $h_k = \frac{2k+1}{2} \Big[\sum_{n=0}^{M} e_{kn} \Big[Q_{1n} (\sigma_n + \delta C_n) - X_{1n} \sigma_n \Big]$

$$+ \sum_{n=M+1}^{n_T} e_{kn} \Big[Q_{1n} (\sigma_n + C_n) - X_{1n} \sigma_n \Big]$$

$$+ \sum_{n=n_T+1}^{\infty} e_{kn} \Big[Q_{1n} (C_n + C_n) - X_{1n} C_n \Big] \Big]$$

$$+ X_{1k} \sigma_k - Q_{1k} (\sigma_k + \delta C_k) \qquad (A.28)$$

Equations (A.26), (A.27) and (A.28) after the substitutions (A.2) and (A.3) give immediately equations (2.105), (2.16) and (2.107) which were to be proven.

APPENDIX B

The deviation of the sea surface from the geoid, known as the Sea Surface Topography (SST) plays an important role when the gravimetric or the altimetric undulation are compared to the ellipsoidal minus orthometric value of the undulation of laser stations on islands. From Figure B1 we can see that the orthometric height (H) of a laser station.

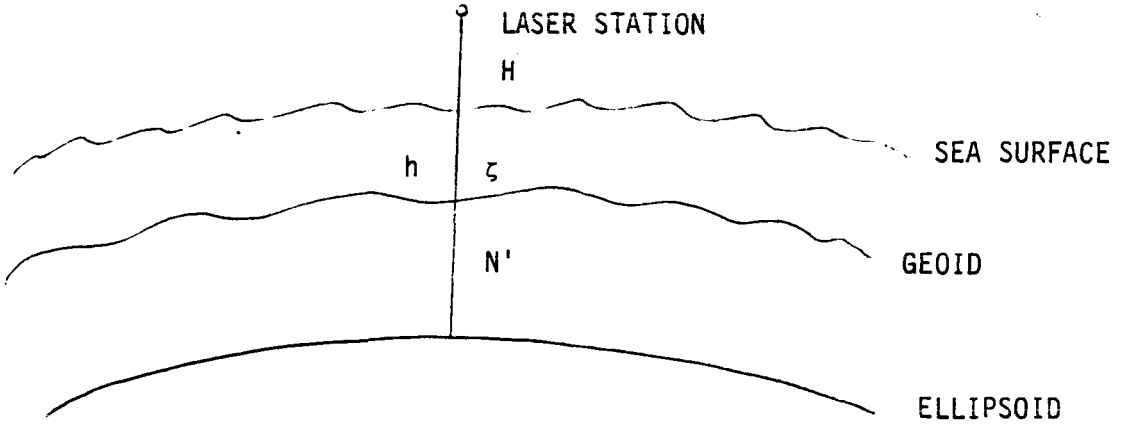

Figure B1. Role of the Sea Surface Topography (ζ) for Undulation Computations in Oceanic Laser Stations.

the SST (ζ), the geoid undulation (N′) and the ellipsoidal height (h) of the laser station satisfy the equation:

$$h = H + \zeta + N' \qquad (B.1)$$

In writing equation (B.1) the basic assumption that has been made is that the vertical datum to which the orthometric height of the laser station refers is assumed to coincide with the mean sea surface as is realized by the altimetric observations. From (B.1) the value of the undulation will be

$$N' = (h-H) - \zeta \qquad (B.2)$$

From Chapter 4, equation (4.2), and from equation (B.2) we take:

$$N' = N_T - \zeta \qquad (B.3)$$

Thus, from the value of the undulation N_T computed in Chapter 4, the value of the SST has to be subtracted, so that the undulation N' obtained can be compared to the gravimetric undulation of the laser station. We thus assume that the gravimetric undulations of the laser stations are free from the effect of SST. This is not rigorously true, since the SST influences the gravity anomaly data which are used to compute the gravimetric undulations, but this effect can be considered negligible (Rapp, 1985b).

Four different SST harmonic coefficient sets described in (Rapp, 1985b, Appendix B) were used to compute ζ. These sets were computed by Engelis (private communication, 1987) similarly as in (Engelis, 1985b) and they are as follows:

Set No. 1: SST harmonic coefficients complete to degree and order 36. The PGS3041 potential coefficient set, an intermediate set for the GEM-T1 (Marsh et al., 1986) has been used to realize the geoid up to degree 36. The high frequencies from degrees

37 to 180 were removed from the SEASAT sea surface heights by using the potential coefficients of the solution described in (Rapp, 1981b).

Set No. 2: SST harmonic coefficients complete to degree and order 36; the PGS3041 set has been used up to degree 36.

Set No. 3: SST harmonic coefficients complete to degree and order 10, based on the Levitus (1982) data.

Set No. 4: A set of 64800 1°x1° global values of SST based on Levitus data.

The computation of the SST at the laser stations using Sets No. 1-3 was done as follows:

$$\zeta = \sum_{n=0}^{M} \sum_{m=0}^{n} (c_{nm}\cos m\lambda + d_{nm}\sin m\lambda)P_{nm}(\sin\bar{\phi}) \qquad (B.4)$$

where c_{nm}, d_{nm} are the SST harmonic coefficients and $\bar{\phi}$ is the geocentric latitude of the laser station. The degree of expansion M was taken 6 for all the three sets.

The computation of the SST at the laser stations using the Set No. 4 was done using the four 1°x1° closest points to the laser station in a bi-linear interpolation with respect to the latitude and longitude of the laser station.

The results of the SST computations using all the four SST sets described above are shown in Table B1 for 5 laser stations. The number and the name of the laser stations appear in the first two columns; the location of the stations appears in the third column; finally

the SST as computed from Sets No. 1-4 ((S1),(S2),(S3),(S4) correspondingly) is shown in columns four-seven. The units for the SST is meters.

Table B1. Sea Surface Topography in meters for 5 Laser Stations Using the Sets No. 1-4.

NUMBER	NAME	OCCUPATION	S1	S2	S3	S4
7210	MAULAS	Maui, Hawaii	0.81	0.88	0.44	0.32
7067	BDILAS	Bermuda Island	0.55	0.61	0.07	0.09
7838	SHOLAS	Simosato, Japan	0.93	0.86	0.43	0.22
7090	YARLAS	Yarragadee, Australia	-0.10	-0.12	0.11	0.00
7943	ORRLAS	Orroral Valey, Australia	0.16	0.10	-0.03	0.00

For the above five laser stations the gravimetric undulations are available using four different methods (See Table 21). We select here the undulations computed using the modified Sjöberg's method to represent the gravimetric undulation of stations 7210-7943 of Table B1. These undulations are shown on the second column of Table B2; then, the N_T value of the undulation computed from (4.2) is shown in the third column; the corrected values of N_T through equation (B.3) using the above four SST sets ($N' = N_T - \zeta$) is shown in columns four-seven. According to our discussion above the undulations of column two should be compatible only with the values of the undulations of columns four-seven of Table B2.

The differences $N-N_T$ and $N-N'$ for the four SST sets are shown on Table B3; Table 37; the corresponded statistics of these differences are shown on Table B4. It can be seen from Table B4 that the mean and the RMS differences were decreased in all cases that the SST correction

Table B2. Gravimetric Value of the Undulation (N), N_T (Uncorrected for SST) and $N' = N_T$ (Corrected for SST Using the Sets No. 1-4) for 5 Laser Stations in meters.

NUMBER	N	N_T	N'(S1)	N'(S2)	N'(S3)	N'(S4)
7210	18.66	20.49	19.68	19.61	20.05	20.17
7067	-31.97	-31.81	-32.36	-32.42	-31.88	-31.90
7838	38.63	39.97	39.04	39.11	39.54	39.75
7090	-24.88	-24.28	-24.18	-24.16	-24.39	-24.28
7943	18.85	20.38	20.22	20.28	20.41	20.38

was applied to the N_T values as compared to the mean and the RMS differences with the uncorrected N_T values. The standard deviation of the differences remained essentially the same when the first two SST sets were used, and slightly decreased (~0.05 m) when the last two SST sets were used.

The accuracy of the SST computed using the four sets as above is thought to be approximately ±20 cm (Rapp, 1985b, p. 106). Considering this accuracy estimate is true, we can say that the inclusion of the SST effect clearly improved the individual and overall comparisons of the gravimetric undulations with the (corrected) N_T value.

Table B3. Differences $N-N_T$, N-N'(S1), N-N'(S2), N-N'(S3) and N-N'(S4) in meters (see Table 36) for the 5 Laser Stations.

NUMBER	$N-N_T$	N-N'(S1)	N-N'(S2)	N-N'(S3)	N-N'(S4)
7210	-1.83	-1.02	-0.95	-1.39	-1.51
7067	-0.16	0.39	0.45	-0.09	-0.07
7838	-1.34	-0.41	-0.48	-0.91	-1.12
7090	-0.60	-0.70	-0.72	-0.49	-0.60
7943	-1.53	-1.37	-1.43	-1.56	-1.53

Table B4. Statistics of the Differences $N-N_T$, $N-N'(S1)$, $N-N'(S2)$, $N-N'(S3)$ and $N-N'(S4)$ in meters (see Table 36) for the 5 Laser Stations.

STATISTICS	$N-N_T$	$N-N'(S1)$	$N-N'(S2)$	$N-N'(S3)$	$N-N'(S4)$
Mean Difference	-1.09	-0.62	-0.63	-0.89	-0.97
RMS Difference	1.25	0.86	0.88	1.04	1.12
Standard Dev Diff	0.61	0.60	0.61	0.54	0.56
Minimum Difference	-1.83	-1.37	-1.43	-1.56	-1.53
Maximum Difference	-0.16	0.39	0.45	-0.09	-0.07

Although the sample of the 5 laser stations used here is small, the systematic improvement of the results when the SST was considered is clear. We thus can say that the SST effect has to always be taken into account when geoid undulations at an accuracy level of 50 cm or better are to be computed.